MONTANUNIVERSITÄT LEOBEN

PETROLEUM ENGINEERING DEPARTMENT

TEXTBOOK SERIES

VOLUME 2

RESERVOIR FLUIDS

by

Zoltán E. HEINEMANN
Professor for Reservoir Engineering

Brigitte E. WEINHARDT
Associate Professor for Reservoir Engineering

Leoben, October 2005

Table of Contents

List of Figures

Chapter 1

Review of Thermodynamic Terminology

When considering hydrocarbon reservoirs, terms such as “oil reservoirs” and “gas reservoirs” are used both in colloquial speech and technical literature. However, these terms are insufficient. Changes in the state of aggregation during production should always be taken into account in consequence of changes of the reservoir pressure and changes of pressure and temperature in the production system (tubing, pipe lines, separator, tank).

Thermodynamics has evolved to a science of studying changes in the state of a system with changes in the conditions, i.e. temperature, pressure, composition. A systematic presentation of basic thermodynamic tools (charts, tables and equations) for sketching the state of a hydrocarbon system as a function of the state variables is one of the objectives of this textbook. Therefore, it may be helpful to refurbish the thermodynamic terminology at the beginning as far as it is indispensable to the understanding of these tools.

Thermodynamic studies are generally focused on arbitrarily chosen systems while the rest of the universe is assumed as “surroundings”. The surface of the system - real or imaginary - is called a “boundary”. A system is called a “closed system” if it does not exchange matter with the surroundings, in opposite to an “open system” which exchanges matter with the surroundings. Both systems may exchange energy with the surroundings.

The concept of a closed system is of major interest in applied hydrocarbon thermodynamics. It is called a “homogeneous” closed system if it contains a single phase, e.g. a natural gas phase or an oil phase. A “heterogeneous” closed system contains more than one phase.

A “phase” is defined as a physically homogeneous portion of matter. The phases of a heterogeneous system are separated by interfaces and are optically distinguishable. It is not obligatory that a phase is chemically homogeneous. It may consists of several compounds, e.g. of a large number of various hydrocarbons.

The thermodynamic properties of a system are classified into “intensive” and “extensive” properties. Intensive properties such as temperature and pressure are independent of the size of the system, i.e. of the amount of the substance in the system. Extensive properties depend on the amount of the substances, such as volume, enthalpy, entropy etc. However,

the extensive properties per unit mass or mole are intensive properties, e.g. the mole volume.

“State functions” or “state variables” are those properties for which the change in state only depends on the respective initial and final state. It is this path-independent characteristic of the state functions that makes it possible to quantify any change of a system.

“Equilibrium” has been defined as a “state of rest”. In an equilibrium state, no further change or - more precisely - no net-flux will take place unless one or more properties of the system are altered. On the other side, a system changes until it reaches its equilibrium state. Any change of a system is called a “thermodynamic interest” in the thermodynamic study of the system:

- adiabatic (no heat added to or removed from the system),
- isothermal (constant temperature),
- isobaric (constant pressure),
- isochoric (constant volume).

A process is called “reversible” if it proceeds through a series of equilibrium states in such a way that the work done by forward change along the path is identical to the work attained from the backward change along the same path. However, all real processes are “irreversible” with varying degrees of departure from a reversible one.

Chapter 2

Phase Behavior

Hydrocarbon reservoirs consist of rock and fluids. Water in brine form and a gaseous and/or liquid hydrocarbon phase are regarded as reservoir fluids. The phase behavior of the actual hydrocarbon mixture in the reservoir can be described as a function of the state of the system.

A system in thermodynamic equilibrium possesses an accurately defined relationship between the state variables. These are united in the so-called "**equation of state**":

$$F(p, V, T) = 0\,. \tag{2.1}$$

By specification of two variables, the third will be stipulated.

2.1 GIBBS' Phase Rule

When referring to the number of phases coexisting in the thermodynamical equilibrium, the phase rule introduced by GIBBS (1928) is applied.

$$F = C - P + 2\,, \tag{2.2}$$

where

- P: number of phases,
- C: number of components,
- F: number of degrees of freedom.

C is defined as the smallest number of constituents by which the coexisting phases can be completely described. F is defined as the number of quantities such as pressure, temperature, concentrations which can be varied within finite boundaries without changing the number of phases in the system.

Eq. 2.2 describes the system in a qualitative and very general manner. However, no reference to the state variables (p,T), to the composition of the particular phases or to the

proportions of the phases are given.

To gain a full understanding, it is best to discuss the phase behavior of pure substances (single-component systems) first. The circumstances in case of 2- or even multi-component systems are much more complicated.

2.2 Single-Component System

2.2.1 Water

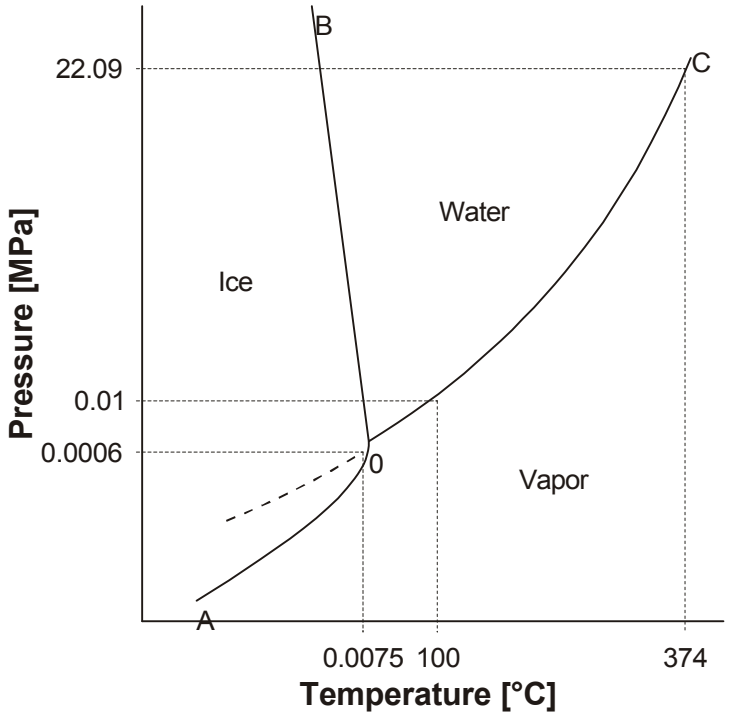

Figure 2.1: Water system - schematic (not drawn to scale)

Water is one of the most thoroughly studied chemical compounds. Therefore, it is discussed as a single-component system in this context. The possible phases are ice (solid state), water (liquid state) and steam (gaseous state). The phase diagram in Figure 2.1 illustrates at which state of the system - characterized by p and T - two or all three phases are in equilibrium:

- The **sublimation curve OA** signifies the equilibrium between the solid and vapor.
- The **melting point curve OB** combines the states of equilibrium between the solid and liquid state.
- The **vapor pressure curve OC** specifies the states of the system at which the liquid and vapor coexist. On this curve, the "wet" vapor is in equilibrium with the

"saturated" liquid.

- At the **triple point O**, all three phases are in equilibrium. In case of water, the thermodynamical data at this point are p = 610.6 Pa and T = 273.16 K.
- The end point *C* of the vapor pressure curve is the **critical point** and signifies the highest temperature and pressure at which the liquid and vapor coexist ($p_c(H_2O)$ = 22.09 MPa, $T_c(H_2O)$= 647.15 K.

Example 2.1

The degree(s) of freedom in different states of a single-component system. by use of Eq. 2.2 (GIBBS' phase rule) and Figure 2.1:

- F = 0 at the triple point (P = 3).
- F = 1 on the curves describing the 2-phase (P = 2) equilibria. Either the temperature or the pressure is freely eligible without counteracting any given phase equilibrium.
- F = 2 in any area of single phase state (P = 1. Both pressure and temperature (naturally inside finite boundaries) are freely eligible without transforming the system into a multi-phase system.

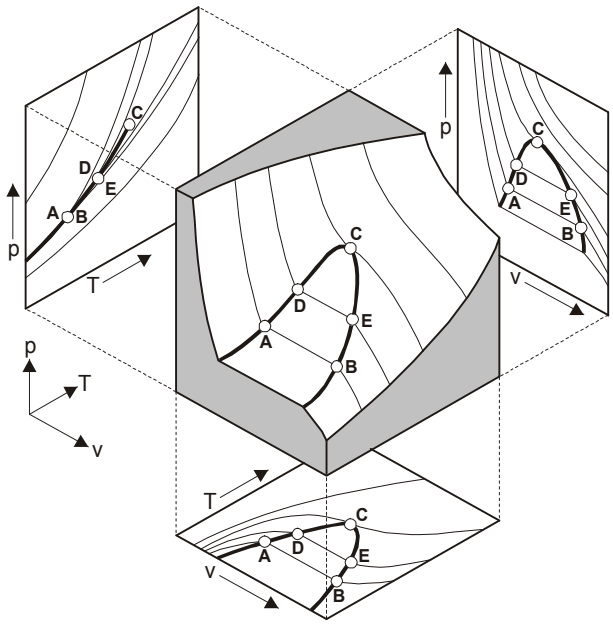

Figure 2.2: Phase equilibrium surface of a pure substance (from GYULAY, 1967)

The state variables, *p*, *T, V* can only assume positive values. Thus, the graphical illustration of the state of any system is only situated in the positive section of the *p,V, T*-coordinate system An example for an equilibrium surface is given in Figure 2.2. The shape of such an equilibrium surface is substance specific.

Assuming that the partial derivatives are steady, it is possible to draw only one single

tangential plane at an optional point of the surface. However, a plane is defined by two vectors which infers that the differential quotients

$$\left(\frac{\partial p}{\partial T}\right)_V, \left(\frac{\partial V}{\partial T}\right)_p, \left(\frac{\partial V}{\partial p}\right)_T$$

are not independent of one another. It is proven that

$$\left(\frac{\partial p}{\partial T}\right)_V = -\frac{\left(\frac{\partial V}{\partial T}\right)_p}{\left(\frac{\partial V}{\partial p}\right)_T}. \tag{2.3}$$

The three differential quotients describe three essential fundamental properties of the system: (i) the isothermal compressibility c, (ii) the cubic expansion coefficient β, and (iii) the pressure coefficient α:

$$c = \left(-\frac{1}{V}\right)\left(\frac{\partial V}{\partial p}\right)_T, \tag{2.4}$$

$$\beta = \frac{1}{V}\left(\frac{\partial V}{\partial T}\right)_p, \tag{2.5}$$

$$\alpha = \frac{1}{p}\left(\frac{\partial p}{\partial T}\right)_V. \tag{2.6}$$

Then, according to Eq. 2.3, the following is valid:

$$\beta = pc\alpha. \tag{2.7}$$

Since the specific volume - in contrast to the representation in Figure 2.1 - appears now as a state variable, the 2-phase state (e.g. water in equilibrium with steam) is characterized by any area surrounded by two curves which converge at the critical point:

- On the **bubble point curve**, an infinitesimal small amount of vapor is in equilibrium with the "saturated" liquid.
- The **dew point curve** characterizes states in which a negligible small amount of liquid is in equilibrium with "wet" vapor.

It is common to simplify the complex spatial illustration of the equilibrium surface by applying normal projections. Figure 2.2 displays that

- the projection into the *p, V*-plane results in **isotherms** (*T = const)*,
- the projection into the *V, T*-plane results in **isobares** (*p = const*),
- the projection into the *p, T*-plane results in **isochores** (*V = const*).

When regarding the projection which represents the 2-phase area (liquid-vapor) in the *p,*

T-plane, the bubble point curve and dew point curve coincide. The resulting single curve is named **vapor pressure curve**.

Of course, the vapor pressure curve is not isochoric. However, it is possible to draw isochores: One upwards into the liquid phase and one downwards into the gas phase. This aspect will be described in detail by discussing the phase behavior of the simple hydrocarbon n-butane.

2.2.2 n-Butane

Projections of the equilibrium surface into two planes of the positive section of the *p,V,T* coordinate system are displayed in Figure 2.3 and Figure 2.4.

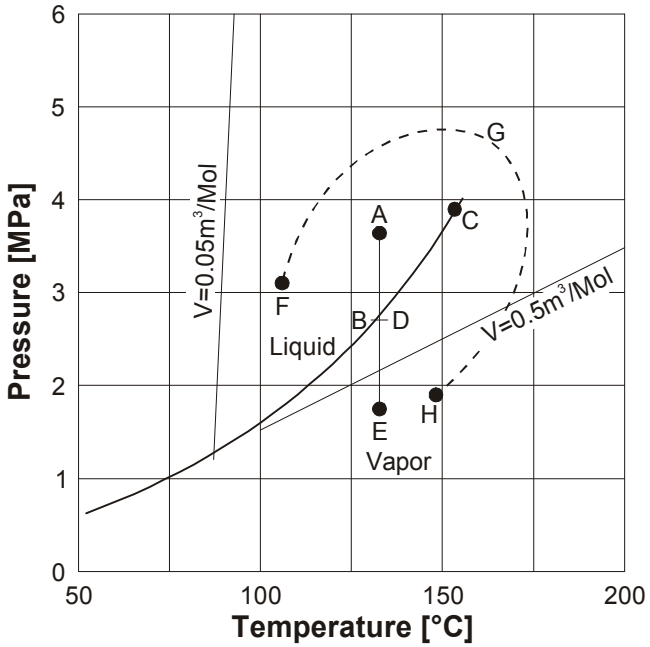

Figure 2.3: Vapor pressure diagram of n-butane (from GYULAY, 1967)

Figure 2.3 illustrates the vapor pressure curve of n-butane, including the critical point *C*. In addition, the isochores $V = 0{,}05$ m^3/kmole inside the liquid phase region and $V = 0.5$ m^3/kmole inside the vapor region are shown. In case of the state *A*, butane is an undersaturated liquid. When moving to the bubble point *B* by isothermal expansion, vaporization commences. Then the continuation of this isothermal expansion includes no further pressure drop in the system until the last molecule has passed over to the gas phase. From this moment, further expansion will result in further pressure decrease. At the point *E*, *n*-butane is in the state of a "dry" vapor. An isochoric change of state must be analogously discussed.

By applying the projection of the equilibrium surface into the *p*, *V*-plane (see Figure 2.4),

it is possible to comprise the whole 2-phase region. In this region, the isothermal vaporization or condensation takes place as an isobaric process.

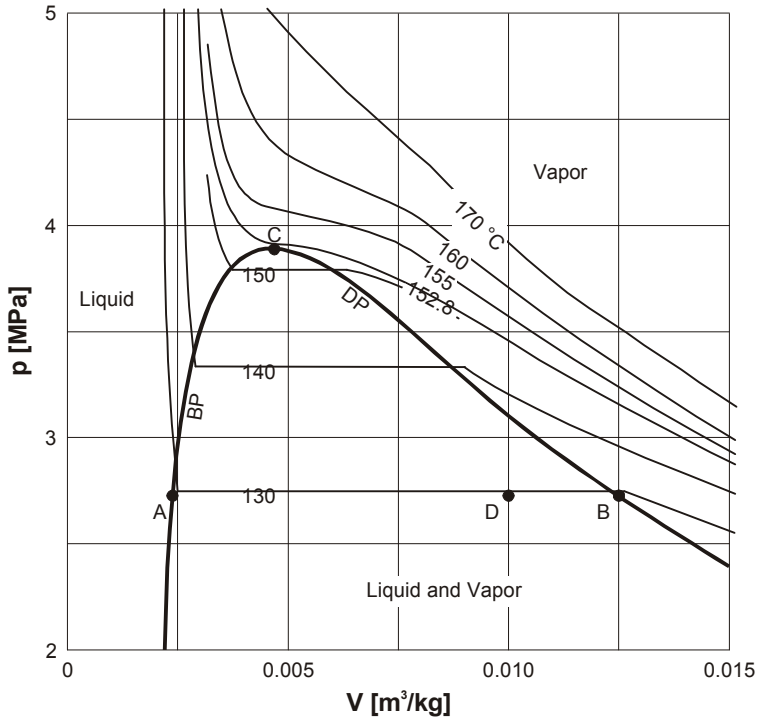

Figure 2.4: Pressure - volume phase diagram of n-butane (from GYULAY, 1967)

Isotherms, which do not intersect the 2-phase region, describe those states of the system without any phase transformation by changing the pressure. The intersection point of all other isotherms with the bubble point curve (e.g. *A*) marks the specific volume of the saturated liquid which is in phase equilibrium with the specific volume of the wet vapor (e.g. marked by point *B*). Considering point *D* within the 2-phase region of the system (specific volume of the system in total), the mass ratio of the liquid and vapor phase being in equilibrium with one another can be calculated by the principle of the lever:

$$m_L / m_v = \overline{DB} / \overline{AD} . \tag{2.8}$$

Example 2.2

100 kg n-butane are filled up in a sealed 10 m^3 container. The volume of the vapor phase at T = 130°C and p = 2.7 MPa can be evaluated from Figure 2.4 using Eq. 2.8

From Figure 2.4:

$$m_L / m_v = \overline{DB} / \overline{AD} = 0.3125 ,$$

$m_L + m_v = 100 = 0.3125\ m_v + m_v$

$m_v = 76.19$ kg.

The specific volume of the vapor phase is marked by point B in Figure 2.4:

$V = 0.0125\ m^3/kg.$

The vapor volume of the system, V_V, can be now calculated by multiplying V with m_V:

$V_V = 0.95\ m^3.$

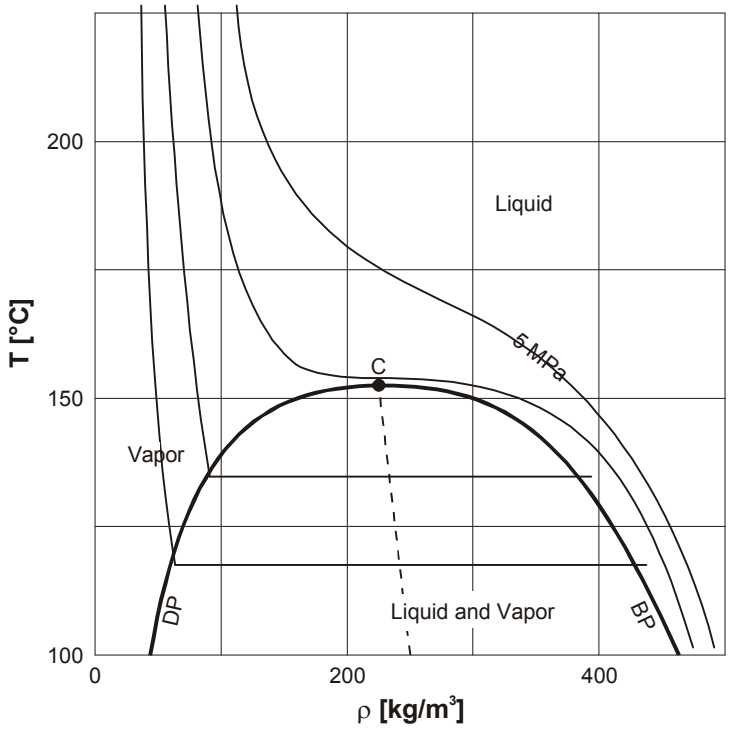

Figure 2.5: Temperature - density phase diagram of n-butane (from GYULAY, 1967)

Figure 2.5 demonstrates the T,ς-diagram of n-butane. The isobar touching the critical point has an inflection point just as the critical isotherm in Figure 2.4. Inside the 2-phase region, average values of fluid and vapor density are located on a straight line. With the help of this rule (CAILLETET-MATHIAS rule (1886)), the critical density can be calculated by extrapolation.

Example 2.3

Use the CAILLETET-MATHIAS rule to evaluate the critical density of methane. The densities of the liquid and the vapor phase being in equilibrium have been measured at different temperatures (see table below). The values of averaged densities have already been

calculated.

Table 2.1:

Temperature T °C	Liquid Density $\rho_{liq,eq}$ kg m^{-3}	Vapor Density $\rho_{v,eq}$ kg m^{-3}	Averaged Density $\overline{\rho_{eq}}$ kg m^{-3}
- 158.3	4.192 E + 2	2.311 E + 0	2.1076 E + 02
- 148.3	4.045 E + 2	2.798 E + 0	2.0365 E + 02
- 138.3	3.889 E + 2	7.624 E + 0	1.9827 E + 02
- 128.3	3.713 E + 2	1.240 E + 1	1.9185 E + 02
- 118.3	3.506 E + 2	1.925 E + 1	1.8493 E + 02
- 108.3	3.281 E + 2	2.899 E + 1	1.7855 E + 02

It is known as the CAILLETET-MATHIAS rule that the averaged densities are situated on a straight line. The slope of a straight line can be evaluated by regression analysis. On the basis of the averaged densities given above:

$$tg\ \alpha = -0,654 kg/m^3 .$$

To evaluate the critical density, ρ_c, the line must be extrapolated to the critical temperature of methane, $T_c = -82,3^o C$:

$$\rho_c = 178.55 - 26 \text{ x } 0.654\ kg/m^3 ,$$

$$\rho_c = 161.546\ kg/m^3 .$$

2.3 Critical State and Quantities of Corresponding States

Figure 2.4 illustrates the inflection point of the critical isotherm at the critical point. At the point of the inflection, both the first and the second partial derivates of $p = p(V)$ equal zero that

$$\left(\frac{\partial p}{\partial V}\right) = 0 = \left(\frac{\partial^2 p}{\partial V^2}\right). \qquad (2.9)$$

The state of the system at this point is characterized by the critical specific volume V_c, the critical pressure p_c, and the critical temperature T_c.

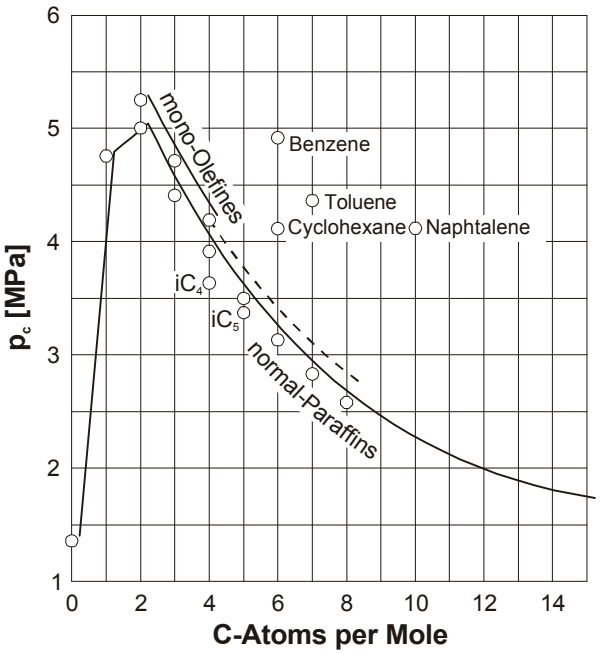

Figure 2.6: Critical pressure as a function of number of *C*-atoms in homologous series (after GYULAY, 1967)

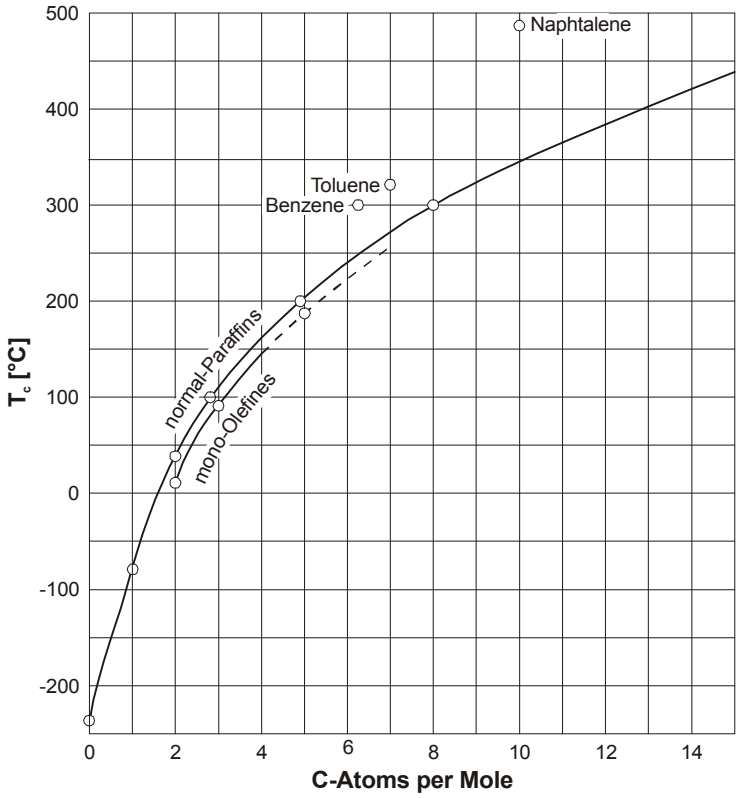

Figure 2.7: Critical temperature as a function of numbers of *C*-atoms in homologous series (after GYULAY, 1967)

Considering the critical data p_c and T_c, the homologous series of hydrocarbons show regularities which can be used for extrapolation. The experimental data in Figure 2.6 and Figure 2.7 refer to the homologous series of paraffins, C_nH_{2n+2}, and olefines, C_2H_{2n}(n = 1,2,... k), with a margin of error 1 to 2%. Because of thermal decomposition, it is not possible to obtain experimentally information about the critical data in case of high molecular weight. However, the critical data of homologous compounds with longer carbon chains can be extrapolated though an increasing error has to be taken into consideration.

The "principle of corresponding states" for chemically similar substances - e.g. for homologous series - results in a close relation between the *p, V, T*-properties of pure hydrocarbons if the state variables are substituted by the so called "reduced quantities" which are

$$p_r = \frac{p}{p_c}; \qquad V_r = \frac{V}{V_c}; \qquad T_r = \frac{T}{T_c}. \tag{2.10}$$

Figure 2.8 shows a p_r, V_r phase diagram which is valid for paraffins from methane *(CH_4)* to hexane *(C_6H_{14})*.

2.4 Binary Systems

If a systems consists of more than one component, its state is also a function of composition. In general, the composition is defined by “mole fractions”.

The mole fraction is defined as the ratio between the number of moles of a certain component and the sum of moles of all components. A system being composed of k components is defined by the specification of *(k - 1)* mole fractions because the sum of the mole fractions always equal 1.Considering a 2-component system, every change in state is described by the equation of state $F(p, V, T, z) = 0$. z may be the mole fraction of one (lighter) component.

The phase behavior of the ethane/n-heptane system is graphically illustrated by the *p, T, z*-coordinate system in Figure 2.9. The volume is equivalent to the mole volume.

In the plane $z = 1$, the vapor pressure curve of ethane appears, whereas in the plane $z = 0$ the one of n-heptane appears. Covering all other *z*-planes, an envelope surface encloses the 2-phase state. This is demonstrated by the example of three additional *z*-planes.

The upper broken line marks the critical points of all compositions which are possible. This curve divides the envelope surface into two parts: the **bubble point surface** and the **dew point surface.** The region of an undersaturated liquid state is positioned outside the bubble point surface (low temperature). Outside of the dew point surface (high temperature), the state of a dry gas is given.

Analogous to the pure substance, the critical state of binary systems is defined as the state at which the intensive properties of the phases are no more distinguishable. Just as in case of 1-component systems, the critical isotherms have an inflection point according to Eq. 2.9.

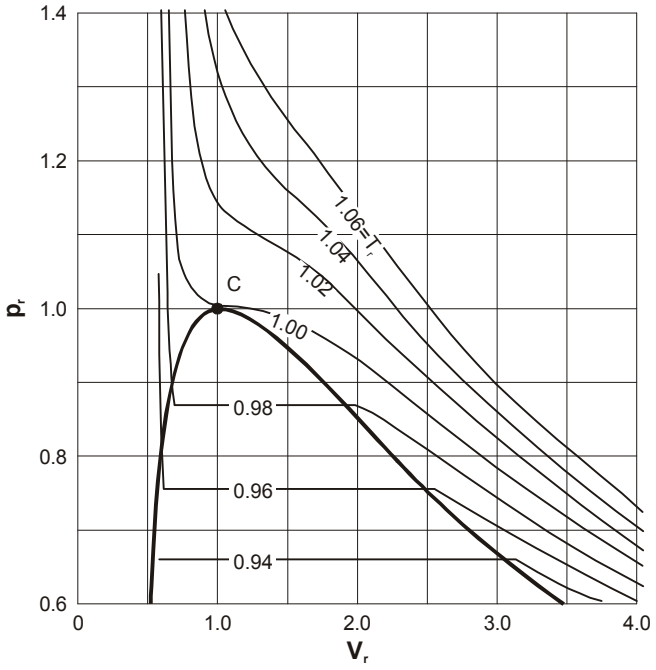

Figure 2.8: Combined reduced pressure - reduced volume phase diagram of paraffins with low molecular weight (after GYULAY, 1967)

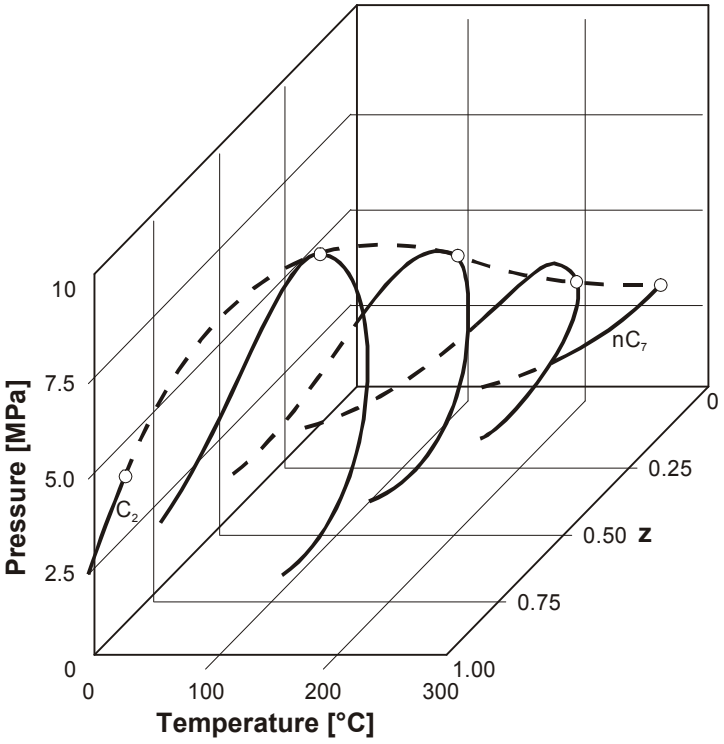

Figure 2.9: Phase equilibrium surface of the binary system ethane/n-heptane (from GYULAY, 1967)

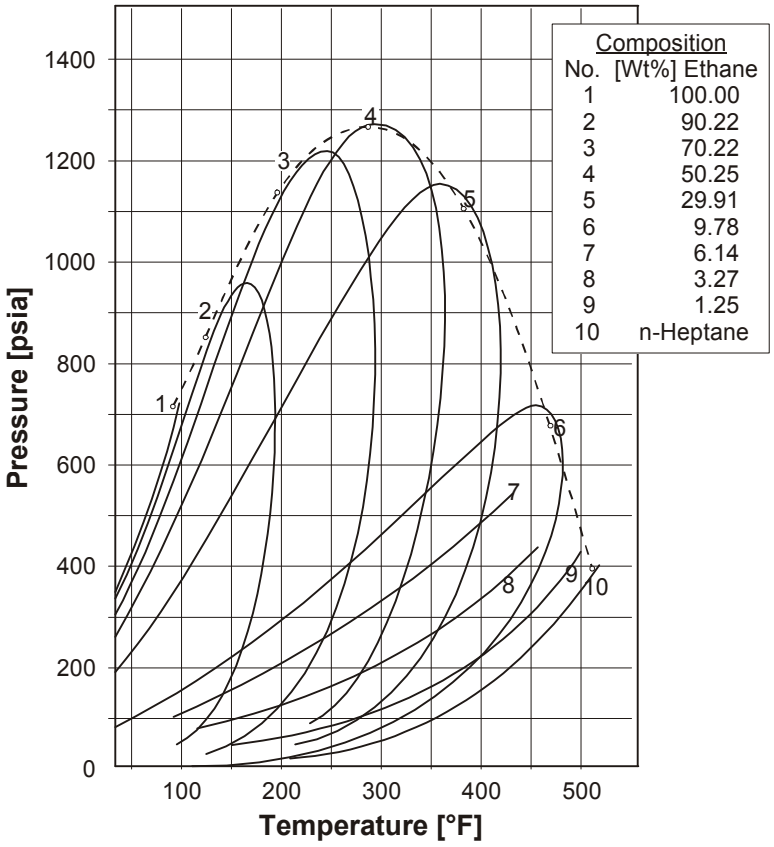

Figure 2.10: Pressure - temperature phase diagram of the binary system ethane/n-heptane (from KAY, 1938)

Figure 2.10 shows the projection of Figure 2.9 into the p, T-plane. At a given pressure, the bubble point temperature of the mixture is always higher than that of the pure lighter component. Physically, it can be explained by the fact that the thermal motion of the lighter molecules is obstructed by the heavier ones which exhibit more inertia.

On the other side, the dew point temperature of the mixture at a given pressure is always lower than that of the pure heavier component. This is due to the fact that lighter molecules partially transfer their higher kinetic energy to the heavier ones by collision. Consequently, the system maintains the state of a gas phase.

Figure 2.10 also shows that T_c of a mixture lies between the critical temperatures of the pure substances. In contrast to this, p_c of the mixture may be obviously higher than the one of the pure substances.

If the mixture consists of two homologous compounds with quite different volatility (in consequence of quite different molecular weights), the critical data curve envelopes a very extensive temperature and pressure region. For example, the maximum of the critical pressure of a methane/n-decane system equals 37 MPa. The smaller the difference between the molecular weights and thus between the volatility, the more flat the envelope curve will be.

Figure 2.11 illustrates the phase behavior of a certain ethane/n-heptane system. Besides the critical point, the curve enveloping the 2-phase region possesses two additional characteristic points:

- C': the point of highest pressure on the curve that is called **cricondenbar**.
- C": the point of highest temperature on the curve that is called **cricondentherm**.

As on Figure 2.11, so called "quality lines" are shown on p,T-diagrams. A quality line represents a certain mole percentage being liquid or vapor in the state of phase equilibrium. In Figure 2.11, the quality line "20%" represents the states in which 20% of the system account for the liquid phase. The bubble point curve and the dew point curve represent 100% and 0% liquid, respectively. All the quality lines (isochores) converge at the critical point.

Figure 2.11 also shows an isothermal decrease along the path EF where E defines the system to be a dry gas. If the constant temperature is higher than T_c but lower than the cricondentherm - like in case of the path EF -, the path surpasses the dew point line twice. Consequently, a condensate drops out at the dew point D'. At some point between D' and D", the volume of condensate (liquid) will be at its maximum. This maximum is given by the intersection point of the path EF with the dotted line connecting C and C". If the decrease in pressure will be continued, the condensate will be vaporized again. As soon as the dew point D" has been reached, the condensated phase has been vaporized in total. This process is called a "retrograde condensation".

Similar phenomena occur when the temperature is changed by an isobaric process where the constant pressure is higher than p_c but lower than the cricondenbar of the system.

In Figure 2.11, the dotted line connecting point C with point C' marks the states of the system which exhibit the highest volume percentage of condensate dropout.

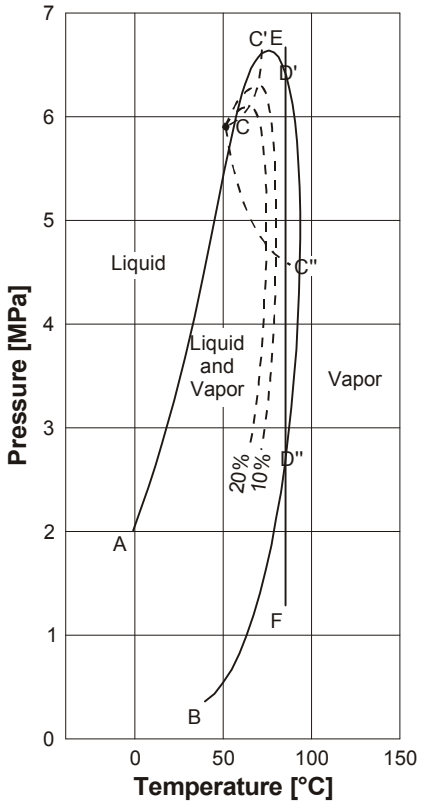

Figure 2.11: Pressure - temperature phase diagram of the binary system ethane (z = 0.9683)/n-heptane

It depends on the composition of the system if the cricondenbar is located on the dew point curve or on the bubble point curve. As far as the system ethane/n-heptane is concerned, Figure 2.10 elucidates that the cricondenbar is located on the bubble point curve at low mole fractions of ethane.

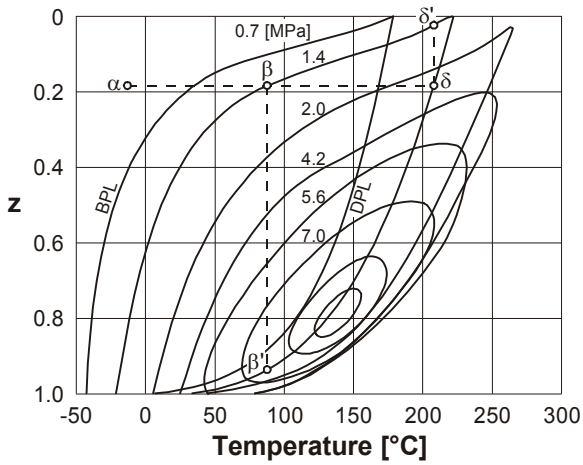

Figure 2.12: Mole fraction(ethane) - temperature diagram of the binary system ethane/n-heptane (from GYULAY, 1967)

In Figure 2.12, the phase behavior of ethane/n-heptane systems is graphically illustrated in the *z,T*-plane corresponding to another possible projection of the surface in Figure 2.9. The mixture α achieves bubble point β due to an isobaric (1.4 MPa) heat supply. Point β symbolizes the composition of the liquid phase which is in equilibrium with an infinitesimal small vapor phase whose composition is symbolized by the point β'. During further increase of temperature, dew point state is reached at point δ. The composition of the infinitesimal small liquid phase in equilibrium with the vapor phase corresponds with point δ'.

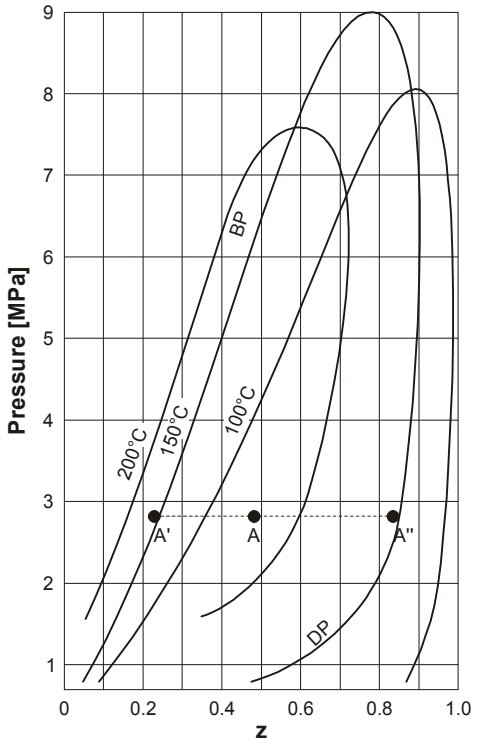

Figure 2.13: Mole fraction (ethane) - Pressure diagram of the binary system ethane/n-heptane (from GYULAY, 1967)

The design of the corresponding p, z-diagram is also possible (see Figure 2.13). An example may be the composition at the point A(T = 150 °C). The composition of the liquid phase is given by point A', the one of the vapor phase by point A". Again the relative masses of both phases can be determined by applying the principle of the lever (see Example 2.4).

Example 2.4.

Determining the phase composition.

A sealed container (p = 2.86 MPa), T = 150°C) is filled up with 100 kg of a ethane(z = 0.47)/n-heptane mixture. The mole number of ethane in the liquid phase and in the vapor phase, respectively, can be evaluated from Figure 2.13 by using the principle of lever.

At first, the mole weights (M_{C2} = 30 kg/mole, M_{C7} = 100 kg/mole) are inserted into

$$z = \frac{m_{C2}/M_{C2}}{m_{C2}/M_{C2} + m_{C7}/M_{C7}}$$

to evaluate the weight of n-heptane in the system, m_{C7}. The weight of ethane, m_{C2}, is given by $m_{C2} = 100 - m_{C7}$.

$$z = 0.47 = \frac{(100 - m_{C7})/30}{(100 - m_{C7})/30 + m_{C7}/100}$$

$$m_{C7} = 79.215 kg$$

$$m_{C2} = 100 - 79.215 = 20.785 kg$$

Now the total mole number of the system, $n = n_{C2} + n_{C7}$, can be calculated:

$$n_{C2} = \frac{m_{C2}}{M_{C2}} = \frac{20.785}{30} = 0.693 kmole,$$

$$n_{C7} = \frac{m_{C7}}{M_{C7}} = \frac{79.215}{100} = 0.792 kmole,$$

$$n = 0.693 + 0.792 = 1.485 kmole.$$

From Figure 2.12

$$\frac{n_{liq}}{n_{vap}} = \frac{\overline{A\,A''}}{A\,A'} = 1.458,$$

where

n_{liq}: total mole number in the liquid phase

n_{vap}: total mole number in the vapor phase

Thus the total mole number in the vapor phase results in

$$n_{vap} = 0.604 \text{ kmole}.$$

The composition of the vapor phase is given by point *A″* in Figure 2.12:

$$z = 0.82$$

The mole number of ethane in the vapor phase can now be calculated by

$$n_{C2,\,vap} = z \times n_{vap} = 0.82 \times 0.672 = 0.495 kmole\ .$$

The composition of the liquid phase is given by point *A'* in Figure 2.12:

$$z = 0.23\ .$$

The total mole number in the liquid phase results in

$$n_{liq} = n - n_{vap} = 1.485 - 0.604 = 0.881 \text{ kmole}\ .$$

The mole number of ethane in the liquid phase can now be calculated by

$$n_{C2,\,liq} = 0.23 \times 0.881 = 0.203 kmole\ .$$

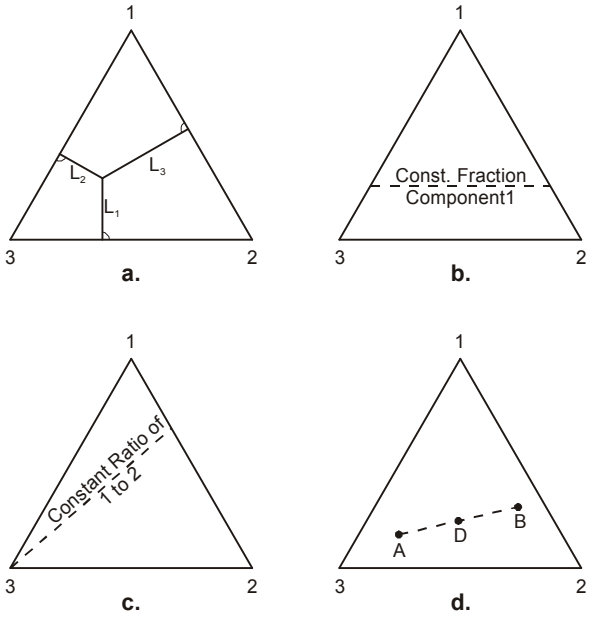

Figure 2.14: Properties of ternary diagrams

2.5 Multi-Component Systems

2.5.1 Ternary Phase Diagrams

It is common to illustrate the phase behavior of 3-component systems at constant pressure and temperature in so called triangular diagrams. Each corner of the triangle represents one pure component. On the basis of the equilaterality of the triangle, the sum of the perpendicular distances from any point to each side of the diagram is a constant equal to length of any of the sides. Thus, the composition - expressed in mole fractions - of a point

in the interior of the triangle is given by

$$z_1 = \frac{L_1}{L_T}, \qquad z_2 = \frac{L_2}{L_T}, \qquad z_3 = \frac{L_3}{L_T}, \tag{2.11}$$

where

$$L_T = L_1 + L_2 + L_3 . \tag{2.12}$$

Several other useful properties of the triangular diagrams are also illustrated by Figure 2.14:

- For mixtures along any line parallel to a side of the diagram, the fraction of the component of the corner opposite to that side is constant.
- Mixtures lying on any line connecting a corner with the opposite side contain a constant ratio of the component at the ends of the side.
- Mixtures of any two compositions lie on a straight line connecting the two initial points on the ternary diagram. The principle of the lever finds application again and

$$\frac{n_A}{n_B} = \frac{\overline{DB}}{\overline{DA}} \tag{2.13}$$

gives the mixing ratio leading to mixture *D*.

Figure 2.15 shows the 2-phase region for chosen *p* and *T*. *A*ny mixture with an overall composition lying inside the binodal curve will split into a liquid and a vapor phase. The "tie lines" connect compositions of liquid and vapor phases in equilibrium. Any overall composition on a certain tie line gives the same liquid and vapor composition being in equilibrium. Only the amounts of the phases change as the overall composition changes.

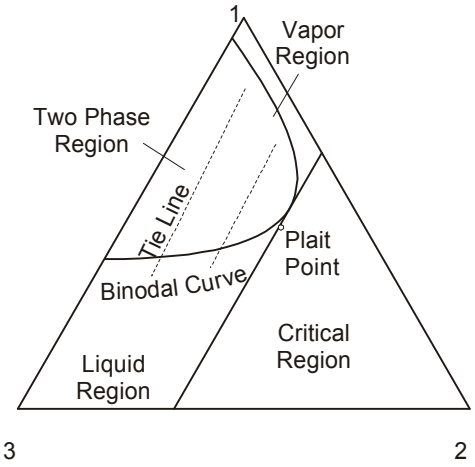

Figure 2.15: Typical features of a ternary phase diagram

The liquid and vapor portions of the binodal curve meet at the "plait point" which represents the critical composition. By drawing the tangent in the plait point on the

binodal curve, the single-phase region is splitted into three sections. Mixtures of a composition being located in the critical region with another one being located in the liquid or vapor region will, in any case, also result in a single-phase system if the straight line connecting the two initial compositions does not intersect the 2-phase region.

Figure 2.16 illustrates the influence of pressure on the phase behavior of a certain ternary system at constant temperature. As pressure increases, the 2-phase region shrinks.

It is useful to comprise the two heavier components of a ternary system and to reduce this system to a fictitious binary system, on the basis of a hypothetical component. Figure 2.17 illustrates a corresponding application by the respective *p,T*-diagram of the methane/propane/n-pentane system. The mole-% of methane are specified along the outermost envelope curve. All envelope curves are characterized by the portion of propane in the hypothetical component (propane/n-pentane) which is given by

$$C = \frac{z_3}{z_3 + z_5}. \tag{2.14}$$

In accordance to this aspect, the critical state properties, p_c and T_c, can be determined for any mixture of the three components (see Example 2.5).

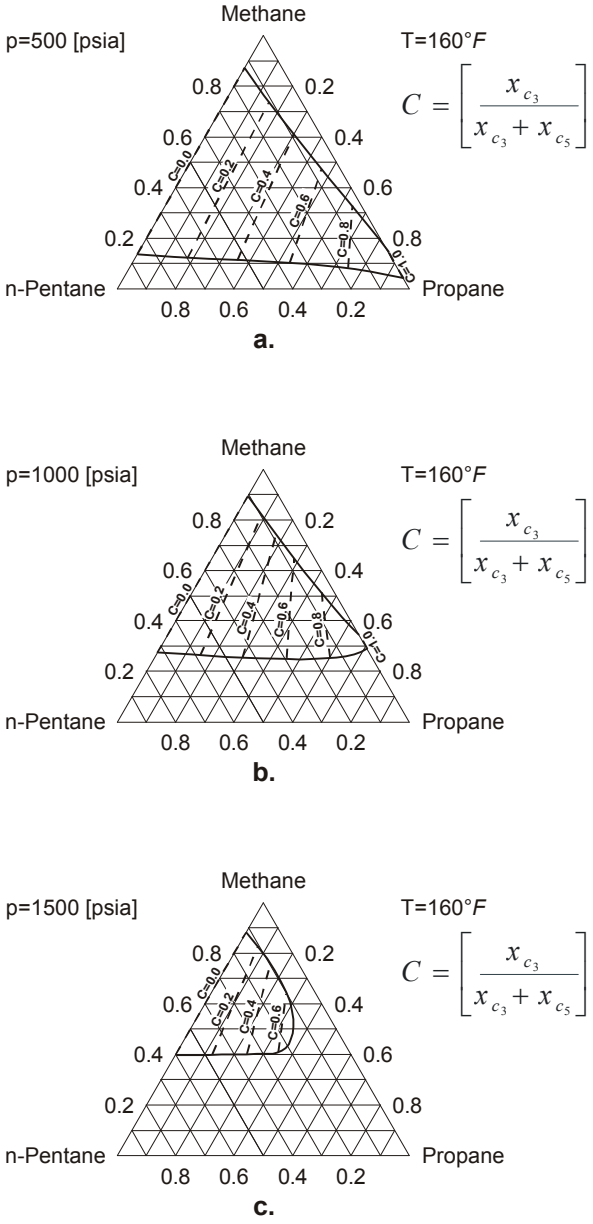

Figure 2.16: Triangular diagrams for the methane/propane/n-pentane system at 160 $^{o}F(71\ ^{o}C)$ (after DOURSON et al., 1943)

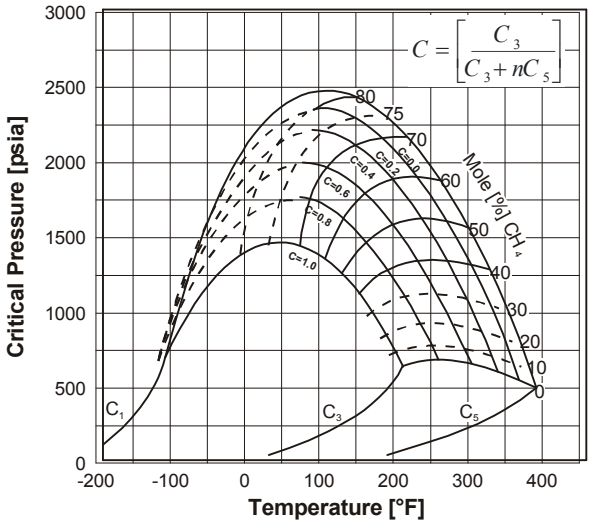

Figure 2.17: Critical loci of methane/propane/n-pentane systems (from KATZ et al., 1959)

Example 2.5

The hydrocarbon mixture is composed of 8 [kg] methane (M = 16[kg kmol^{-1}], 13,2 [kg] propane (M = 44.1[kg kmol^{-1}]) and 32.5 [kg] n-pentane (M = 72.2[kg kmol^{-1}]). The critical data of this mixture can be evaluated by use of Figure 2.17.

At first, the mole numbers and the respective mole fractions must be calculated.

$$n_1 = \frac{8}{16} = 0.5 kmole,$$

$$n_3 = \frac{13.2}{44.1} = 0.3 kmole,$$

$$n_5 = \frac{32.5}{72.2} = 0.45 kmole,$$

$$z_1 = \frac{0.5}{0.5 + 0.3 + 0.45} = 0.4,$$

$$z_3 = \frac{0.3}{0.5 + 0.3 + 0.45} = 0.24,$$

$$z_5 = \frac{0.45}{0.5 + 0.3 + 0.45} = 0.36.$$

The portion of propane in the hypothetical component propane/n-pentane is given by

$$C = \frac{z_3}{z_3 + z_5} = \frac{0.24}{0.24 + 0.36} = 0.4 .$$

From Figure 2.17 at $C = 0.4$ and 40 mole percent methane:

$$T_c = 262.5°F = 128°C$$

and

$$p_c = 1344\ psia = 9.27 MPa .$$

The application of the triangular diagram is not solely confined to ternary systems. For example it is possible to partition the paraffinic hydrocarbons into three pseudo-components which are

- methane *(C_1)* as the light component,
- the lighter pseudo-component including ethane to hexane *(C_2-C_6),*
- the heavier pseudo-component including heptane and higher hydrocarbons *(C_{7+})*.

2.5.2 Classification of Hydrocarbon Reservoirs

Anyway, only poor information of complex natural hydrocarbon systems has been reported until now. Nevertheless, some generalization makes a description of these complex systems possible - according to known data. The phase behavior of several complex and natural hydrocarbon systems are demonstrated in Figure 2.18 to Figure 2.22 by *p, T*-phase diagrams. For the classification of natural hydrocarbon systems, it is essential to know

- if the critical temperature is lower or higher than the reservoir temperature,
- which state will be achieved at surface conditions (separator).

Not considered in this classification are changes in composition during production.

Figure 2.18 represents a hydrocarbon system whose critical temperature is significantly lower than the reservoir temperature. In case of an isothermal pressure decrease (full line from point 1 to 2), which occurs in the reservoir adjacent to the production well the course of production, the system remains in the single-phase (gaseous) state. Even in case of both pressure and temperature decrease (dotted line), no liquid phase will drop out. Consequently, the considered hydrocarbon mixture is called a “dry gas”. Dry gases contain mainly methane, small amounts of ethane, possibly propane and some hydrocarbons of higher molecular weights.

A so called “wet gas” (see Figure 2.19) remains in a single-phase (gaseous) state in the

reservoir during production (line 1-2). Anyway, condensate will drop out under separator conditions.

In case of the system shown in Figure 2.20, the reservoir temperature is higher than the critical one but lower than the cricondentherm. The initial conditions given by Point 1 specifies the hydrocarbon mixture as a dry gas. If the pressure will decrease adjacent to the production well during production, the dew point of the system is reached at point 2. Consequently, condensate drops out inside the reservoir. The pressure at point 3 corresponds to the state in which the condensed liquid phase reaches the maximum (in mole%). In the separator, the amount of condensate is larger than in case of wet gases. Systems as shown in Figure 2.20 are called “gas condensates”.

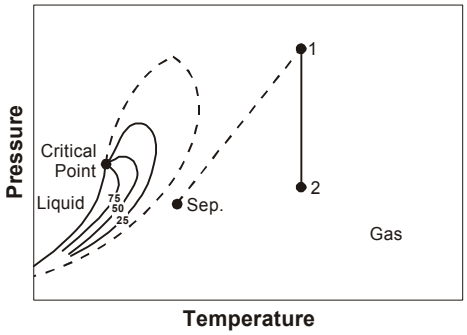

Figure 2.18: Phase diagram of a dry gas (from McCain, 1973)

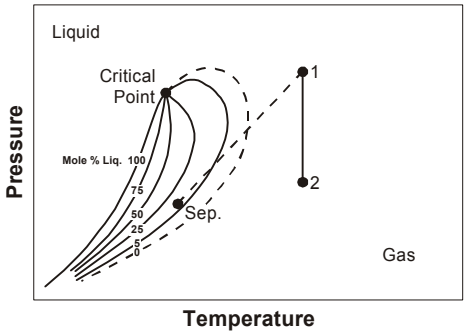

Figure 2.19: Phase diagram of a wet gas (from McCain, 1973)

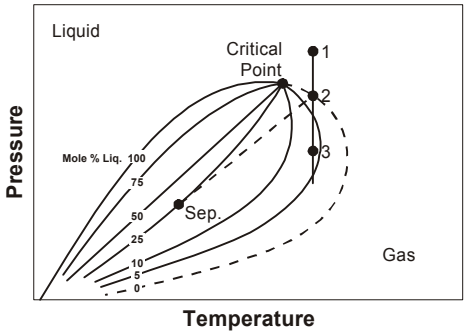

Figure 2.20: Phase diagram of a retrograde gas condensate (from McCain, 1973)

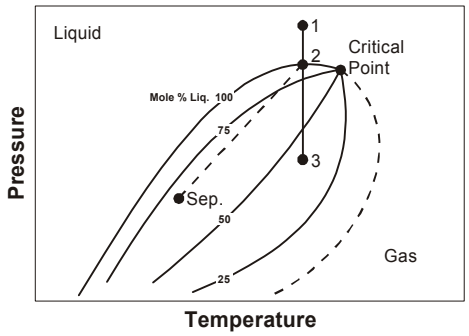

Figure 2.21: Phase diagram of a high-shrinkage crude oil (from McCain, 1973)

The so called "white oils" - as characterized in Figure 2.21 - are referred to as "high shrinkage oils". The reservoir temperature is below the critical temperature. Since the bubble point curve will be reached by the decrease in pressure due to production, from the initial pressure (point 1) to the pressure 2, a further pressure drop in the reservoir will lead to point 3 and thus to an increased development of the vapor phase. At separator conditions, about 65% of the produced hydrocarbon mixture will exist as liquid phase if the reservoir is produced at bubble point conditions.

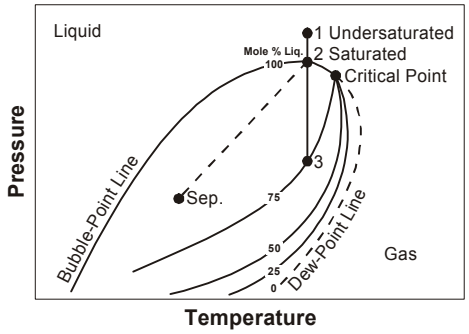

Figure 2.22: Phase diagram of a low shrinkage crude oil (from McCain, 1973)

Figure 2.22 shows a "black oil" or "low shrinkage oil". The initial state is characterized by point 1 at which the state of the system can be regarded as "undersaturated" liquid. If the pressure in the neighborhood of the production well will decrease during production to point 2, the bubble point curve is reached and the state of the system is now considered "saturated". The separator conditions are near the bubble point curve. Consequently, about 85 mole% of the produced hydrocarbon mixture is in the liquid phase at separator conditions. In accordance to this fact, the shrinkage of the oil due to gas liberation is less pronounced than in case "white oils" (see Figure 2.21).

If the hydrocarbon mixture in the reservoir is a 2-phase state under initial reservoir conditions, oil and gas phase can be considered apart from one another (see Figure 2.23). The equilibrium conditions at the initial state of the system are given by the intersection point of the dew point curve of the gas cap and the bubble point curve of the oil zone.The gas cap shows a "retrograde" behavior, if the intersection point is located on the dew point curve of the gas cap between the critical point and the cricondentherm.

Just as in case of binary systems (see Figure 2.9), the phase behavior of natural hydrocarbon mixtures can also be illustrated in *p, T, z*-diagrams.

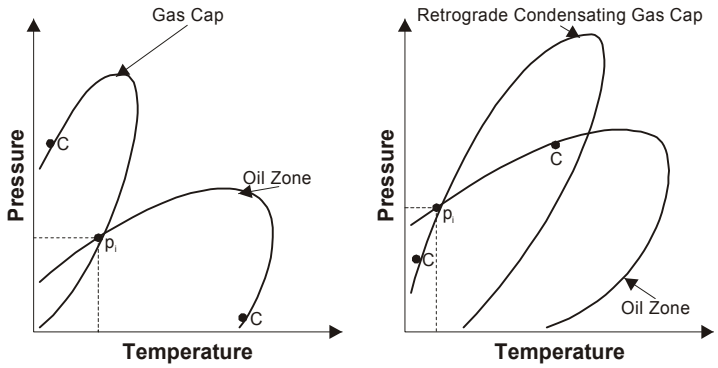

Figure 2.23: Phase diagram pairs of gas cap and oil zone

In Figure 2.24, composition I represents the separator gas while composition IV represents the corresponding separator oil of the well stream. Furthermore, the phase behavior of two representative mixtures of I and IV are given by the compositions II and III. The system of composition II corresponds to a gas-condensate system, the one of composition III to a white oil. Inside the 2-phase region of system II and III, isochores of the liquid phase and - as dotted lines - the locations of maximum retrograde condensation are drawn. Again an envelope surface comprises the 2-phase region in dependence on the composition. The spatial curve, which connects the critical points, splits the surface into two parts which are the dew point surface and the bubble point surface. Outside the envelope surface, the system is in a single-phase state.

By projecting the phase surface into the *p, z*-plane, information about the composition of the system will be obtained. If the state of the system is represented by point 1, the equilibrium composition of the liquid (x_1), and the one of the vapor phase, (y_1), is given by point 4 in the *p, z*-plane.

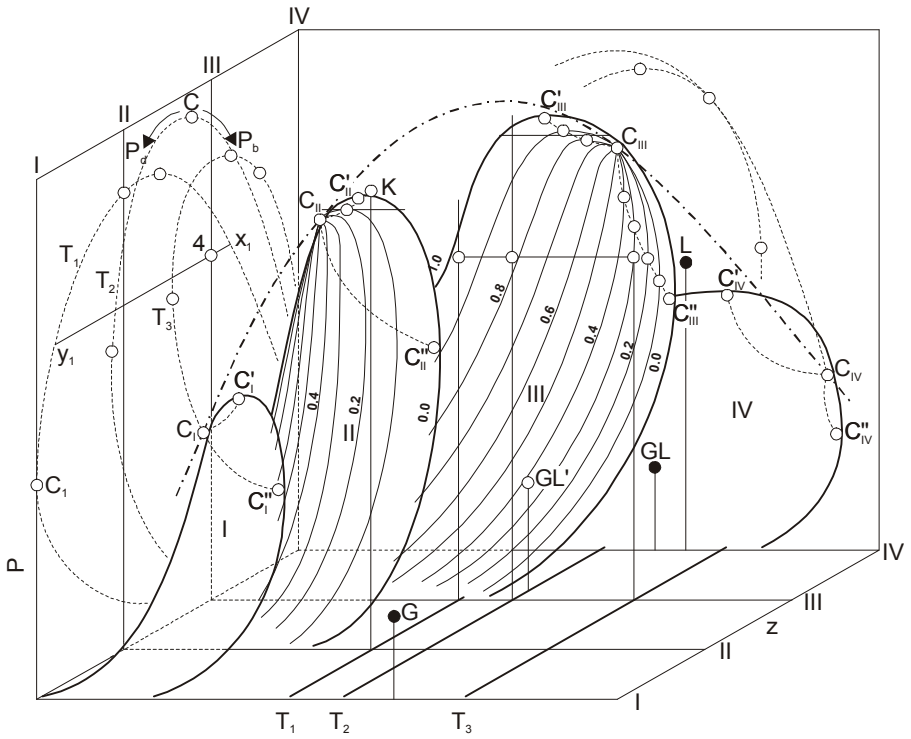

Figure 2.24: Phase equilibrium surface of oil/natural gas systems (from GYULAY, 1967)

Chapter 3

Equations of State

The preliminary chapter included graphical illustrations of equilibrium surfaces and their normal projections into the *(p,T), (p,V), (p,z)* etc. planes. The application of such diagrams enable the determination of the respective volume for certain states defined by the corresponding pressure *p* and temperature *T*. However, a pure graphical application of the state functions is not very practical and - on top of that - impossible for multi-component systems. This aspect obviously makes a mathematical consideration of these problems necessary.

On the basis of Eq. 2.1, the following relation regarding the *p, V, T*-data is valid in case of any chemically homogeneous phase:

$$V = V(p, T)\,. \tag{3.1}$$

In this context, V must be defined as the volume of one mole (intensive property). In case of a 2-phase system:

$$n = n_{liq} + n_{vap}\,, \tag{3.2}$$

and therefore

$$nV_t = n_{liq}V_{liq} + n_{vap}V_{vap}\,, \tag{3.3}$$

where

V_t: mole volume of the system
V_{liq}: mole volume of the liquid phase
V_{vap}: mole volume of the vapor phase
n: number of moles in the system
n_{liq}: number of moles in the liquid phase
n_{vap}: number of moles in the vapor phase.

If phase equilibrium is given, the phases can be regarded as separate thermodynamic systems. If a phase - may be the liquid - phase consists of *k* components, the corresponding equation of state may be written as follows:

$$F(p,\ V,\ T,\ x_1, x_2, \ldots x_p) = 0\,, \tag{3.4}$$

or

$$V = V(p, T, x_1, x_2, \ldots x_k)\,, \tag{3.5}$$

where x_i is defined as the mole fraction of the component i in the (liquid) phase. Considering the mole fractions, the so called "constraint equation" is valid:

$$\sum_{i=1}^{k} x_i = 1\,. \tag{3.6}$$

In various cases of even practical interests, a multi-component phase behaves as an ideal mixture and the volumes are strictly additive. If V_i is defined as the mole volume of component i in the phase, the mole volume of the phase will result in

$$V = \sum_{i=1}^{k} x_i V_i\,. \tag{3.7}$$

If Eq. 3.7 is valid, the enthalpy of the system must be generally considered additive. This means that the enthalpy of the system is equal to the sum of the enthalpies of the single components. In this case, no thermal effect will take place during the mixing procedure. Put into other words: The mixing energy will be zero.

Regarding Eq. 3.6 in discussing Eq. 3.5, it is obvious that V is a function of 2 + (k - 1) = k + 1 variables. It is impossible to approximate the equilibrium surface for the entire (*p, V, T, x_k*)-space by one single equation of state. Therefore some procedure bit by bit is necessary.

3.1 Change of State at Low Compressibility

The expansion of Eq. 3.1 - or just the same of Eq. 3.5 at constant composition - into a TAYLOR-Series leads to

$$\begin{aligned} V(p, T) = V(p_o, T_o) + \left(\frac{\partial V}{\partial p}\right)_T (p - p_o) + \frac{1}{2}\left(\frac{\partial^2 V}{\partial p^2}\right)_T (p - p_o)^2 + \\ + \left(\frac{\partial V}{\partial T}\right)_p (T - T_o) + \frac{1}{2}\left(\frac{\partial^2 V}{\partial T^2}\right)_p (T - T_o)^2 + \ldots\ldots \end{aligned} \tag{3.8}$$

By assuming that the higher derivations are negligible, Eq. 3.8 may be truncated to

$$V(p,T) = V_o\left[1 + \frac{1}{V_o}\left(\frac{\partial V}{\partial p}\right)_T (p - p_o) + \frac{1}{V_o}\left(\frac{\partial V}{\partial T}\right)_p (T - T_o)\right], \tag{3.9}$$

where

$$V_o = V(p_o, T_o).$$

Considering the Eq. 2.4 and Eq. 2.5, Eq. 3.9 may be transformed to

$$V(p, T) = V_o[1 - c(p - p_o) + \beta(T - T_o)], \tag{3.10}$$

where

c : isothermal compressibility

β : cubic expansion coefficient

Eq. 3.10 can at best be applied for fluids in a 1-phase state. Experience and practice have shown that the cubic equations of state are most sufficient and beneficial for calculating the state of gases and of 2-phase systems. Of course, there may exist equations which approximate the measured values more accurately. Anyway, the constants included in these equations are not always given. Therefore, only the cubic equations of state, particularly the PENG-ROBINSON equation, will be discussed in this textbook. In doing so, the proceedings of generalization in derivating this equation of state will be elucidated.

3.2 Equation of State of Perfect and Real Fluids

A fluid is defined as perfect, if the intermolecular forces are negligible.

Then for a molar system:

$$pV = RT, \tag{3.11}$$

where R is defined as “universal gas constant” and

$R = 8.31434\ J/mole\ K.$

The compressibility factor Z is defined as

$$Z = \frac{pV}{RT} \tag{3.12}$$

or

$$Z = \frac{V_{actual}}{V_{ideal}}, \tag{3.13}$$

respectively.

For ideal gases, the factor Z equals 1. For real gases, Z is a state variable and depends on the pressure, the temperature and the composition. The critical point is defined by the pressure p_c, temperature T_c, and specific volume V_c and may be determined experimentally for 1-component systems.

The critical compressibility factor, Z_c, can be evaluated by substituting the critical data p_c, T_c and V_c into Eq. 3.12:

$$Z_c = \frac{p_c V_c}{R T_c}. \tag{3.14}$$

Example 3.1

Evaluation of a Z-factor from laboratory data. A cylinder with volume of 0.075 m^3 has been filled with a gas under atmospheric pressure and at a temperature of 90.5°C. Then the volume of the cylinder has been isothermally reduced to 0.00035 m^3 (volume reduction in consequence of mercury insertion). After the volume reduction, the pressure has been recorded as 13.79 MPa.

If the gas would show an ideal behavior at 90°C and 13.79 MPa, the specific volume could be calculated by

$$P_1 V_1 = P_2 V_2$$

and so

$$V_2 = V_1 \frac{p_1}{p_2},$$

$$V_2 = 75 \times 10^{-3} \frac{101 \times 10^{-3}}{1379 \times 10^{2}} = 55 \times 10^{-5}\ m^3 .$$

By use of Eq. 3.13 and considering the measured volume amounting to 0.00035 m^3:

$$Z = \frac{35 \times 10^{-5}}{55 \times 10^{-5}} = 0.63$$

3.3 Cubic Equations of State

If the pressure of any gaseous system is low, the ideal gas equation remains sufficient to describe the volumetric behavior. In the year 1873, VAN DER WAALS deducted the first equation of state which is able - up to a certain degree - to describe the continuity from gaseous to the liquid state:

$$\left(p + \frac{a}{V^2}\right)(V - b) = RT. \tag{3.15}$$

a and b are substance specific constants. b can be interpreted as the inherent volume of the molecules which is not available for the thermal motion of the molecules. The term a/V^2 regards the pressure reduction in consequence of intermolecular attraction.

Eq. 3.15 may also be written in the following form:

$$p = \frac{RT}{(V - b)} - \frac{a}{V^2}. \tag{3.16}$$

Figure 3.1 illustrates the VAN DER WAALS isotherms in the vicinity of the critical point. The dotted section of the isotherms represents the data which are predicted by using the VAN DER WAALS equation. Obviously, Eq. 3.16 cannot predict the real behavior of the system during the vaporization, respectively condensation. The real behavior is shown by the straight full line $\overline{BD}$ inside the 2-phase region.

The cubic equations of state, which have been formulated by REDLICH and KWONG (1949), SOAVE (1972), and PENG and ROBINSON (1976), have achieved much better results.

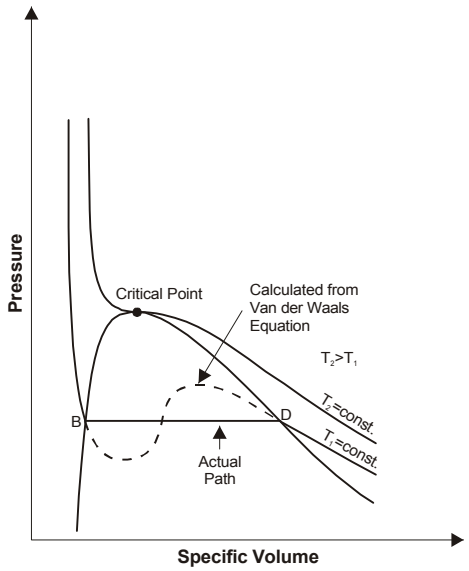

Figure 3.1: The VAN DER WAALS isotherms near the critical point

The REDLICH-KWONG equation is given as

$$p = \frac{RT}{(V-b)} - \frac{a}{V(V+b)}, \tag{3.17}$$

where b again is a substance specific constant. Anyway. a is now a function of the temperature. It is useful to write the parameter a as follows:

$$a = a' f(T), \tag{3.18}$$

where a' is constant. The original REDLICH-KWONG equation included

$f(T) = T^{-0.5}$.

By multiplication of Eq. 3.17 with

$V(V+b)(V-b)/p$

and after arrangement of V corresponding to its order of power:

$$V^3 - \frac{RT}{p}V^2 + \left(\frac{a}{p} - \frac{bRT}{p} - b^2\right)V - \frac{ab}{p} = 0. \tag{3.19}$$

At the critical point $(V = V_c)$:

$$(V-V_c)^3 = V^3 - 3V_c V^2 + 3V_c^2 V - V_c^3 = 0. \tag{3.20}$$

The comparison of Eq. 3.19 and Eq. 3.20 leads to

$$3V_c = \frac{RT_c}{p_c}, \tag{3.21}$$

$$3V_c^2 = \frac{a_c}{p_c} - \frac{bRT_c}{p_c} - b^2, \tag{3.22}$$

$$V_c^3 = \frac{a_c b}{p_c}, \tag{3.23}$$

where

$$a_c = a' f(T_c). \tag{3.24}$$

Substitution of Eq. 3.21 and Eq. 3.23 into Eq. 3.22 results in

$$3V_c^2 = \frac{V_c^3}{b} - 3bV_c - b^2, \tag{3.25}$$

or after rearrangement, in

$$b^3 + 3b^2 V_c + 3bV_c^2 + V_c^3 = 2V_c^3, \tag{3.26}$$

$$(b + V_c)^3 = 2V_c^3, \tag{3.27}$$

$$b = (2^{1/3} - 1)V_c. \tag{3.28}$$

Furthermore, Eq. 3.28 and Eq. 3.21 can be combined to

$$b = \frac{(2^{1/3} - 1)RT_c}{3p_c} = \Omega_b \frac{RT_c}{p_c}. \tag{3.29}$$

Inserting Eq. 3.21 and Eq. 3.23 into Eq. 3.29:

$$a_c = \frac{(RT_c)^2}{9(2^{1/3} - 1)p_c} = \Omega_a \frac{(RT_c)^2}{p_c}. \tag{3.30}$$

The constants Ω_b and Ω_a have the following numerical values:

$\Omega_b = 0.08664$,

$\Omega_a = 0.42748$.

From Eq. 3.18 and Eq. 3.24:

$$a = a_c \frac{f(T)}{f(T_c)} = a_c \alpha. \tag{3.31}$$

It is obvious that $\alpha = 1$, if $T = T_c$.

The substitution of $V = ZRT/p$ into the Eq. 3.19 and the arrangement of Z corresponding to its order of power results in

$$\left(\frac{ZRT}{p}\right)^3 - \frac{RT}{p}\left(\frac{ZRT}{p}\right)^2 + \left(\frac{a}{p} - \frac{bRT}{p} - b^2\right)\frac{ZRT}{p} - \frac{ab}{p} = 0. \tag{3.32}$$

Therefore:

$$Z^3 - Z^2 + \left[\frac{ap}{(RT)^2} - \frac{bp}{RT} - \frac{b^2 p^2}{(RT)^2}\right]Z - \frac{ap}{(RT)^2}\frac{bp}{RT} = 0 \tag{3.33}$$

or

$$Z^3 - Z^2 + (A - B - B^2)Z - AB = 0\,, \tag{3.34}$$

where

$$A = \frac{ap}{(RT)^2} \tag{3.35}$$

and

$$B = \frac{bp}{RT}. \tag{3.36}$$

The substitution of Eq. 3.29 and Eq. 3.30 into Eq. 3.35 and Eq. 3.36 leads to

$$A = 0{,}42748\left(\frac{p_r}{T_r^2}\right)\alpha \tag{3.37}$$

and

$$B = 0.08664\,\frac{p_r}{T_r}. \tag{3.38}$$

In the original REDLICH-KWONG equation:

$$f(T) = T^{-0.5}\,, \tag{3.39}$$

and so

$$\alpha = T_r^{-0.5}\,. \tag{3.40}$$

Eq. 3.34 includes only two parameters which are p_c and T_c. Please note that the ideal gas equation contains no substance-specific parameters. Since the Redlich-Kwong cubic equations of state consider these two substance-specific parameters, it has improved the calculation of *PVT*-properties in a fundamental way. Anyway, the increasing yield of experimental data has more and more indicated that the behavior of many liquids with a non-spherical molecule structure deviates greatly from the predicted one. This made the introduction of a third factor necessary.

Beginning with the year 1951 (MEISSNER and SEFERIAN), several proposals for a third parameter have been made. The so called “acentric factor”, ω, has become the one with greatest acknowledgement:

$$\omega = -\left(lgp_r^s + 1\right) \quad at\ T_r = 0{,}7\,, \tag{3.41}$$

where $p_r^s = p^s / p_c$ is the reduced boiling point pressure.

The equation of state from SOAVE (1972) only differs from the REDLICH-KWONG equation with respect to the definition of the factor

$$\alpha^{0.5} = 1 + (0.48 + 1.574\omega - 0.176\omega^2)(1 - T_r^{0.5})\,. \tag{3.42}$$

The weakness of all these equations ranging from the original REDLICH-KWONG equation to all its modifications (including the SOAVE equation) is the fact of an universal unrealistic $\boldsymbol{Z}_c$ factor of $1/3$. Moreover, the prediction of liquid density is combined with large errors.

Improved approximation has been achieved with the PENG-ROBINSON equation:

$$p = \frac{RT}{V-b} - \frac{a}{V(V+b) + b(V-b)}, \tag{3.43}$$

where a is given by Eq. 3.18 and b is further a substance specific constant.

Just as in case of the REDLICH-KWONG equation, the following terms and equations can be obtained:

$$V^3 - \left(\frac{RT}{p} - b\right)V^2 + \left(\frac{a}{b} - \frac{2bRT}{p} - 3b^2\right)V - \left(b\frac{a}{p} - \frac{RT}{p}\,b - b^2\right) = 0\,, \tag{3.44}$$

$$V_c = 0.307\,\frac{RT_c}{p_c}, \tag{3.45}$$

$$b = 0.07796\,\frac{RT_c}{p_c}, \tag{3.46}$$

$$a = a_c\alpha\,, \tag{3.47}$$

$$a_c = 0.457235\,\frac{(RT_c)^2}{p_c}, \tag{3.48}$$

$$Z^3 - (1-B)Z^2 + (A - 2B - 3B^2)Z - -AB - B^2 - B^3 = 0, \tag{3.49}$$

$$A = 0.457325 \cdot \left(\frac{p_r}{T_r^2} \right) \alpha , \tag{3.50}$$

$$B = 0.07796 \cdot \frac{p_r}{T_r} , \tag{3.51}$$

$$. \alpha^{0.5} = 1 + m(1 - T_r^{1/2}) \tag{3.52}$$

$$m = 0.3676 + 1.54226\omega - 0.26992\omega^2 \tag{3.53}$$

or for the modification of 1979, m is given by

$$m = \begin{cases} 0{,}37464 + 1{,}54226\omega_i - 0{,}26992\omega_i^2, \text{ if } \omega \le 0{,}4 \\ 0{,}3796 + 1{,}485\omega_i - 0{,}1644\omega_i^2 + 0{,}01667\omega_i^3 \quad , \text{if } \omega > 0{,}4 \end{cases} \tag{3.54}$$

Analogies between Eq. 3.44 to Eq. 3.52 on the one side and between Eq. 3.19, Eq. 3.21, Eq. 3.29 to Eq. 3.31, Eq. 3.34 to Eq. 3.38, and Eq. 3.42 on the other side are obvious. The universal critical Z-factor of the PENG-ROBINSON equation results in 0.307 which is much better than $1/3$ but still far away from reality. Anyway, the calculated fluid densities are much more accurate than the ones calculated by the equations of state previously discussed.

Eq. 3.16, Eq. 3.17, and Eq. 3.43 have been established for pure substances. The extension for multi-component systems requires the calculation of the respective data of the pure components and mixing rules in order to get the parameters of the mixture.

The mixing rule for the parameter b, which is included in the equations of REDLICH-KWONG, SOAVE and PENG-ROBINSON, is universally defined as an arithmetic average by using

$$b = \sum_{i=1}^{k} x_i b_i . \tag{3.55}$$

For the temperature-dependent coefficient a, different mixing rules exist and are presented below.

REDLICH-KWONG:

$$a = \left[\sum_{i=1}^{k} x_i a_i^{0.5} \right]^2 . \tag{3.56}$$

where a_i can be calculated on the basis of the critical data of each component by using Eq. 3.30 and Eq. 3.40 into Eq. 3.31.

SOAVE:

$$a = \sum_{i=1}^{k} \sum_{j=1}^{k} x_i x_j (a_i a_j)^{0.5} (1 - k_{ij}), \tag{3.57}$$

where a_i and a_j, respectively, can be evaluated by Eq. 3.30 and Eq. 3.42.

PENG-ROBINSON:

$$a = \sum_{i=1}^{k} \sum_{j=1}^{k} x_i x_j (a_i a_j)^{0.5} (1 - k_{ij}), \tag{3.58}$$

where a_i is defined by Eq. 3.48 and Eq. 3.52.

The mixing rules used by SOAVE and PENG-ROBINSON consider the binary interaction between the molecules of the components *i* and *j*. In Eq. 3.55 and Eq. 3.56, the terms k_{ij} are **binary interaction coefficients** which are assumed to be independent of pressure and temperature.

Values of the binary interaction coefficients must be obtained by fitting the equation of state to gas-liquid equilibria data for each binary mixture. They have different values for each binary pair and also take on different values for each equation of state.

Obviously, Eq. 3.55 and Eq. 3.56 reduce to the form of Eq. 3.54 if all binary interaction coefficients are zero.

Another possibility of obtaining this coefficient - if no data are available - is by mean of matching the phase behavior of multi-component systems.

Example 3.2

Calculation of the pressure by use of the PENG-ROBINSON equation of state. A laboratory cell at temperature of 100 ^{o}C with volume of 0.00025 m^3 contains 0.25 mole of gas. The composition of the system, the critical data and the acentric factors of the components are tabled below.

Component	Composition y_i	Critical Data $T_{c,i}$ ^oK	$p_{c,i}$ MPa	Acentric Factor ω_i
C_1	0.75	190.6	4.60	0.0115
C_2	0.20	305.4	4.88	0.0908
n - C_4	0.05	425.2	3.80	0.1928

First, the parameters *b* and *a* must be calculated for each component.

For methane from Eq. 3.46:

$$b_1 = 77796 \times 10^{-6} \frac{831434 \times 1907 \times 10^6}{463 \times 10^8} = 2677 \times 10^{-5},$$

from Eq. 3.48:

$$a_{c,1} = 457235 \times 10^{-6} \frac{(831434 \times 1907 \times 10^6)^2}{463 \times 10^8} = 0.2494,$$

from Eq. 3.52 by inserting the acentric factor for methane

$$\omega_1 = 0.0115$$

and the reduced temperature of methane

$$T_{r,1} = \frac{273.15}{190.6} = 1.958:$$

$$\alpha_1^{0.5} = 0.8954$$

and thus

$$\alpha_1 = 0.8018,$$

and from Eq. 3.47:

$$\alpha_1 = 0.2494 \times 0.8018 = 0.1999.$$

Correspondingly to the calculations for methane, the parameters of ethane and n-butane were evaluated. They are tabled below.

Component	b_i	$a_{c,i}$	α_i	a_i
C_1	2.677 E-5	0.2494	0.8018	0.1999
C_2	4.048 E-5	0.6042	1.0010	0.6045
n - C_4	7.245 E-5	1.5050	1.2130	1.8260

The parameter *b* can be calculated by use of Eq. 3.53:

$$b = 0.75 \times 2.67\text{E} - 5 + 0.20 \times 4.\ 048\text{E} - 5 + 0.05 \times 7.245\text{E} - 5$$

$$b = 3.\ 180\text{E} - 5\ .$$

To calculate the coefficient *a* by use of Eq. 3.56, the interactive coefficients, K_{ij}, must be known. They are given below:

	C_1	C_2	n - C_4
C_1	0.0000 E+0	0.2648 E-2	0.1464 E-1
C_2	0.2648 E-2	0.0000 E+0	0.4904 E-2
n - C_4	0.1464 E-1	0.4904 E-2	0.0000 E+0

$$\begin{aligned}
a = {} & 0.75 \times 0.75(0.1999 \times 0.1999)^{0.5}(1 - 0.000000) + \\
& + 0.75 \times 0.20(0.1999 \times 0.6045)^{0.5}(1 - 0.002648) + \\
& + 0.75 \times 0.05(0.1999 \times 1.8260)^{0.5}(1 - 0.014640) + \\
& + 0.20 \times 0.75(0.6045 \times 0.1999)^{0.5}(1 - 0.002648) + \\
& + 0.20 \times 0.20(0.6045 \times 0.6045)^{0.5}(1 - 0.000000) + \\
& + 0.20 \times 0.05(0.6045 \times 1.8260)^{0.5}(1 - 0.004904) + \\
& + 0.05 \times 0.75(1.8260 \times 0.1999)^{0.5}(1 - 0.014640) + \\
& + 0.05 \times 0.20(1.8260 \times 0.6045)^{0.5}(1 - 0.004904) + \\
& + 0.05 \times 0.05(1.8260 \times 1.8260)^{0.5}(1 - 0.000000) = 0.3108
\end{aligned}$$

Now the pressure can be calculated through Eq. 3.43 and by inserting

$$V = \frac{0.00025}{0.25} = 0.001\ m^3/mole\ ,$$

$$T = 373.15\ K\ ,$$

$$R = 8.31434\ J/K \times mole$$

$$b = 3.18 \times 10^{-5}$$

and

$$a = 0.3108 .$$

The calculation procedure results in

$$p = 2.328\ MPa$$

Example 3.3

Calculation of the density of methane by use of the PENG-ROBINSON equation of state. 2.0 kg methane *(MC_1 = 16 kg k/mol*e is hold at temperature of *305.12 K* and at pressure of *9.26 MPa*. The critical data and the acentric factor of methane are known as

$$T_c = 190.6\ K ,$$

$$p_c = 4.63\ MPa ,$$

$$\omega = 0.0115 .$$

First, the parameters *a* and *b* have to be calculated.

From Eq. 3.46:

$$b = 0.077796 \frac{8.31434 \times 190.6}{4.63 \times 10^6} = 2.662 \times 10^{-5} .$$

From Eq. 3.48:

$$a_c = 0.457235 \frac{(8.31434 \times 190.6)^2}{463 \times 10^4} = 0.248 .$$

From Eq. 3.52 by inserting the acentric factor and the reduced temperature of the system

$$T_{r,1} = \frac{305.12}{190.6} = 1.601 ,$$

$$\alpha^{0.5} = 0.8954$$

and thus

$$\alpha = 0.8018 ,$$

and from Eq. 3.47:

$$a = 0.248 \times 0.8018 = 0.1988 .$$

Now the mole volume of methane at the given state variables has to be evaluated through Eq. 3.44. To solve this cubic equation of

state, the CARDAN equation is applied for

$$x^3 + rx^2 + sx + t = 0$$

where

$$r = -\left(\frac{RT}{p} - b\right),$$

$$s = \left(\frac{a}{p} - \frac{2bRT}{p} - 3b^2\right)$$

and

$$t = -b\left(\frac{a}{p} - \frac{RT}{p}b - b^2\right).$$

The calculation of r, s and t result in

$$r = -0.2473 \times 10^{-3},$$

$$s = 0.4755 \times 10^{-8},$$

and

$$t = -0.3585 \times 10^{-12}.$$

By substitution of

$$x = y - \frac{r}{3},$$

the formula

$$x^3 + rx^2 + sx + t = 0$$

is reduced to

$$y^3 + py + q = 0$$

where

$$p = \frac{3s - r^2}{3}$$

and

$$q = \frac{2r^3}{27} - \frac{rs}{3} + t.$$

The calculation of p and q result in

$$p = -1.563 \times 10^{-8}$$

and

$$q = -1.089 \times 10^{-12}.$$

The discriminant D is defined as

$$D = \left(\frac{p}{3}\right)^3 + \left(\frac{q}{2}\right)^2$$

and thus

$$D = 1.53776 \times 10^{-25}.$$

Based on the relationships

$$u = \sqrt[3]{-\frac{q}{2} + \sqrt{D}},$$

$$v = \sqrt[3]{-\frac{q}{2} - \sqrt{D}}$$

and

$$y = u + v,$$

the mole volume can be calculated through

$$x = y - \frac{r}{3}:$$

$$u = 9.7800 \times 10^{-5},$$

$$v = 5.3272 \times 10^{-5},$$

$$y = 1.5107 \times 10^{-4}$$

and thus

$$V = 2.3350 \times 10^{-4}\ m^3/mole,$$

and

$$\rho = \frac{m}{nV} = \frac{M}{V} = 68.522\ kg/m^3.$$

3.4 Virial Equation of State

All cubic equations of state mentioned above are more or less empirical or at best semi-theoretical. However, they are obviously qualified for practical application.

In contrast, the virial equation of state has some theoretical background in statistical mechanics. However, the form of an infinite series concerning the volume is not very appropriate for practical application.

The pressure is expressed as

$$p = RT\left(\frac{1}{V} + \frac{B}{V^2} + \frac{C}{V^3}\ldots\right). \tag{3.59}$$

The virial coefficients B, C etc. are solely a function of temperature. Sometimes Eq. 3.57 is applied for the calculation of gaseous states (e.g. natural gas) by considering only the first two or three terms (depending on the availability of the virial coefficients).

If V is substituted into Eq. 3.57 according to the gas law by $Z\,RT/p$, then:

$$Z = 1 + \frac{Bp}{ZRT} + \frac{Cp^2}{(ZRT)^2} + \ldots. \tag{3.60}$$

The second virial coefficient B can be shown to be the slope of isotherms on a plot of $Z = Z(p)$ at $p = 0$. When p approaches zero, the third term in Eq. 3.58 may be neglected so that

$$B = ZRT \lim_{p \to 0}\left(\frac{Z-1}{p}\right). \tag{3.61}$$

Since also Z becomes *zero* as p goes to zero, de l'Hospital's rule can be applied resulting at constant T in

$$B = RT \lim_{p \to 0}\left(\frac{\partial Z}{\partial p}\right)_T. \tag{3.62}$$

Eq. 3.60 implies that the 2. virial coefficient vanishes at the BOYLE-temperature. The BOYLE temperature is defined as the temperature above which Z-values become greater than *1* for all pressures.

Chapter 4

Calculation of Phase Equilibria

4.1 Mixtures

4.1.1 Definitions

In case of thermodynamical phase equilibrium of a multi-component system, all phases are - in physical terms - homogeneous mixtures. Vaporized compounds are always mixable in all relations, independent of their chemical characteristics. Therefore, only one vapor phase exists.

Compounds existing in a liquid phase are only mixable in all relations if they are chemically similar. Since hydrocarbons - especially whose which belong to the same homologous series - exhibit such chemical conformity, their mixtures will be physically homogeneous, independent of the composition of the mixture.

The composition of the system and its phases are specified by mole fractions. The mole fraction of the component *i* is given by the ratio between its mole number, n_i, and the total mole number in the system (in the respective phase), *n*. The sum of all mole fractions equals 1. In the following, the different mole fractions are marked by

z_i: mole fraction of the component *i* in the total system,

x_i: mole fraction of the component *i* in the liquid phase,

y_i: mole fraction of the component *i* in the vapor phase,

so that in the system in total

$$z_i = \frac{n_i}{\sum_{i=1}^{k} n_i}, \tag{4.1}$$

$$x_i = \left(\frac{n_i}{\sum_{i=1}^{k} n_i} \right)_{liq}, \tag{4.2}$$

$$y_i = \left(\frac{n_i}{\sum_{i=1}^{k} n_i} \right)_{vap}. \tag{4.3}$$

If a multi-component system is in the state of thermodynamic phase equilibrium, the distribution of the component *i* among the vapor and the liquid phase is characterized by its distribution coefficient, the so called "*K*-factor":

$$K_i = \frac{y_i}{x_i}. \tag{4.4}$$

The numerical value of K_i depends on the state of the system. Accordingly, the composition of the phases will change at any variation in state.

4.1.2 K-Factors

Ideal liquid mixtures have the property of being met by RAOULT's law so that

$$x_i = \frac{p_i}{p_i^o}, \tag{4.5}$$

where

p_i: partial pressure of the component *i,*

p_i^o: tension of component *i* as a single-component system,

x_i: mole fraction of component *i* in the liquid phase.

The total pressure of the system adds up to

$$p = \sum_{i=1}^{k} p_i = \sum_{i=1}^{k} x_i p_i^0. \tag{4.6}$$

If a vapor phase exhibits perfect behavior, DALTON's law can be applied and

$$y_i = \frac{p_i}{p}. \tag{4.7}$$

The combination of Eq. 4.5 and Eq. 4.7 results in

$$y_i p = x_i p_i^o, \tag{4.8}$$

or using the definition Eq. 4.3:

$$K_{i(id)} = \frac{y_i}{x_i} = \frac{p_i^o}{p}. \tag{4.9}$$

The subscript *id* should show that Eq. 4.9 is only valid under ideal conditions, which means at low pressure and at Z = 1. For real systems the concept of "partial pressures" had to be replaced by the fugacity as a measure of the real volatility of a given compound at a defined state. Note, that a state is defined by pressure, temperature and composition of the system. Consequently, the fugacity is also a functions of those state variables. Two phases are in equilibrium if the molecules from both phases have the same tendency to change their states, also their fugacities in both phases are equal:

$$f_{iV} = f_{iL}. \tag{4.10}$$

To express the fugacity by introducing a "fugacity coefficient" is a formal step, and serves to express the *K*-factor with this concept:

$$f_{iL} = x_i \phi_{lL} p,$$

$$f_{iV} = y_i \phi_{lL} p,$$

and so

$$K_i = \frac{y_i}{x_i} = \frac{\phi_{iV}}{\phi_{iL}}. \tag{4.11}$$

Figure 4.1: Fugacity of natural gases (from Brown, 1945)
Figure 4.2: Ideal and real K-factors of n-butane at 60°C]

The fugacity coefficients can be calculated from the equation of states. For example from the PENG-ROBINSON equation:

$$\ln\phi_i = \frac{b_i}{b}(Z-1) - \ln(Z-B) - \frac{A}{2\sqrt{2}B}\left[\frac{2\sum_{j=1}^{k} x_j a_{ij}}{a} - \frac{b_i}{b}\right] \ln\left(\frac{Z+2{,}414B}{Z-0.414\mathrm{B}}\right), \tag{4.12}$$

where

$$a_{ij} = a_i^{0,5}\, a_j^{0,5}\, (1-\delta_{ij}). \tag{4.13}$$

4.2 Composition of Phases in Equilibrium

4.2.1 Definitions

If the system at a given pressure, temperature and composition is in a liquid-vapor phase equilibrium, the following must be valid (on the basis of an overall and particular material balance, respectively):

$$n = n_{liq} + n_{vap}, \tag{4.14}$$

$$z_i n = x_i n_{liq} + y_i n_{vap}; \qquad (i = 1, \ldots, \mathrm{k}), \tag{4.15}$$

where

n: total mole number of the system,

n_{liq}: mole number of the liquid phase,

n_{vap}: mole number of the vapor phase,

x_{i}: mole fraction of component i in the liquid phase,

y_{i}: mole fraction of component i in the vapor phase,

z_{i}: mole fraction of component i in the system.

After substitution of Eq. 4.9 into Eq. 4.14 and after rearrangement, the following is valid:

$$x_i = \frac{z_i n}{n_{liq} + n_{vap} K_i}, \tag{4.16}$$

$$y_i = \frac{z_i n}{n_{liq}/K_i + n_{vap}}. \tag{4.17}$$

If the numerical value for n_{liq} and has $\mathrm{n_{vap}}$ have been chosen correctly, the calculations of x_{i} and y_{i}*(i = 1,...k)* (Eq. 4.15 and Eq. 4.16) result in

$$\sum_{i=1}^{k} x_i = \sum_{i=1}^{k} \frac{z_i n}{n_{liq} + n_{vap} K_i} = 1, \tag{4.18}$$

and

$$\sum_{i=1}^{k} y_i = \sum_{i=1}^{k} \frac{z_i n}{n_{liq}/K_i + n_{vap}} = 1. \tag{4.19}$$

Example 5.1 will demonstrate that it is possible to use the Eq. 4.17 and Eq. 4.18 for

iterative calculation purposes which result in the evaluation of the phase compositions at given *p, T* and system composition.

If $n = 1$, Eq. 4.13 gives

$$n_{vap} = 1 - n_{liq},$$

and Eq. 4.17 becomes

$$\sum_{i=1}^{k} x_i = \sum_{i=1}^{k} \frac{z_i}{n_{liq} + K_i(1 - n_{liq})} = 1. \tag{4.20}$$

Eq. 4.19 elucidates that

n_{liq} must be chosen larger in the following iteration if $\sum x_i > 1$,

n_{liq} must be chosen smaller in the reverse case of $\sum x_i < 1$.

Example 4.1

Determination of the gas and liquid phase compositions at $p = 14$ MPa and $T = 92\ ^{\circ}C$ through an iterative calculation procedure. The actual composition of the hydrocarbon system is tabled below.

FIRST ITERATION: $n_{\text{liq}} = 0.790$

$n_{\text{vap}} = 0.210$

n_{liq} must be chosen smaller in the following iteration because of

Component	System Composition z_i	K-Factor K_i	$n_{vap}K_i$	$nl_{iq}+n_{vap}K_i$	$x_i = \frac{z_i}{n_{liq} + n_{vap}K_i}$
C_1	0.4404	2.85	0.598	1.388	0.3173
C_2	0.0432	1.17	0.246	1.036	0.0417
C_3	0.0405	0.68	0.143	0.933	0.0434
C_4	0.0284	0.41	0.086	0.876	0.0324
C_5	0.0174	0.24	0.051	0.841	0.0207
Σ	1.0000				0.9963

Component	System Composition z_i	K-Factor K_i	$n_{vap}K_i$	$nl_{iq}+n_{vap}K_i$	$x_i = \frac{z_i}{n_{liq} + n_{vap}K_i}$
C_6	0.0290	0.15	0.031	0.821	0.0353
C_{7+}	0.4011	0.01	0.003	0.793	0.5055
Σ	1.0000				0.9963

$\sum x_{i<1}$.

SECOND ITERATION: n_{liq} = 0.776

n_{vap} = 0.224

THIRD ITERATION: n_{liq} = 0.778

n_{vap} = 0.222

Component	Iteration II $x_i = \frac{z_i}{n_{liq} + n_{vap}K_i}$	Iteration III $x_i = \frac{z_i}{n_{liq} + n_{vap}K_i}$	Iteration III $y_i = \frac{z_i}{n_{liq}/K_i + n_{vap}}$
C1	0.3114	0.3123	0.8896
C2	0.0416	0.0416	0.0487
C3	0.0436	0.0436	0.0296
C4	0.0327	0.0327	0.0134
C5	0.0210	0.0209	0.0051
C6	0.0358	0.0357	0.0054
C7+	0.5145	0.5132	0.0082
Σ	1.0006	0.9999	1.0000

At the bubble point of the system, the amount of vapor is infinitesimal small and thus

$n_{vap} = 0$, $n_{liq} = n$ and $x_i = z_i$.

Eq. 4.18 then becomes

$$\sum_{i=1}^{k} \frac{z_i n}{n_{liq}/K_i + n_{vap}} = \sum_{i=1}^{k} K_i z_i = \sum_{i=1}^{k} K_i x_i = 1. \tag{4.21}$$

Example 4.2 illustrates the iterative process of calculating the bubble point pressure, p_b, for a given hydrocarbon composition and for a fixed temperature. Naturally, $K_i = K_{i(p)}$ must be known.

In the vicinity of the bubble point, $K_i x_i$ are in a linear relation to pressure. Therefore, linear interpolation can be applied for acceleration purposes.

Example 4.2

Determination of the bubble point pressure of a crude oil. The composition of the system is given in Example 4.1.

Component	System Compos. z_i	1. Assumption p_b = 21 MPa K_i	$y_i = K_i z_i$	2. Assumption p_b = 22.5 MPa K_i	$y_i = K_i z_i$	3. Assumption p_b = 23.2 MPa K_i	$y_i = K_i z_i$
C_1	0.4404	2.1500	0.9469	2.060	0.9072	2.020	0.8896
C_2	0.0432	1.0300	0.0445	1.025	0.0443	1.020	0.0441
C_3	0.0405	0.6720	0.0272	0.678	0.0274	0.680	0.0275
C_4	0.0284	0.4400	0.0125	0.448	0.0127	0.450	0.0128
C_5	0.0174	0.3000	0.0052	0.316	0.0055	0.323	0.0056
C_6	0.0290	0.2150	0.0062	0.230	0.0067	0.239	0.0069
C_{7+}	0.4701	0.0235	0.0094	0.250	0.0100	0.026	0.0104
Σ	1.0000		1.0519		1.0138		0.9969

By interpolation: $p_b = 23$ MPa

At the dew point of the system, the amount of liquid phase is infinitesimal small and thus

$$n_{liq} = 0, n_{vap} = n \quad \text{and} \quad y_i = z_i .$$

From Equation 4.21:

$$\sum_{i=1}^{k} \frac{z_i n}{n_{liq} + n_{vap} K_i} = \sum_{i=1}^{k} \frac{z_i}{K_i} = \sum_{i=1}^{k} \frac{y_i}{K_i} = 1 . \tag{4.22}$$

In analogy of the iterative process demonstrated by Example 4.2 (evaluation of p_b), it is theoretically possible to evaluate the dew point pressure by use of Eq. 4.21 by summing up the y_i / K_i values and by variating the pressure as long as $\Sigma y_i / K_i = 1$.

However, the evaluation of the *K*-factor for heavier components is crucial. Therefore, the calculation of the dew point pressure of hydrocarbon systems by using Eq. 4.21 may be too inaccurate. This notion is mostly used to check the *K*-factors which have been evaluated for certain state conditions.

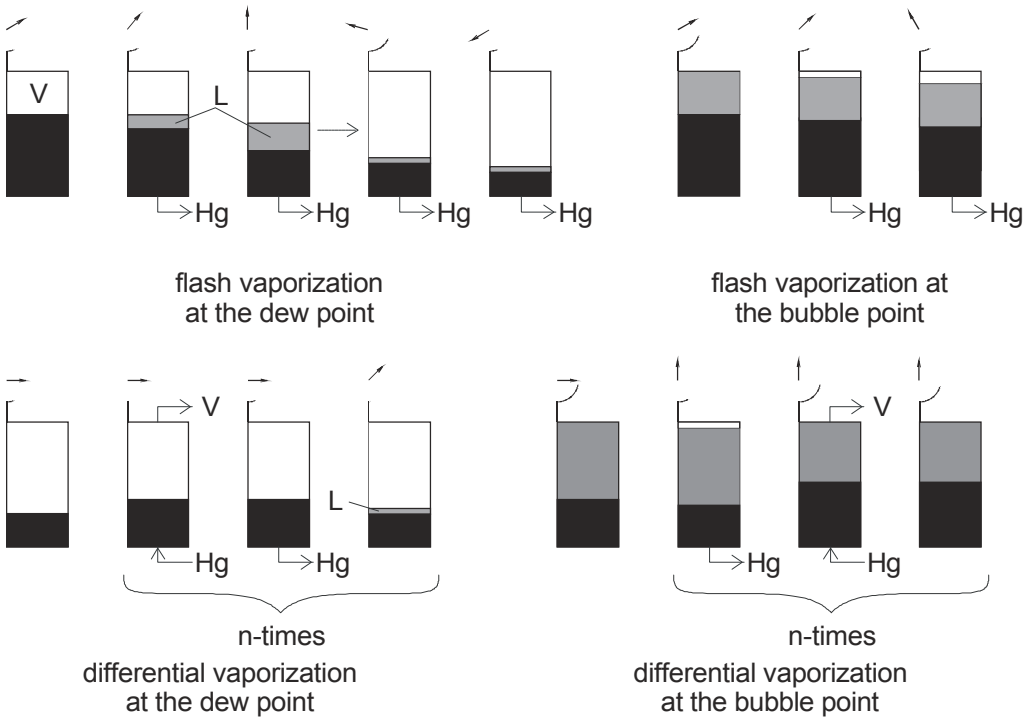

Figure 4.3: Flash and differential vaporization

In evaluating hydrocarbon systems, two characteristic processes are of importance. These are illustrated schematically in Figure 4.3:

- Mass and composition of the system remain constant (closed system). The portions of the phases and their compositions in various states of thermodynamic equilibrium (p and V are variables) are to be evaluated. This process is specified as the "flash vaporization (condensation)".
- Preceding every further change of state, mass and composition of the system are changed in removing one phase - in most cases the vapor phase - as soon as the previous phase equilibrium is achieved (open system). Such a process is called "differential vaporization (condensation)".

In case of a flash process, it is of importance whether the system is signified as liquid at bubble point pressure or as a vapor at dew point pressure. In both cases, the volume increases during an isothermal pressure decrease.

If the temperature of a dry gas system ranges between T_c and the cricondentherm, a condensate will drop out below the dew point. The amount of the condensate will increase up to a certain value as a function of pressure decrease (retrograde condensation). Below this point, further pressure decrease will now effect the vaporization of the condensate.

In case of an undersaturated liquid system, the vapor phase appears below bubble point pressure. At the same time, the liquid volume diminishes. Correspondingly, the oil phase shrinks at decreasing pressure.

The equilibria states appearing at a flash vaporization in series after one another can be calculated independent of one another by Eq. 4.15 to Eq. 4.17 in regard of their phase composition. However, the *K*-factors must always correspond to the given pressure and temperature.

In case of a differential vaporization, some material balance has to be applied. The volume remains constant meanwhile every change in state is connected with a change of the mole number in the system and its composition (open system).

This would correspond to the following reflections: In case of a saturated liquid, the amount of component *i* will decrease by $y_i dn_v$ resulting from the liberation and production of an infinitesimal small amount of gas dn_v, and

$$y_i dn_{vap} = n_{liq} x_i - (n_{liq} - dn_{vap})(x_i - dx_i) . \tag{4.23}$$

Since $y_i = K_i x_i$ and $dn_{vap} = dn_{liq}$, the following is obtained after neglection of the term $dn_{vap} dx_i$:

$$K_i x_i dn_{liq} = x_i dn_{liq} + n_{liq} dx_i . \tag{4.24}$$

Eq. 4.23 cannot be integrated, because K_i is a function of *p*. Therefore, the method of finite differences is often applied. The integral is then substituted by summation formulae. Results have been often proved to correspond with the experimental data in a most accurate way (see Example 4.3).

Example 4.3

Determination of tank oil composition after 3-stage separation on the basis of the system composition in Example 5.1.

FIRST SEPARATOR: p = 3.33 MPa

T = 48.7 °C

n_{liq} = 0.582

n_{vap} = 0.418

Component	Well Stream Composition z_i	K-Factor K_i	Fluids Liquid x_i	Fluids Vapor y_i
C_1	0.4404	8.100	0.1110	0.8991
C_2	0.0432	1.650	0.0339	0.0560
C_3	0.0405	0.590	0.0489	0.0288
C_4	0.0284	0.230	0.0419	0.0096
C_5	0.0174	0.088	0.0281	0.0025
C_6	0.0290	0.039	0.0485	0.0019
C_{7+}	0.4011	0.003*	0.6877	0.0021
$\Sigma =$	1.0000		1.0000	1.0000

*$K_{7+} = 0.15\ K_{C7}$

SECOND SEPARATOR: p = 0.44 MPa

T = 48.7 °C

n_{liq} = 0.844

n_{vap} = 0.156

Component	Feed Composition z_i	K-Factor K_i	Fluids Liquid x_i	Fluids Vapor y_i
C_1	0.1110	60.000	0.0109	0.6530
C_2	0.0339	10.600	0.0135	0.1430
C_3	0.0489	3.400	0.0355	0.1207
C_4	0.0419	1.250	0.0403	0.0504
C_5	0.0281	0.415	0.0309	0.0128
C_6	0.0485	0.170	0.0557	0.0095
C_{7+}	0.6877	0.013*	0.8132	0.0106
$\Sigma =$	1.0000		10000	10000

*$K_{7+} = 0.15\ K_{C7}$

TANK: p = 0.1 MPa

T = 48.7 °C

n_{liq} = 0.9486

n_{vap} = 0.0514

*$K_{7+} = 0.15K_{C7}$

Component	Feed Composition z_i	K-Factor K_i	Fluids Liquid x_i	Fluids Vapor y_i
C_1	0.109	265.0	0.0007	0.1965
C_2	0.0135	46.6	0.0038	0.1885
C_3	0.0355	14.3	0.0210	0.3022
C_4	0.0403	5.35	0.0330	0.1775
C_5	0.0309	1.72	0.0299	0.0513
C_6	0.0557	0.70	0.0566	0.0396
C_{7+}	0.8132	0.052*	0.8550	0.0444
Σ =	1.0000		1.0000	1.0000

One mole reservoir crude oil produced amounts to n_{liq1} x n_{liq2} x n_{liq3} = 0.582 x 0.844 x 0.9486 = 0.466 mol tank oil

4.2.2 Evaluation of *K*-Factors Using Convergence Pressures

As already mentioned, the *K*-factors in real systems not only depend on temperature and pressure, but also on composition. KATZ and HACHMUTH (1937) have been the first to provide for appropriate data of gas/oil-systems. Since then the collection of data has been continuously enlarged.

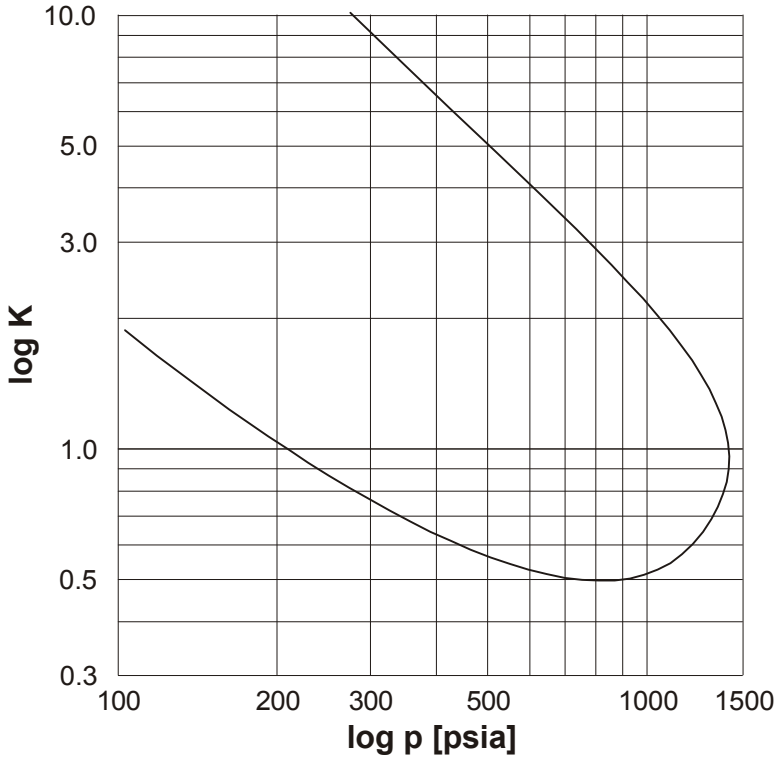

Figure 4.4: K-factors for methane-propane at $T_c = 100\ ^oF$ (from SAGE, LACEY and SCHAAFSMA) (1934)

The most simple relations exist in any 2-component system. Figure 4.4 is a plot of the *K*-factors for the methane-propane system at the critical temperature of the mixture $T_c = 100\ ^oF$. At any pressure - at which the vapor and the liquid phase are in equilibrium - $K > 1$ for the highly volatile component methane. The K-factor decreases with pressure.

On the other side $K<1$ for the less volatile component propane since its concentration in the vapor phase is less than in the liquid. At any isothermal change in state, *K* for the less volatile component propane will equal 1 at two different pressures. One corresponds - just as in case of the highly volatile component - with the critical pressure of the mixture and the other one with the vapor pressure of the pure substance. Above the critical pressure of the system, K-factors have no longer physical meaning.

Generally, the K-factors increase with increasing *T* at constant pressure. However, methane shows some irregular behavior. Its *K*-factor increases with temperature up to a certain limit and decreases beyond that.

Even if the temperature of the system is not equal to the critical temperature T_c, the two K-isotherms will also converge. This point is also characterized by $K = 1 (y = x)$. However, this convergence is only an "apparent" convergence. In contrast to the critical isotherms, the K-values have no physical meaning up to the point of apparent convergence because of the existence of only one phase beyond a certain pressure limit. Anyway, the isotherms may be extrapolated to K = 1 defining the pressure at this point as

the **convergence pressure** p_k of the system at the actual temperature.

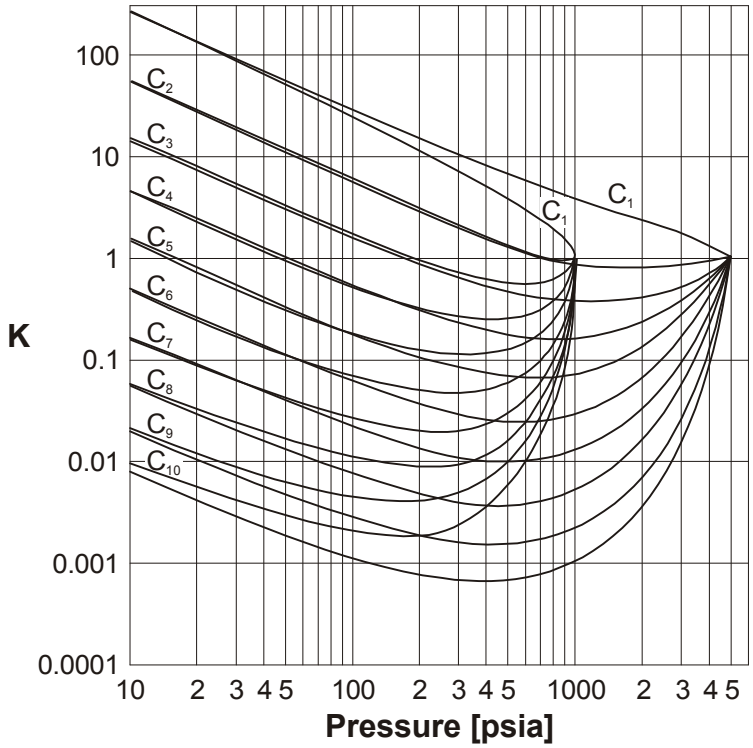

Figure 4.5: Comparison of *K-factors* at 1*00 °F* for *1,000* and *5,000-psia* convergence pressure (from NGAA, 1957)

It has been proved that multi-component systems have properties very similar to those of the binary systems with respect to the convergence of all *K*-isotherms. The (apparent) convergence pressure p_k is a function of the composition of the mixture. Figure 4.5 emphasizes the dependence of the K-factors on the convergence pressure being a function of the system composition. The differences in *K*-values for the two convergence pressures at pressures below 0.7 MPa (100 psia) are not significant for the lighter hydrocarbons ethane through pentane. It then becomes apparent that at low pressures and temperatures, the K-factors are nearly independent of composition.

In 1957, the NGAA **(Natural Gasoline Association of America)** published a diagram series $lgK = f(lg\ p)_T$ in its "Equilibrium Ratio Data Book". The diagrams were based on average values of already available data from various gas condensates and gas/crude oil-systems. This series includes the paraffinic homologous compounds - methane through decane - just as ethylene, propylene, nitrogen, carbon dioxide and hydrogen sulfide within the pressure range from 0.07 to 140 MPa and for temperatures ranging from - 148 to +260 °C.

Figure 4.6 and Figure 4.7 present the respective charts for methane and hexane, respectively, in case of the convergence pressure p_k = 34.5 MPa (5000 psia). The values for this convergence pressure can be used for a large number of hydrocarbon systems. Today, these data are already available for data-processing with computers.

If p_k is known, it is possible to choose from the measured series those K-factors, which are best suited to describe the phase equilibrium vapor/liquid of the given system.

The second parameter, which has to be evaluated to proceed with the prediction of the phase and volumetric behavior of complex hydrocarbon systems, is the *K*-factor of the heaviest component. In conventional analyses of hydrocarbon fluids, everything heavier than hexane is grouped together and reported as the pseudo-component *"C_{7+}"*. This fraction is a mixture of materials of varying volatility. However, the vapor pressure curves and the critical properties of the hydrocarbons heavier than hexane are fairly close together. Thus, it is possible to characterize the mixture *"C_{7+}"* by an average set of *K*-values.

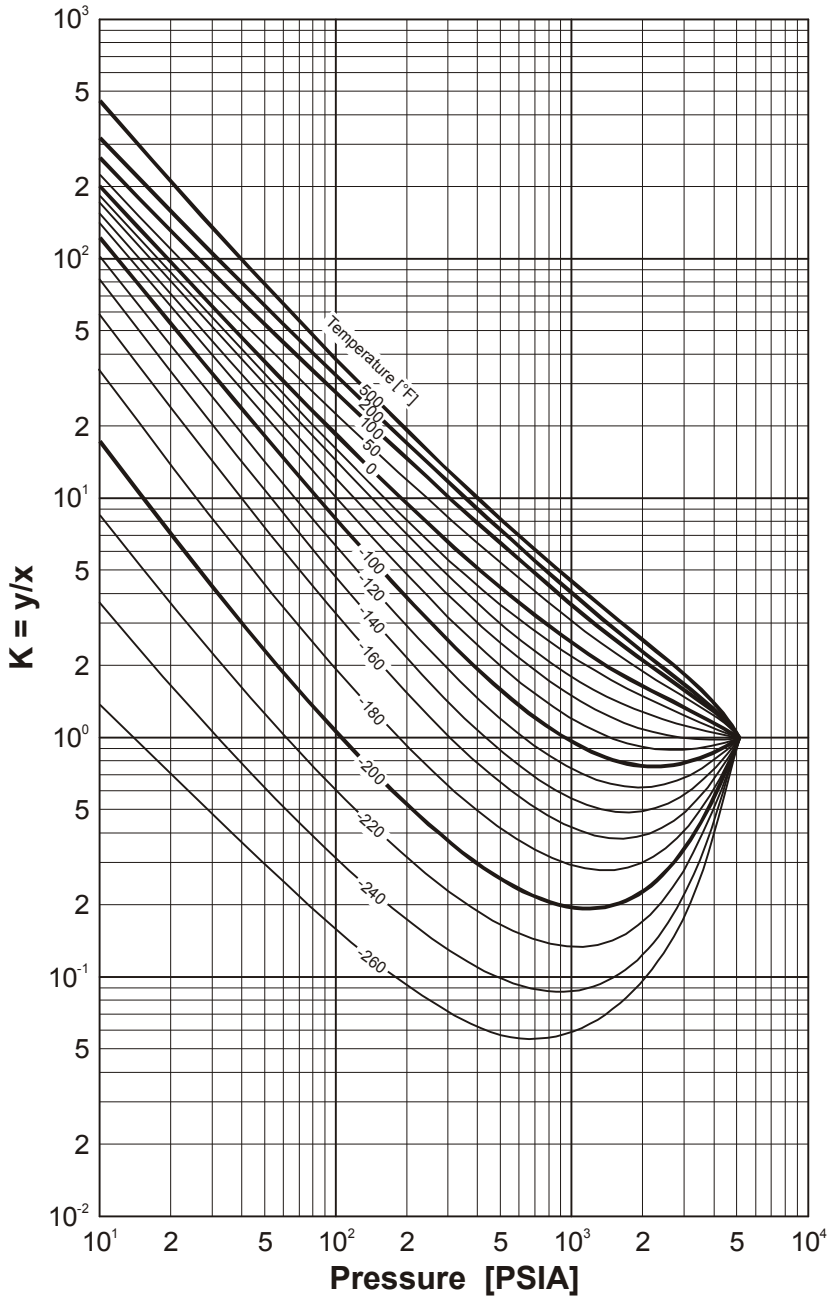

Figure 4.6: K-factors for methane, 5,000 psia convergence pressure (from NGAA, 1957)

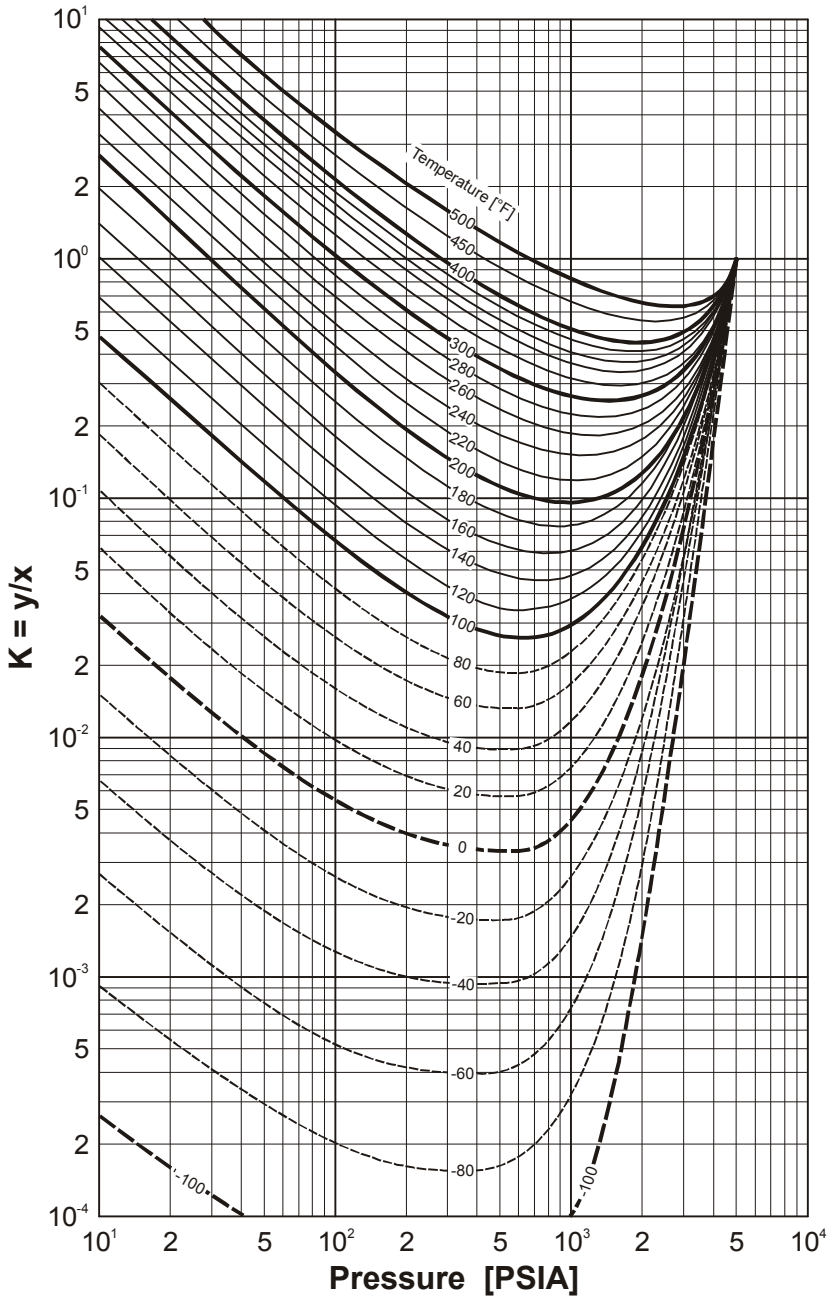

Figure 4.7: K-factors for hexane, 5,000 psia convergence pressure (from NGAA, 1957)

4.2.3 Evaluation of Convergence Pressure

Several iterative methods of estimating p_k have been proposed. One of the most convenient methods is based on the assumption of a pseudo-binary system and consists of the following steps:

- A certain convergence pressure is assumed and the K-factors of components are evaluated from the NGAA-diagrams (examples are given through Figure 4.6 and Figure 4.7).
- The respective composition of the liquid phase being in equilibrium are evaluated by a flash process (see Example 4.1).
- With exception of the lightest component methane, all other components are summarized in a second fictitious component. The pseudo-critical temperature of the pseudo-component C_{2+} in the liquid phase is evaluated in calculating the averaged mole weights in the liquid phase, W_i, through

$$W_i = x_i M_i \tag{4.25}$$

and the pseudo-critical temperature of C_{2+} through

$$T_{pc} = \frac{\sum_{i=2}^{k} W_i T_{ci}}{\sum_{i=2}^{k} W_i}. \tag{4.26}$$

- The critical point of the component C_{2+} is plotted on Figure 4.8 which shows the vapor pressure curves of homologous hydrocarbons.
- The "binary" critical envelope curve of methane with this pseudo-component is drawn.
- For the given temperature, the convergence pressure p_k can be read off because it coincides with the critical pressure of one of the possible mixing ratios in the "binary" system.
- If this numerical value of the convergence pressure does not coincide with the value initially assumed, the whole procedure has to be repeated starting with the assumption of another convergence pressure. The iterative process must go on until correspondence of the assumed convergence pressure and the evaluated one will be achieved.

This iterative method will be demonstrated by Example 4.4.

The K-factors obtained through this method exhibit only satisfactory results, if the operating pressure is considerably lower than p_k. As the operating pressure approaches p_k, the K-factors become very sensitive to the convergence pressure used and care must be taken in the selection of the correct value of p_k. However, charts exist only for some distinct convergence pressure (800, 1000, 1500, 2000, 3000, 5000 and 10,000 psia). Thus the interpolation - inevitable in estimating the *K*-values - may lead to great errors.

4.2.4 Flash Calculation by use of the PENG-ROBINSON Equation of State

With help of the "successive solution method", the *K*-factors of the components of the system can be evaluated by an iterative process like the one presented through Example 4.5:

- The composition of the system, the pressure and temperature as well as the critical data of the components, their acentric factors and the interactive coefficients must be initially known.
- On the basis of assumed K-factors, the phase compositions are calculated through an iterative calculation procedure (see Example 4.1).
- On the basis of the calculated phase compositions, the EOS-parameters *a, b, A*, and *B* after PENG-ROBINSON are calculated for both phases.
- The *Z*-factors both for the liquid and the vapor phase can be evaluated solving the equation of state (Eq. 3.49) through use of the method of CARDAN (see Example 3.3).
- The fugacity coefficients for both phases are evaluated by use of Eq. 4.12 and Eq. 4.13:

$$\ln\phi_i = \frac{b_i}{b}(Z-1) - \ln(Z-B) - \frac{A}{2\sqrt{2}B}\left[\frac{2\sum_{j=1}^{k} x_j a_{ij}}{a} - \frac{b_i}{b}\right]\ln\left(\frac{Z+2{,}414B}{Z-0.414\mathrm{B}}\right).$$

- New *K*-values can be evaluated by inserting these values in Eq. 4.18:
- $K_i = \dfrac{\phi_{i,\,liq}}{\phi_{i,\,vap}}$
- On the basis of the evaluated *K*-values, the calculation procedure is repeated. The steps described above will be repeated until the K-factors converge within a certain limit.
- The last flash iteration results in the evaluation of the mole number in the liquid phase, n_{liq}, the mole number in the vapor phase n_{vap} and in the evaluation of the composition of the phases.
- Using Z_{liq} and Z_{vap}, the volume and the density of the two phases can be calculated, too.

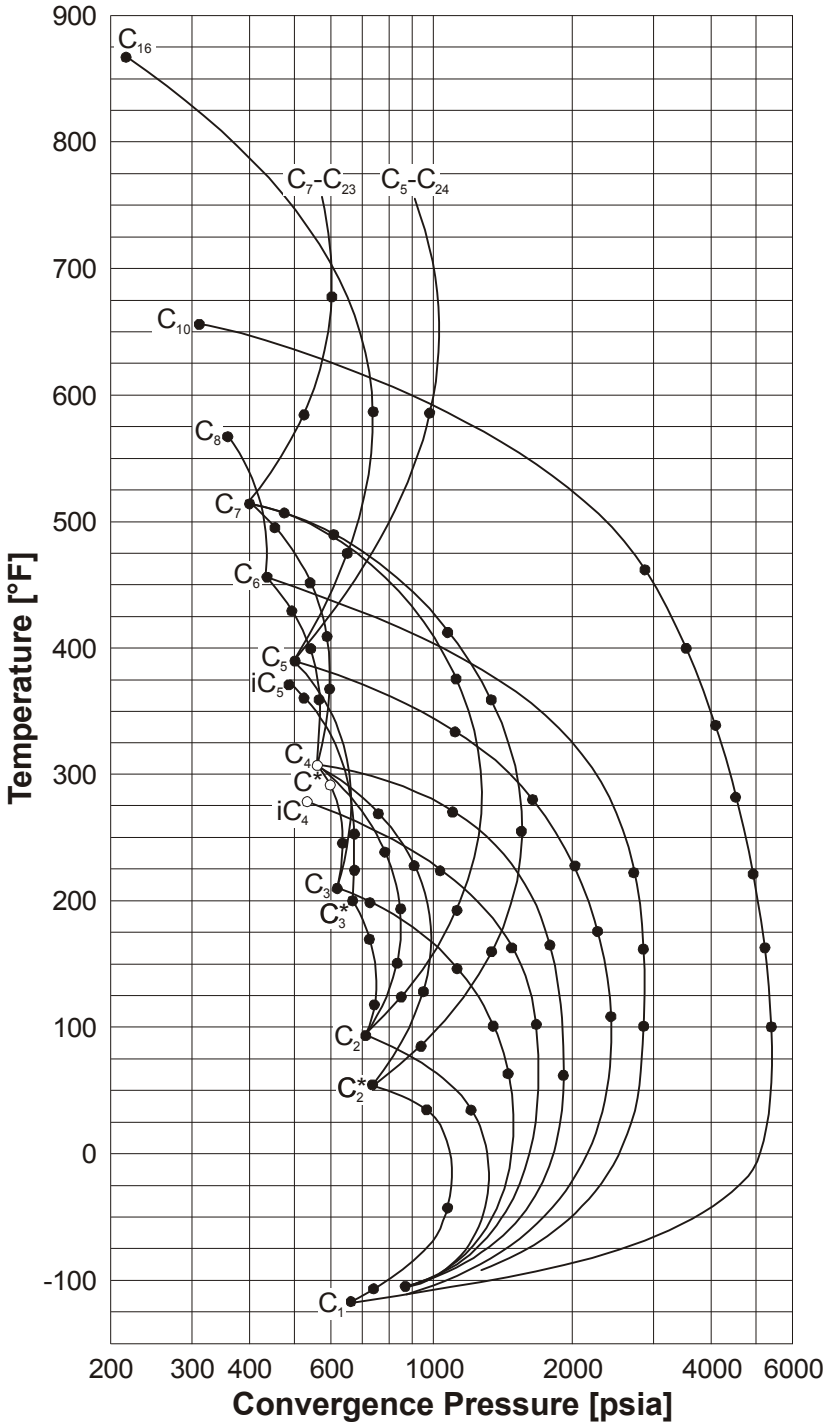

Figure 4.8: Convergence pressure data - methane for binary hydrocarbon mixtures (from WINN, 1952)

Example 4.4

Evaluation of the convergence pressure by the iterative NGAA process described above. The composition of the system is tabled below, and the temperature and the pressure are fixed as $T = 49\ ^{\circ}C$ and $p = 15.5$ MPa.

FIRST ITERATION: p_k = 26.7 MPa (4000 psia)

n_{liq} = 0.5876

n_{vap} = 0.4124

Component	z_i	M_i kg/kmole	$T_{c,i}$ K	K_i	x_i	$W_i=x_iM_i$	W_iT_{ci}
C_1	0.6973	-	-	1.6500	0.5499	-	-
C_2	0.0318	30.07	305.4	0.9000	0.0332	0.998	304.79
C_3	0.0194	44.09	369.8	0.6300	0.0229	1.010	373.50
nC_4	0.0223	58.12	425.2	0.4300	0.0292	1.697	721.56
nC_5	0.0221	72.15	469.7	0.2250	0.0325	2.345	1101.45
nC_{6*}	0.0309	86.17	507.4	0.1700	0.0470	4.050	2054.97
C_{7*}	0.1762	114.22	568.8	0.0720	0.2854	32.598	18541.74
Σ					1.0000	42.698	23098.01

*assumption: $C_{7+} \approx nC_8$

$$T_{pc} = \frac{\sum_{i=2}^{k} W_i T_{c,i}}{\sum_{i=2}^{k} W_i} = \frac{23098.01}{42.698} = 540.96\ K = 514.06\ ^oF$$

On Figure 4.8 T_{pc} = 514.06°F is close to T_c of pure n-heptane. For the given temperature of the system (T = 49 °C and 120 °F, respectively), the convergence pressure p_k can be read off on the envelope curve between methane and n-heptane at

$p_k = 3150\ psia = 21.72\ MPa.$

This value does not coincide with the initially assumed value. Thus a second iteration must be done.

SECOND ITERATION: p_k = 20.4 MPa (3000 psia)

n_{liq} = 0.5604

n_{vap} = 0.4496

Component	K_i	x_i	$W_i = x_i M_i$	$W_i T c_i$
C_1	1.700	0.5332	-	-
C_2	0.8800	0.0336	1.010	308.45
C_3	0.6200	0.0233	1.027	379.78
nC^4	0.4200	0.0299	1.738	739.00
nC5	0.2200	0.0336	2.424	1138.55
nC_{6*}	0.1800	0.0483	4.162	2111.80
C_{7*}	0.0700	0.2980	34.038	19360.81
Σ		1.0000	44.399	24038.39

*assumption: $C_{7+} \approx nC_8$

$$\frac{\sum_{i=2}^{k} W_i T_{c,i}}{\sum_{i=2}^{k} W_i} = \frac{24038.39}{44.399} = 541.42K = 514.9\ ^oF$$

From Fig. 4.8:

$$p_k = 3150 psia$$

and thus

$$p_k = 21.72 MPa\,.$$

The agreement with the assumption is now satisfactory. Further refinement is impossible (*K*-values only evaluated for 1000 *psia* steps in p_k).

Example 4.5

Evaluation of the K-factors of the three components of a system at *p = 1.38 MPa* and *T = 338.7 K*. The successive solution method is used on the basis of the composition of the system, the critical and reduced data as well as the acentric factors which are given below in Table 4.1. Table 4.2 presents the interaction coefficients K_{ij} which must be known, too.

Table 4.1: Composition of the System, Critical Data and Acentric Factors

Component	Composition	Critical Data		Reduced Data		Acentric Factor
	z_i	T_c K	p_c MPa	T_r	p_r	ω_i
C_3	0.61	369.8	4.245	0.916	0.325	0.152
n - C_4	0.28	425.2	3.800	0.797	0.363	0.193
n - C_5	0.11	469.6	3.374	0.721	0.409	0.251

Table 4.2: Interaction Coefficients of the Components

	C_3	n - C_4	n - C_5
C_3	0.000	0.001	0.003
n - C_4	0.001	0.000	0.001
n - C_5	0.003	0.001	0.000

For the first iteration of a flash process,K-factors as well as the mole numbers in the phases, n_{liq} and n_{vap}, are not assumed. The gas and the liquid phase compositions are calculated through an iterative calculation procedure (see Example 4.1). The assumed K-factors as well as the evaluated phase compositions are given in Table 4.3.

Table 4.3: Assumed K-Factors and evaluated phase compositions

FIRST ITERATION: $n_{liq} = 0.52$

$n_{vap} = 0.48$

Component	K-Factor	$x_i = \frac{z_i}{n_v K_i + n_L}$	$y_i = \frac{z_i}{n_L / K_i + n_v}$
C_3	1.745	0.440	0.767
n - C_4	0.537	0.369	0.198
n - C_5	0.182	0.191	0.035
Σ		1.000	1.000

Then the iteration starts with the evaluation of *a* and *b*. At first the parameters *b* and *a* for each component have to be evaluated through

$$b_i = 0.0778 \frac{RT_c}{p_c},$$

$$a_{c,i} = 0.45724 \frac{R^2 T_c^{\,2}}{p_c},$$

$$\alpha_i^{0.5} = 1 + (0.37646 + 1.54226\omega - 1.54226\omega^2)(1 - T_r^{0.5}),$$

(see Eq. 3.52) and through

$$a_i = (a_c \alpha)_i.$$

The results of these calculations are given in Table 4.4).

Table 4.4: First Iteration: Determination of *a* and *b* for the components

Component	b_i	a_i
C_3	5.635 E-5	1.072
n - C_4	7.247 E-5	1.729
n - C_5	9.003 E-5	2.557

By use of Eq. 3.53

$$b = \sum_{i=1}^{k} x_i b_i$$

and Eq. 3.56

$$a = \sum_{i=1}^{k} \sum_{j=1}^{k} x_i x_j (a_i a_j)^{0.5} (1 - K_{ij}),$$

a and *b* for the liquid phase as well as for the vapor phase are calculated on the basis of phase compositions evaluated in Table 4.3) The calculation procedure is presented through Example 3.2.

Then the parameters *A* and *B* are calculated after PENG-ROBINSON using Eq. 3.35

$$A = \frac{ap}{R^2 T^2}$$

and Eq. 3.36

$$B = \frac{b\,p}{R\,T}.$$

The evaluated numerical values of the parameters a, b, A and B for both phases are summarized in Table 4.5.

Table 4.5: First Iteration: Evaluation of the EOS parameters using mixing rules.

	a	b	A	B
Liquid Phase	1.551	6.873 E-5	0.2699	3.368 E-2
Vapor Phase	1.232	6.072 E-5	0.2144	2.975 E-2

Now the *Z*-factors both for the liquid and the vapor phase can be evaluated solving the equation of state given by Eq. 3.49:

$$Z^3 - (1-B)Z^2 + (A - 2B - 3B^2)Z - (AB - B^2 - B^3) = 0.$$

To solve this cubic equation of state, the CARDAN equation is applied for

$$x^3 + rx^2 + sx + t = 0,$$

where

$$r = -(1-B),$$

$$s = (A - 2B - 3B^2)$$

and

$$t = -(AB - B^2 - B^3).$$

The factors *r*, *s* and *t* have to be evaluated both for the liquid and the vapor phase.

By substitution of

$$x = y - \frac{r}{3},$$

the formula

$$x^3 + rx^2 + sx + t = 0$$

is reduced to

$$y^3 + py + q = 0,$$

where

$$p = \frac{3s - r^2}{3}$$

and

$$q = \frac{2r^3}{27} - \frac{rs}{3} + t.$$

The discriminant D is defined as

$$D = \left(\frac{p}{3}\right)^3 + \left(\frac{q}{2}\right)^2.$$

Contrary to Example 3.3, D < 0 both in case of the liquid phase and in case of the vapor phase. Thus the cubic equation of state has three real solutions, respectively. In defining

$$\varsigma = \sqrt[2]{-\frac{p^3}{27}}$$

and

$$\cos\varphi = -\frac{q}{2\varsigma},$$

the three solutions for the reduced form

$$y^3 + py + q = 0$$

are given by

$$y_1 = 2\sqrt[3]{\varsigma}\cos(\varphi/3)$$

$$y_2 = 2\sqrt[3]{\varsigma}\cos(\varphi/3 + 2\pi/3)$$

and

$$y_3 = 2\sqrt[3]{\varsigma}\cos(\varphi/3 + 4\pi/3).$$

Introducing y_1, y_2, and y_3 into

$$x = y - \frac{r}{3},$$

the Z-factors(=x) of the phases can be evaluated. The solutions are summarized in Table 4.6.

Table 4.6: First Iteration Solution f or the Z-Factors after CARDAN

	z_1	z_2	z_3
Liquid Phase	0.0523	0.2172	0.6968

	z_1	z_2	z_3
Vapor Phase	0.0526	0.1325	0.7852

Obviously, the actual Z-factor of the liquid phase must be identical with the smaller one of the three solutions for the liquid phase, meanwhile the actual Z-factor for the vapor phase is equal to the greatest one of the three solutions for the vapor phase. Thus the first iteration results in

$$Z_{liq} = 0.0523$$

and

$$Z_{vap} = 0.7852 .$$

The Z-factors are introduced into Eq. 4.13.

$$\ln\phi_i = \frac{b_i}{b}(Z-1) - \ln(Z-B) - \frac{A}{2\sqrt{2}B}\left[\frac{2\sum_{j=1}^{k} x_j a_{ij}}{a} - \frac{b_i}{b}\right]\ln\left(\frac{Z+2{,}414B}{Z-0.414B}\right),$$

respectively, to evaluate the fugacity coefficients ϕ_3 (of propane), ϕ_4, of n-butane) and ϕ_5 (of n-pentane) both for the liquid and the vapor phase. The results of this calculation procedure are summarized in Table 4.7.

Table 4.7: First Iteration Fugacity Coefficients

	ϕ_3	ϕ_4	ϕ_5
Liquid Phase	1.2580	0.4707	0.1831
Vapor Phase	0.8473	0.7519	0.6672

As a result of the first iteration flash, K-factors are evaluated through Eq. 4.18

$$K_i = \frac{\phi_{i,liq}}{\phi_{i,vap}}$$

and summarized in Table 4.8

Table 4.8: First Iteration

Components	K-Factor
C_3	1.4847
n - C_4	0.6260
n - C_5	0.2744

These K-factors are the basis of the second iteration which starts again with the iterative calculation procedure presented through Example 4.1 (see Table 4.9)

On the basis of the data in Table 4.4 and in Table 4.9 the numerical values of the parameters a, b, A and B for both phases are evaluated again and summarized in Table 4.10.

Now the Z-factors both for the liquid and the vapor phase can be evaluated solving the equation of state given by Eq. 3.49

$$Z^3 - (1 - B)Z^2 + (A - 2B - 3B^2)Z - (AB - B^2 - B^3) = 0$$

through the CARDAN equation. Again D < 0 both in case of the liquid phase and in case of the vapor phase. Correspondingly, the cubic equation of state has three real solutions. The solutions are summarized in Table 4.11.

Table 4.9:

SECOND ITERATION: n_{liq}= 0.556

n_{vap}= 0.444

Component	K-Factor	$x_i = \frac{z_i}{n_v K_i + n_L}$	$y_i = \frac{z_i}{n_L / K_i + n_v}$
C_3	1.4847	0.5020	0.7453
n - C_4	0.6260	0.3358	0.2102
n - C_5	0.2742	0.1623	0.0445
Σ		1.0001	1.0000

Table 4.10: Second Iteration

	a	b	A	B
Liquid Phase	1.490	6.725 E-5	0.2592	3.296 E-2
Vapor Phase	1.249	6.116 E-5	0.2173	2.997 E-2

Table 4.11: Second Iteration Solution for the Z-Factors, after CARDAN

	Z_1	Z_2	Z_3
Liquid Phase	0.0521	0.1988	0.7161
Vapor Phase	0.0525	0.1364	0.7812

Once more again, the actual Z-factor of the liquid phase must be identical with the smallest one of the three solutions for the liquid phase, meanwhile the actual Z-factor for the vapor phase is equal to the greatest one of the three solutions for the vapor phase. Thus the second iteration results in

$$Z_{\text{liq}} = 0.0521$$

and

$$Z_{\text{vap}} = 0.7812.$$

The Z-factors are introduced into Eq. 4.13

$$\ln\phi_i = \frac{b_i}{b}(Z-1) - \ln(Z-B) - \frac{A}{2\sqrt{2}B}\left[\frac{2\sum_{j=1}^{k} x_j a_{ij}}{a} - \frac{b_i}{b}\right]\ln\left(\frac{Z+2{,}414B}{Z-0.414B}\right),$$

respectively, to evaluate the fugacity coefficients ϕ_4 (of n-butane)and ϕ_5 (of n-pentane) both for the liquid and the vapor phase. The results of this calculation procedure are summarized in Table 4.12.

Table 4.12: Second Iteration
Fugacity Coefficients

	ϕ_3	ϕ_4	ϕ_5
Liquid Phase	1.2520	0.4717	0.1846

	ϕ_3	ϕ_4	ϕ_5
Vapor Phase	0.8477	0.7511	0.6655

The K-factors are evaluated through Eq. 4.18

$$K_i = \frac{\phi_{i,\,liq}}{\phi_{i,\,vap}}$$

and given in Table 4.13

Table 4.13: Second Iteration

K-Factors

Components	K-Factor
C_3	1.4769
n - C_4	0.6280
n - C_5	0.2773

The K-factors from the two flash iterations exhibit satisfactory convergence. On the basis of the K-factors given in Table 4.13, a final iterative calculation procedure analogous to Example 4.1 results in the mole numbers and in the composition of the phases.

Table 4.14: Final Results

FINAL RESULTS: n_{liq} = 0.562

n_{vap}= 0.438

Component	**K-Factor**	$x_i = \frac{z_i}{n_v K_i + n_L}$	$y_i = \frac{z_i}{n_L / K_i + n_v}$
C_3	1.4769	0.5046	0.7452
n - C_4	0.6280	0.3345	0.2101
n - C_5	0.2773	0.1609	0.0446
Σ		1.0000	0.9999

Chapter 5

Phase Properties

5.1 Natural Gases

5.1.1 Volume

As previously discussed in Chap. 3, the state of ideal gases is defined by the following equation of state:

$$pV = nRT, \tag{5.1}$$

where R is the universal gas constant and n is the number of moles. The value R depends on the system of units. In the *SI*-system:

$$R = 8.31432\ J/K\ mole.$$

In case of ideal gases, no intermolecular forces are acting. At any isothermal change of state, the decrease in volume is directly proportional to the increase in pressure. It has been observed that in many cases - e.g. in case of natural gases - the volume becomes less than half if the pressure is doubled. This behavior of a gas in called a real one.

Below the BOYLE temperature, the real gases are more compressible than an ideal one, because of intermolecular forces of attraction and repulsion. If the pressure is low (the forces of attraction can be neglected because of the great distance of molecules) or in case of high temperatures (dominance of the kinetic energy of the molecules), real gases behave similarly to perfect gases.

In case of real gases, the change in state can be well described by the equations of state which are also presented in Chap. 3 (VAN DER WAALS, REDLICH-KWONG, PENG-ROBINSON). In the petroleum industry, the basic relation of Eq. 3.12

$$pV = ZnRT \tag{3.12}$$

is commonly used because of its easy applicability.

The *Z*-factor is the so called "deviation factor" or "compressibility factor". It is defined as the ratio of the volume of a real gas to the volume of a perfect one at identical temperature and pressure. Let m be the mass and M the molecular weight, then

$$n = \frac{m}{M}, \tag{5.2}$$

and for unit mass (m = 1 g) Eq. 3.12 can be transformed into

$$pV = \frac{ZRT}{M}. \tag{5.3}$$

Here V is the specific volume and its reciprocal is the phase density:

$$\rho_g = \frac{1}{V} = \frac{pM}{ZRT}. \tag{5.4}$$

The atmospheric density of the gas is often related to the atmospheric density of air at the same standard temperature. In doing so, the "specific gravity" of the gas γ_g is defined by

$$\gamma_g = \frac{\rho_g^o}{\rho_{g,a}^o} = \frac{M}{M_a} = \frac{M}{28.97}, \tag{5.5}$$

where the subscript "a" indicates the values for air and the superscript "o" those at standard conditions (atmospheric pressure).

If Eq. 5.5 is combined with Eq. 5.3, the gas density results in

$$\rho_g = \frac{1}{V} = \frac{M_a}{R}\gamma_g\frac{p}{ZT} = 0.003473\gamma_g\frac{p}{ZT}. \tag{5.6}$$

As expected, the *Z*-factor depends both on pressure and temperature. Z-factors of different gases, which can be determined experimentally, vary considerably. Figure 5.1 shows the *Z*-factor of methane, ethane and propane as a function of the pressure.

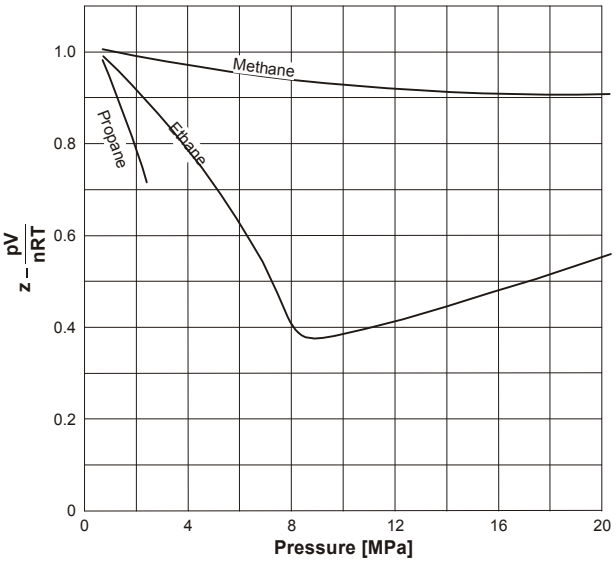

Figure 5.1: Z-factor of methane, ethane and propane versus pressure at $T = 140\ ^oF$ (from STANDING, 1977)

5.1.2 Formation Volume Factor

In petroleum industry, the term "formation volume factor" is widely used. It expresses which volume is taken up by one cubic meter (at standard state conditions, p^o and V^o) at a pressure p and a temperature T.

The formations volume factor for gases, B_g, is defined by

$$B_g = B_g(p, T) = \frac{V}{V^o}, \tag{5.7}$$

where the standard conditions p^o and T^o are generally defined in

Europe: p^o: *1.00 bar*

T^o: *273.15 K*

and in

USA: p^o: *14.7 psia (1.01325 bar)*

T^o: *60.0* ^oF *(15* ^oC*).*

In case of one mole, Eq. 5.4 results for standard conditions in

$$p^o T^o = Z^o R T^o . \tag{5.8}$$

If Eq. 5.4 and Eq. 5.8 are substituted in Eq. 5.7, then

$$B_g(p,\mathrm{T}) = \frac{ZT}{p}C, \tag{5.9}$$

where

$$C = \frac{p^o}{Z^o T^o}.$$

5.1.3 Compressibility

On the basis of the gas law, the isothermal gas compressibility results in

$$c_g = -\frac{1}{V}\left(\frac{\partial V}{\partial p}\right)_T = -\frac{1}{B_g}\left(\frac{\partial B_g}{\partial p}\right)_T = \frac{1}{p} - \frac{1}{Z}\left(\frac{\partial Z}{\partial p}\right). \tag{5.10}$$

For ideal gases: Z = 1, i.e. $\frac{\partial Z}{\partial p} = 0$.

Therefore, the gas compressibility is only a function of pressure and is inversely proportional to the pressure.

5.1.4 Correlation of the *Z*-Factor

5.1.4.1 STANDING-KATZ Correlation

In general, the components of natural gases are homologous paraffins with similar molecular structures and the theorem of corresponding states can be applied. Figure 5.2 shows the excellent correspondence of the *Z*-factors of methane, propane and pentane as a function of reduced pressure for a series of reduced temperatures.

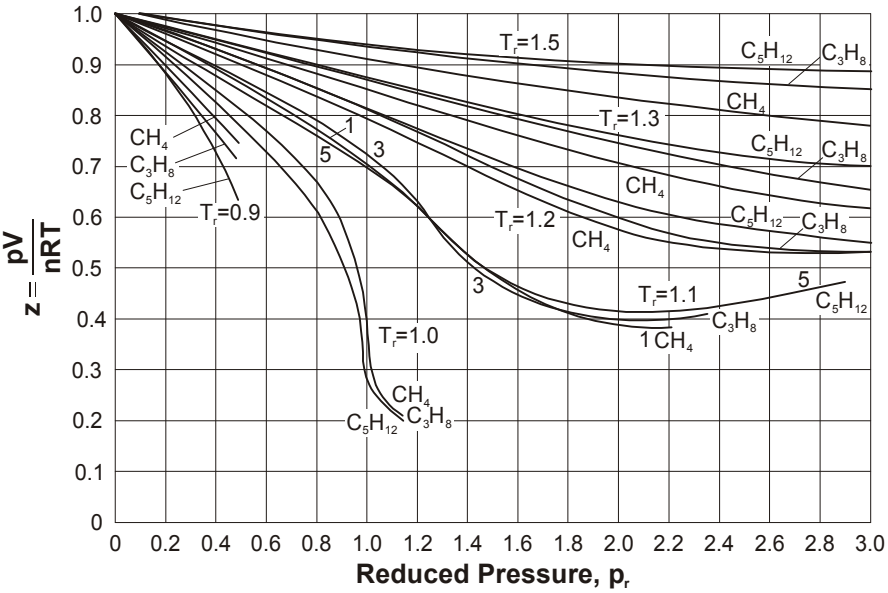

Figure 5.2: *Z*-factor as a function of reduced pressure for a series of reduced temperatures (from SAGE and LACEY, 1949)

The theorem of corresponding states can also be applied to gas mixtures, using KAY´s mixing rule for calculation of the evaluation of "pseudo-critical" data, T_{pc} and p_{pc}, which are given by

$$T_{pc} = \sum_{i=1}^{k} y_i T_{c,\mathrm{i}}, \tag{5.11}$$

and

$$p_{pc} = \sum_{i=1}^{k} y_i p_{c\mathrm{i}}, \tag{5.12}$$

where
p_{ci}: critical pressure of component *i,*
T_{ci}: critical temperature of component *i,*
y_i: mole fraction of component *i* in the gas phase.

Then, the "pseudo-reduced" data, T_{pr} and p_{pr}, can be evaluated:

$$T_{pr} = \frac{T}{T_{pc}}, \tag{5.13}$$

$$p_{pr} = \frac{p}{p_{pc}}, \tag{5.14}$$

where
T: operating temperature,
p: operating pressure.

Note, that both T and T_{pc} in Eq. 5.13 must be absolute temperatures, either given in K (Kelvin, SI unit) or in R (Rankine, Field Unit).

The definition of corresponding states on the basis of the pseudo-reduced data results in a generalized plot of *Z*-factors for natural gases (see Figure 5.3). This plot can be used to evaluate the *Z*-factor of a natural gas on the basis of its composition and the critical data (see Example 5.1).

Several natural gases contain considerable amounts of heavy components which will be combined - depending on the feasibility of chemical analysis - to the pseudo components C_{7+} or C_{9+}. The compositions of these mixtures cannot exactly be defined. In the laboratory practice, the C_{7+} fraction is obtained as liquid residue from a fractional destillation and two properties - averaged molecular weight and specific gravity - are determined. These properties have been correlated with the pseudo-critical data of this fraction (see Figure 5.4). On the basis of these correlations, the engineer is able to calculate pseudo-reduced properties of natural gases for which conventional analyses are available.

In many cases, the data of fractional distillation are not available. Anyway, several diagrams have been published which correlate the pseudo-critical functions of state with the gas gravity. By means of these diagrams, the *Z*-factor can be determined even if the gas composition is not known. These diagrams are only valid for a given quality or only for one area, formation, reservoir, basin, etc. The respective diagram for Oklahoma City gases is given in Figure 5.5 (see also Example 5.2.)

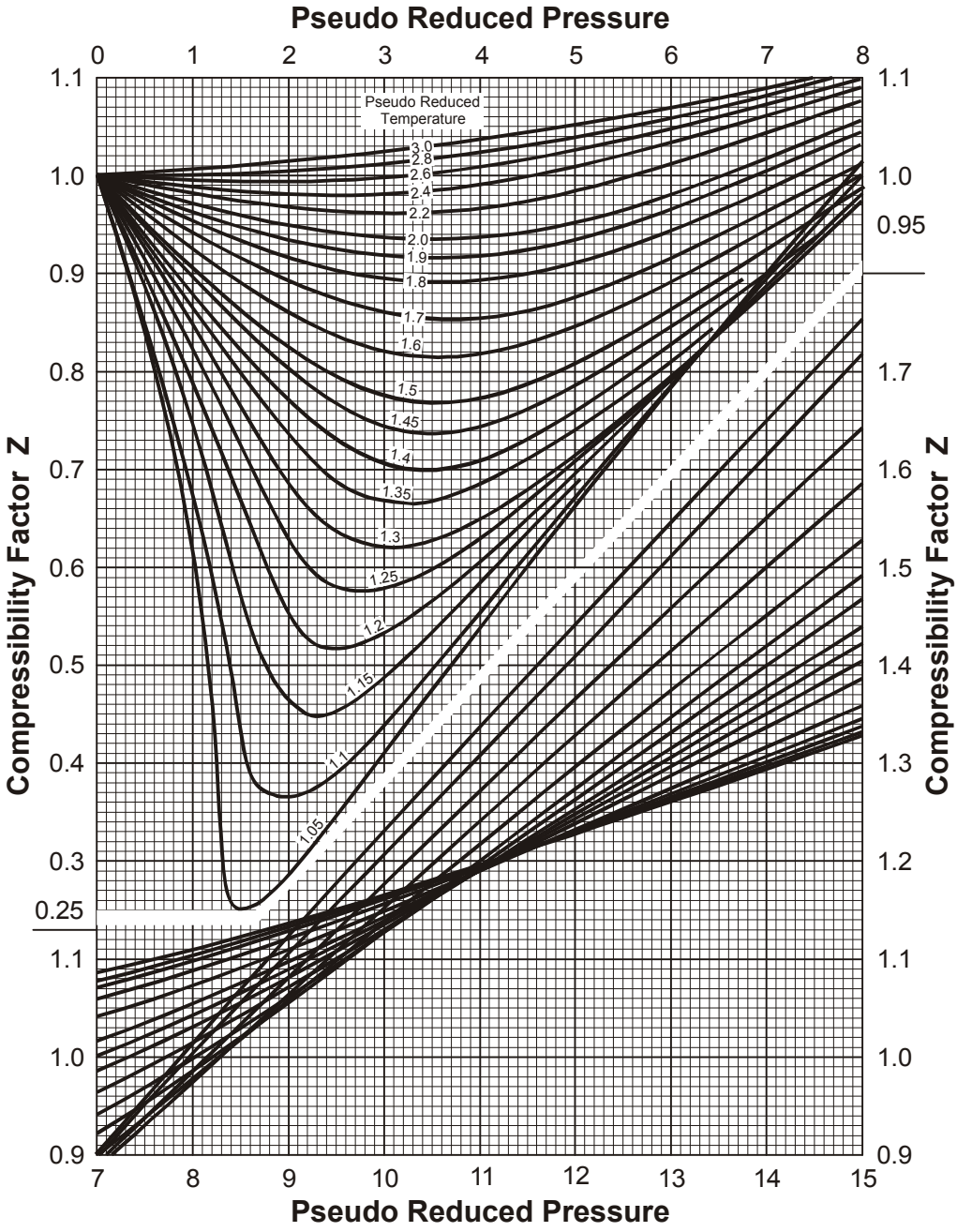

Figure 5.3: *Z*-factor for natural gases (from BROWN et al., 1948)

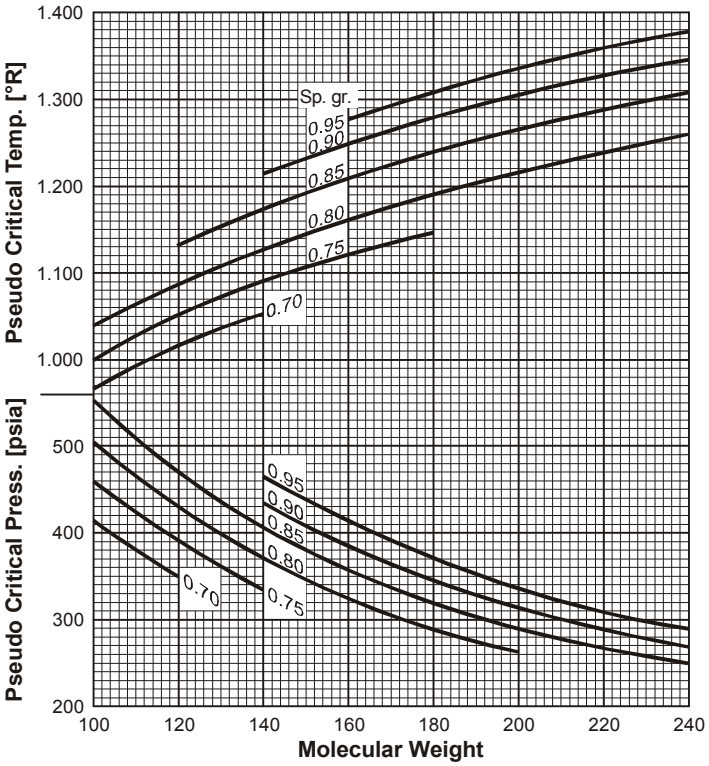

Figure 5.4: Pseudo-critical temperatures and pressures for heptanes and heavier (from MATTHEWS et al, 1942)

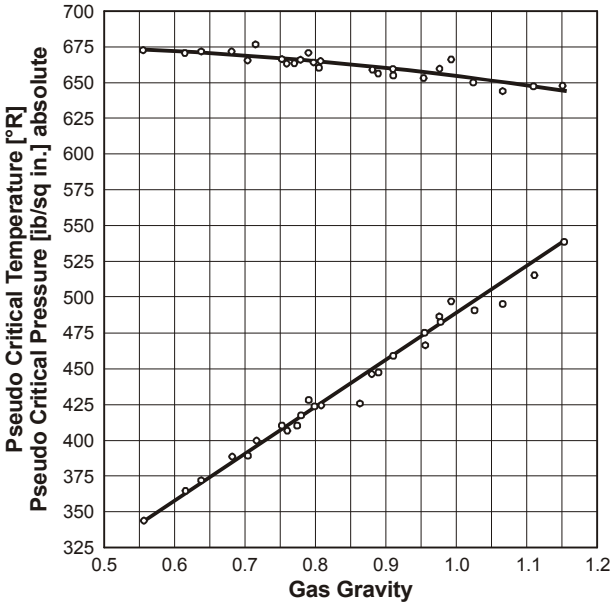

Figure 5.5: Pseudo-critical properties of Oklahoma City Gases (from MATTHEWS et al., 1942)

Example 5.1

Evaluation of the density of a natural gas at $T = 105\ ^{o}C$ and at $p = 22.55$ MPa. The Z-factor is determined by using Figure 5.3 The table below summarizes the composition of the gas, the critical data as well as the calculated reduced data of the components.

Component	M_i kg/kmole	y_i	$y_i M_i$ kg/kmole	$T_{c,i}$ K	y_i x T_{ci} K	p_{ci} MPa	y_i x p_{ci} MPa
C_1	16.0	0.9443	15.109	190.6	179.98	4.60	4.344
C_2	30.1	0.0158	0.476	305.4	4.83	4.88	0.077
C_3	44.1	0.0132	0.582	369.8	4.88	4.25	0.056
iC_4	58.1	0.0051	0.296	408.1	2.08	3.65	0.019
nC_4	58.1	0.0053	0.308	425.2	2.25	3.79	0.020
iC_5	72.2	0.0023	0.166	461.4	1.06	3.38	0.008
nC_5	72.2	0.0021	0.152	469.7	0.99	3.37	0.007
C_6	86.2	0.0033	0.284	507.4	1.67	3.01	0.010
C^{*}_{7+}	114.23	0.0086	0.982	568.8	4.89	2.48	0.021
Σ		1.000	18.355		202.63		4.562

assumption: $C_{7+} \approx C_8$

$$T_{pr} = \frac{T}{T_{pc}} = \frac{105 + 273.15}{202.63} = 1.87,$$

$$p_{pr} = \frac{p}{p_{pc}} = \left(\frac{22.5}{4.562} = 4.93\right)$$

From Figure 5.3

$Z = 0.925$

which is introduced in

$$\rho_g = \frac{p\sum_{i=1}^{k} y_i M_i}{ZRT},$$

where

$R = 8.31432[J°K^{-1}mol^{-1}]$.

$$\rho_g = \frac{225.5\ E+5 \times 18.355\ \text{E - 3}}{0.925 \times 8.31432 \times 378.15} kg/m^3 \ ,$$

$$\rho_g = 142.32 kg/m^3 .$$

Example 5.2

Evaluation of the density and the formation volume factor of an Oklahoma City Gas of the specific gravity $\gamma_g = 0.7018$ at temperature T = 90.5 ^{o}C(655 R)and pressure p = 12.5 MPa(1813 psia). At first the pseudo critical data are read off from Figure 5.5 as

$$T_{pc} = 390R$$

and

$$p_{pc} = 670 psia .$$

Now the pseudo reduced data are calculated as

$$T_{pr} = \frac{T}{T_{pc}} = \frac{655}{390} = 1.68$$

and

$$p_{pr} = \frac{p}{p_{pc}} = \frac{1813}{670} = 2.71 .$$

On the basis of the pseudo-reduced data,

$$Z = 0.86$$

results from Figure 5.3.

Because

$$\rho_g = \frac{M_a}{R}\gamma_g \frac{p}{ZT},$$

where

M_a = 28.97 E-3 kg/mole,

and

R = 8.31432J/K mole,

the density can be calculated through

$$\rho_g = \frac{0.02897 \times 0.7018 \times 125\ E+5}{8.31432 \times 0.86 \times 363.65} kg/m^3 \ ,$$

so that

$\rho_g = 97.774\ \text{kg/m}^3$.

The formation volume factor can be evaluated through Eq. 5.9

$$B_g(p,\mathrm{T}) = \frac{ZT}{p}C,$$

where

$$C = \frac{p^o}{Z^o T^o}.$$

Assuming that the gas is a perfect one at European standard conditions

$$p^o = 1\,bar$$

and

$$T^o = 273.15\ \mathrm{K},$$

so that Z = 1.0, its formation volume factor results in

$$B_g = \frac{0.86 \times (90.5 + 273.15)}{12.5}\frac{0.1}{273.15},$$

$$B_g = 0.00916.$$

STANDING and KATZ presented a generalized Z-factor chart (Figure 5.3), which has become industry standard for predicting the volumetric behavior of natural gases. Many empirical equations and EOS's have been fit to the original STANDING-KATZ chart:

5.1.4.2 HALL-YARBOROUGH Correlations

HALL and YARBOROUGH presented an accurate, powerful method to numerically reproduce the STANDING and KATZ chart. The calculation steps are the following:

$$Z = \frac{\alpha p_{pr}}{y}, \tag{5.15}$$

where

$$\alpha = 0{,}06125\,t\exp[-1{,}2(1-t)^2]. \tag{5.16}$$

p_{pr} is the pseudoreduced pressure and t is the reciprocal of the pseudoreduced temperature.

y is a reduced density parameter, the product of a VAN DER WAALS co-volume and density, which is obtained by solving the following equation by NEWTON-RAPHSON iteration:

$$f(y) = 0 = -\alpha p_{pr} + \frac{y + y^2 + y^3 + y^4}{(1-y)^3} - (14{,}76t - 9{,}76t^2 + 4{,}58t^3)y^2 \quad , \tag{5.17}$$
$$+ (90{,}7t - 242{,}2t^2 + 42{,}4t^3)y^{2{,}18 + 2{,}82t}$$

An initial value of $y = 0.001$ can be used with the NEWTON-RAPHSON procedure, where convergence should be obtained in 3 to 10 iterations for $|f(y)| = 1 \times 10^{-8}$.

The derivative $\frac{\partial Z}{\partial p}$ used in the definition of c_g is given by

$$\left(\frac{\partial Z}{\partial p}\right)_T = \frac{\alpha}{p_{pc}}\left[\frac{1}{y} - \frac{\alpha(p_{pr}/y^2)}{df(y)/dy}\right], \tag{5.18}$$

where

$$\frac{df(y)}{dy} = \frac{1 + 4y + 4y^2 - 4y^3 + y^4}{(1-y)^4} \tag{5.19}$$
$$-(29{,}52t - 19{,}52t^2 + 9{,}16t^3)y$$
$$+ (2{,}18 + 2{,}82t)\left(90{,}7t - 242{,}2t^2 + 42{,}4t^3\right)y^{1{,}18 + 2{,}82t}$$

The HALL and YARBOROUGH (DRANCHUK and ABOU-KASSEM) equations give the most accurate representation for a broad range of temperatures and pressures. The STANDING and KATZ Z-factor correlation may require special treatment for wet gas and gas condensate fluids containing significant amounts of heptanes-plus material and for gas mixtures with significant amounts of non-hydrocarbons. An apparent discrepancy in the STANDING and KATZ Z-factor chart for $1.05 < T_r < 1.15$ has been smoothed in the HALL and YARBOROUGH correlations. This correlation is recommended for most natural gases.

5.1.4.3 WICHERT-AZIZ Correlation

The STANDING-KATZ chart is not applicable, if significant quantities of non-hydrocarbon components such as CO_2 or H_2S are present. WICHERT and AZIZ suggest corrections in the calculation of the pseudocritical values, based on the non-hydrocarbon mole fractions, as follows:

$$T_{pc} = \widehat{T}_{pc} - \varepsilon, \tag{5.20}$$

$$p_{pc} = \frac{\widehat{p}_{pc}(\widehat{T}_{pc} - \varepsilon)}{\widehat{T}_{pc} + y_{H_2S}(1 - y_{H_2S})\varepsilon}, \tag{5.21}$$

and

$$\varepsilon = 120\left[(y_{CO_2} + y_{H_2S})^{0,9} - (y_{CO_2} + y_{H_2S})^{1,6}\right] + 15\left(y_{CO_2}^{0,5} + y_{H_2S}^{4}\right) \tag{5.22}$$

$\widehat{T}_{pc}$ and $\widehat{p}_{pc}$ are the mixture pseudocriticals on the basis of KAY´s mixing rule.

If only gas gravity and nonhydrocarbon content are known, the hydrocarbon specific gravity is first calculated from

$$\gamma_{gHC} = \frac{\gamma_g - (y_{N_2}M_{N_2} + y_{CO_2}M_{CO_2} + y_{H_2S}M_{H_2S})/M_{air}}{1 - y_{N_2} - y_{CO_2} - y_{H_2S}}. \tag{5.23}$$

Hydrocarbon pseudocriticals are then calculated from the following correlations suggested by SUTTON.

$$T_{pcHC} = 169{,}2 + 349{,}5\gamma_{gHC} - 74{,}0\gamma_{gHC}^2, \tag{5.24}$$

and

$$p_{pcHC} = 756{,}8 - 131{,}0\gamma_{gHC} - 3{,}6\gamma_{gHC}^2. \tag{5.25}$$

and these values are adjusted for non-hydrocarbon content on the basis of KAY'S mixing rule:

$$\widehat{p}_{pc} = (1 - y_{N_2} - y_{CO_2} - y_{H_2S})p_{pcHC} + y_{N_2}p_{cN_2} + y_{CO_2}p_{cCO_2} + y_{H_2S}p_{cH_2S} \tag{5.26}$$

and

$$\widehat{T}_{pc} = (1 - y_{N_2} - y_{CO_2} - y_{H_2S})T_{pcHC} + y_{N_2}T_{cN_2} + y_{CO_2}T_{cCO_2} + y_{H_2S}T_{cH_2S} \tag{5.27}$$

$\widehat{T}_{pc}$ and $\widehat{p}_{pc}$ are used in the WICHERT-AZIZ equations with CO_2 and H_2S mole fractions to obtain mixture T_{pc} and p_{pc}.

Gases containing significant amounts of CO_2 and H_2S non-hydrocarbons should always be corrected with the WICHERT-AZIZ equations.

5.1.5 Water Content

The conventional gas analysis does not indicate any water content. However, the natural gas in a reservoir is in thermodynamic equilibrium with the connate water. Therefore, the gas is saturated with water vapor. The mole fraction of the water, y_w, can be calculated by the DALTON law (see Eq. 5.8).

$$y_w = \frac{p_w}{p}, \tag{5.28}$$

where

p_w: vapor pressure of water at operating temperature,

p: operating pressure of the system.

The water vapor pressure will be calculated from an empirical correlation by J.L. HAAS as a function of temperature and salinity. Figure 5.6 shows the resulting vapor pressure curves for water and brine.

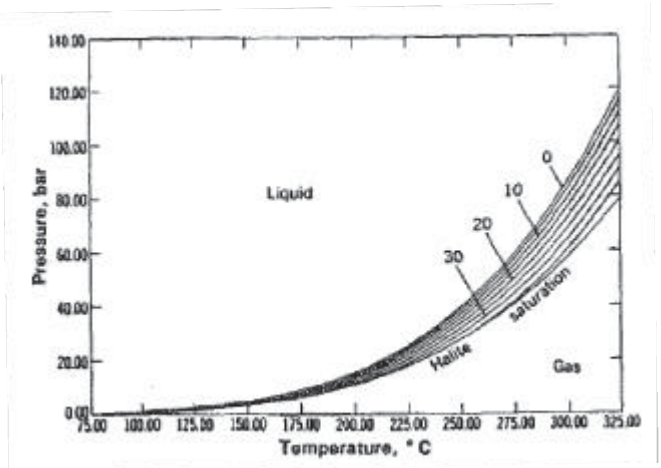

Figure 5.6: Water and brine vapor pressure curves after HAAS

The gas-water ratio $R_{g,w}$ is then obtained from

$$R_{g,w} = 801 \cdot \frac{y_w}{1 - y_w}. \tag{5.1}$$

The coefficient yields $R_{g,w}$ in [kg H_2O/1000 sm^3 gas], if $R_{g,w}$ should be in [STB/MMscf] replace 801 with 135.

The water content of a natural gas as a function of pressure and temperature can be evaluated based on the KATZ chart given in Figure 5.7. Example 5.3 shows the procedure.

Example 5.3

Evaluate the water content of a natural gas as a function of operating pressure and temperature:

This can be done by correlation through Figure 5.7

FIRST STATE: p = 13.8 MPa(2000 psia)

T = 93.3 ^{o}C (200 $^{\circ}$F)

The water content at this state is evaluated through Figure 5.7 as

$3.8\,\mathrm{E}-4 lb/cu\ \mathrm{ft} = 6.1\,E-3 kg/m^3$.

SECOND STATE: p = 3.45 MPa (500 psia)

T = 60 $^{\circ}$C (140 $^{\circ}$F)

The water content at this state was evaluated through Figure 5.7 as

$3.25\,\mathrm{E}-4\ \mathrm{lb}/cu\ \mathrm{ft} = 5.2\,E-3 kg/m^3$.

THIRD STATE: p = 2.8 MPa (400 psia)

T = 60 $^{\circ}$C (140 $^{\circ}$F)

The water content at this state was evaluated through Figure 5.7 as

$3.8\,\mathrm{E}-4\ \mathrm{lb}/cu\ \mathrm{ft} = 6.1\,E-3\ \mathrm{lb}/cu\ \mathrm{ft}$.

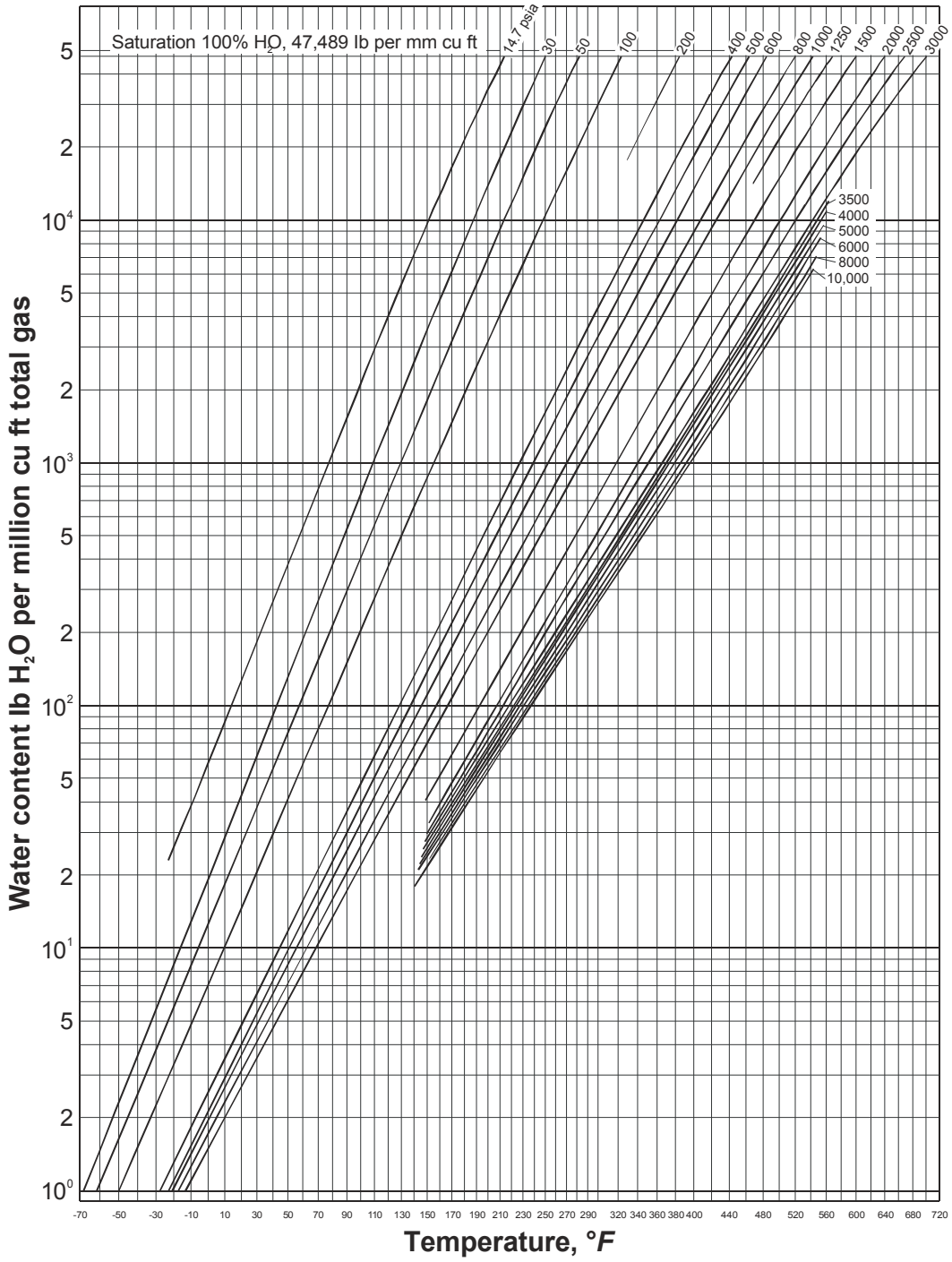

Figure 5.7: Water content of natural gas in equilibrium with liquid water (from KATZ et al., 1959)

Natural gas and liquid water will combine to form solids resembling wet snow at temperatures somewhat above the crystallization temperature of pure water. These solids are called “gas hydrates”. Because these solids can form at temperatures and pressures normally encountered in natural-gas pipelines, this phenomenon is of particular interest to the petroleum industry. The conditions for the gas hydrate formation will be summarized later on.

5.1.6 Viscosity

5.1.6.1 Viscosity of Pure Gases

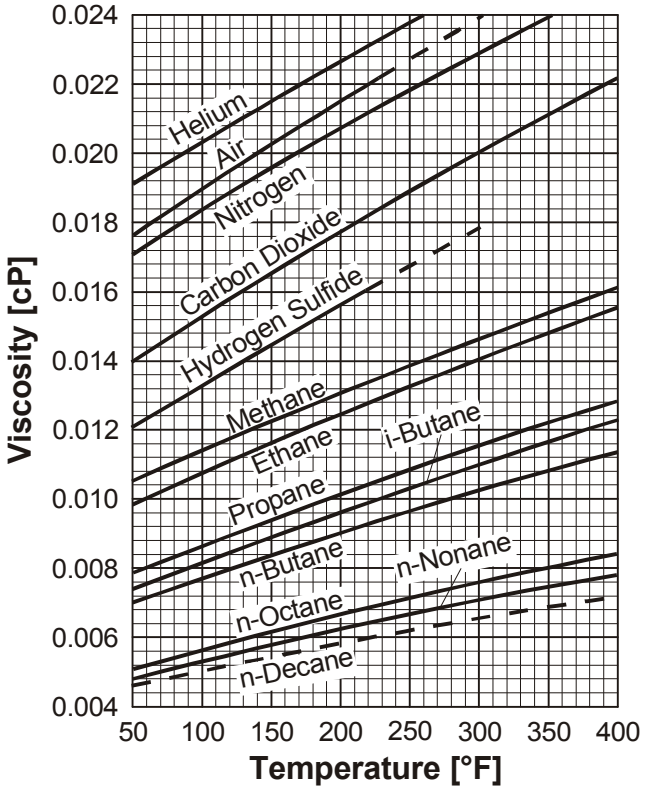

Figure 5.8: Viscosity of gases at atmospheric pressure (from CARR et al., 1954)

In general, the gas viscosity μ_g decreases with the mole weight and increases with the temperature. Figure 5.8 shows the dependence of the viscosity of pure gases on the temperature at atmospheric pressure (0.1 MPa and 14.7 psi, respectively).

5.1.6.2 Viscosity of Natural Gas at Atmospheric Pressure

Figure 5.9 presents the viscosity of natural gases at atmospheric pressure as a function of the average molecular weight. This diagram elucidates that the viscosity decreases along with increasing molecular weight. It also contains correction functions for CO_2, N_2 and H_2S.

Like all intensive physical properties, the viscosity is completely described by

$$\mu = F(p, T, y_1, y_2, y_3 \ldots y_{k-1}) . \tag{5.29}$$

Eq. 5.29 simply states that the viscosity is a function of pressure, temperature and composition.

The correlations (suggested by CARR) presented below may be viewed as modifications of Eq. 5.29. The assumptions are practical because the composition is frequently not known. Anyway, the assumptions are sufficiently valid so that these correlations are frequently used for reservoir engineering computations.

5.1.6.3 Gas Viscosity at Actual Pressure

The theorem of corresponding states has been proved to be valid once more again. The viscosity at any state of the gaseous system can be predicted through the reduced viscosity which is defined by

$$\mu_{g,r}(p_{pr}, T_{pr}) = \frac{\mu_g(p,T)}{\mu_{g,1}(p = 1, T)} . \tag{5.30}$$

The procedure to evaluate μ at certain p and T is the following (see Example 5.4):

- From Figure 5.9, the atmospheric viscosity $\mu_{g,1}$ has to be evaluated for the given gravity (or averaged molecular weight) of the gas and the operating temperature.
- According to Figure 5.4 and Figure 5.5, the pseudo-critical pressure, p_{pc}, and the pseudo-critical temperature, T_{pc}, are determined.
- After the calculation of the pseudo-reduced state quantities p_{pr} and T_{pr}, the reduced viscosity $\mu_{g,r}$, which is given by the ratio between the actual viscosity and the one at atmospheric pressure, is evaluated by use of Figure 5.10.
- The actual gas viscosity can be calculated through Eq. 5.30, where
- $\mu_g = \mu_{g,r}\mu_{g,1}$.

The gas viscosity determined through this method deviates from laboratory measurements by 3% at the maximum. This is a satisfactory solution for practical purposes.

5.1.6.4 LOHRENZ-BRAY-CLARK Correlations

LOHRENZ, BRAY and CLARK have provided a general correlation to calculate the phase viscosity, applicable for gas as well as liquid. The method is described in Chap. 6.

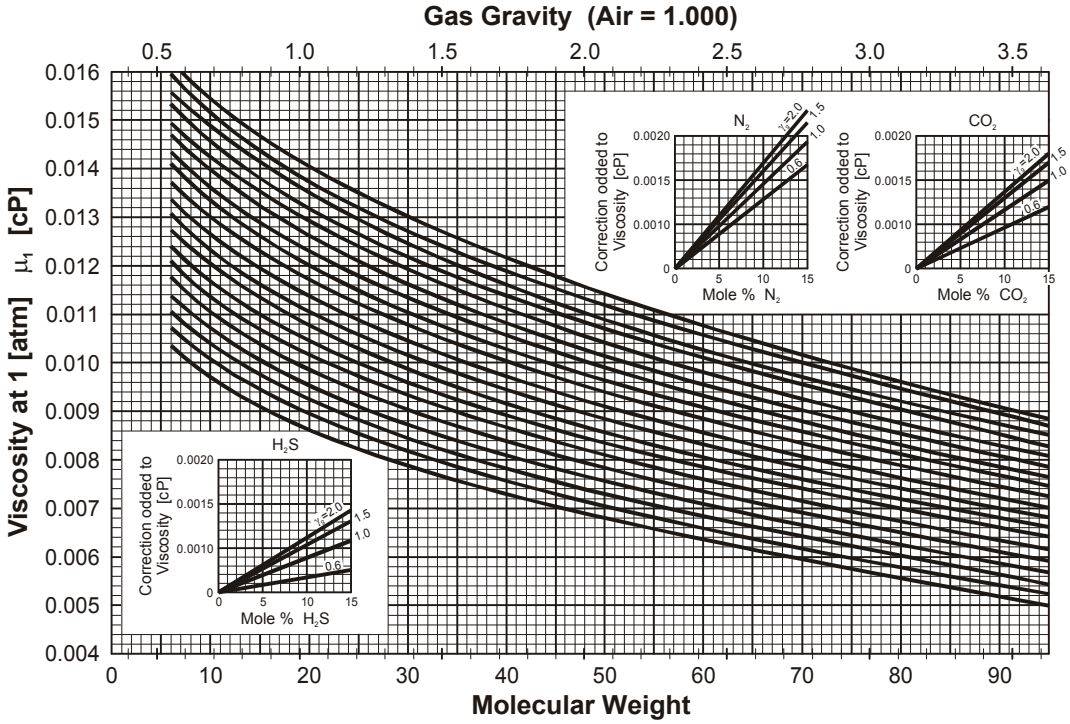

Figure 5.9: Viscosity of natural gases at atmospheric pressure (from CARR et al, 1954)

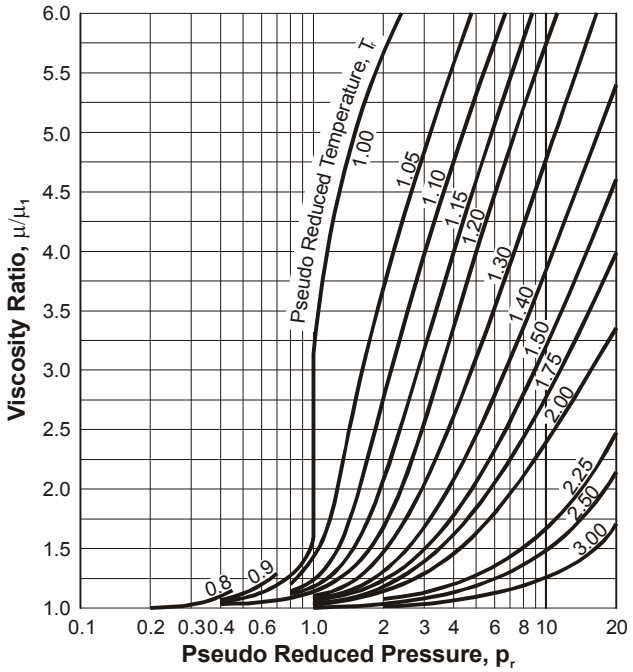

Figure 5.10: Correlation of viscosity ratio with pseudo-reduced pressure and temperature (from CARR et al., 1954)

Example 5.4

Determination of the gas viscosity at temperature *T = 90.5 °C (194.9 °F, 654.7 R)* and at pressure *p = 12.5 MPa (1800 psia)*. The specific gas gravity was found as $\gamma_g = 0.7018$.

From Figure 5.9, the viscosity at atmospheric pressure and operating temperature can be read off as

$$\mu_{g,1} = 0.0122\text{cP}.$$

Then the pseudo-critical data of the system are evaluated from Figure 5.5 where

$$p_{pc} = 670\,psia$$

and

$$T_{pc} = 385^{o}R.$$

The calculation of the pseudo-reduced data of the system result in

$$p_{pr} = \frac{p}{p_{pc}} = \frac{1800}{670} = 2.69$$

and

$$\frac{T}{T_{pc}} = \frac{654.6}{385} = 1.70\,.$$

The ratio between the actual gas viscosity, $\mu_{g,,}$ and its viscosity at atmospheric pressure, $\mu_{g,1}$, can now be read off from Figure 5.10:

$$\mu_{g,r} = 1.35\,,$$

so that

$$\mu_g = \mu_{g,r} \times \mu_{g,1} = 1.35 \times 0.0122 = 0.0165\,cP$$

and

$$\mu_g = 0.0165\ \text{mPa s}\,,$$

respectively.

5.2 Hydrocarbon Liquids

5.2.1 Volume and Density

5.2.1.1 STANDING and KATZ Method

For practical purposes, it is sufficient to consider hydrocarbon liquids as ideal mixtures whose volumes can be calculated by adding up the volumes of the components.

The interesting properties (density, viscosity, etc.), which depend on the oil composition, can be easily determined at the standard (normal) state (atmospheric pressure and T = 60°F (15 °C)). The theorem of corresponding states can be applied again to determine the properties at any other state of the system (e.g. at reservoir conditions).

However, a crude oil does not remain in the single-phase state at "normal" conditions if it contains any high mole fraction of light components which will be liberated at atmospheric pressure and surface temperature. This inconvenience can be avoided by attributing "apparent densities" or "apparent specific volumes" at standard conditions to the dissolved and easily volatilized components. Then the respective "pseudo-liquid" data of any hydrocarbon liquid at standard conditions may be evaluated from the real one at standard conditions and from the apparent data of the liberated light components.

STANDING and KATZ (1942) examined the properties of many crude oils. They established that the apparent densities of the two light components methane and ethane depend on the density of the system (see Figure 5.11). Based on these data and assuming that propane and heavier components follow the rule of additive volumes, they developed a method for computing the density of hydrocarbon mixtures.

It is based on Figure 5.12 presenting the correlation of the density of a system containing methane and ethane with the density of the propanes-plus fraction, the weight -% ethane in the ethanes-plus and the weight-% methane in the system.

The density of the propane-plus can be calculated through

$$\rho_{C3+} = \frac{\sum_{i=3}^{k} z_i M_i}{\sum_{i=3}^{k} V_i} . \qquad (5.31)$$

The weight -% ethane in the ethane-plus material can be calculated through

$$w_{C2} = \frac{z_2 M_2}{\sum_{i=2}^{k} z_i M_i} \times 100 \tag{5.32}$$

and the weight -% methane in the entire system through

$$w_{C1} = \frac{z_1 M_1}{\sum_{i=1}^{k} z_i M_i} \times 100\,. \tag{5.33}$$

Then, the resulting pseudo-liquid density of the system containing methane and ethane has to be corrected with regard to the operating temperature and pressure. Figure 5.13 and Figure 5.14 serve this purpose. This calculation procedure is also presented through Example 5.5.

The correlation method after STANDING and KATZ is satisfactory for stock-tank liquids which have low concentrations of methane and ethane.

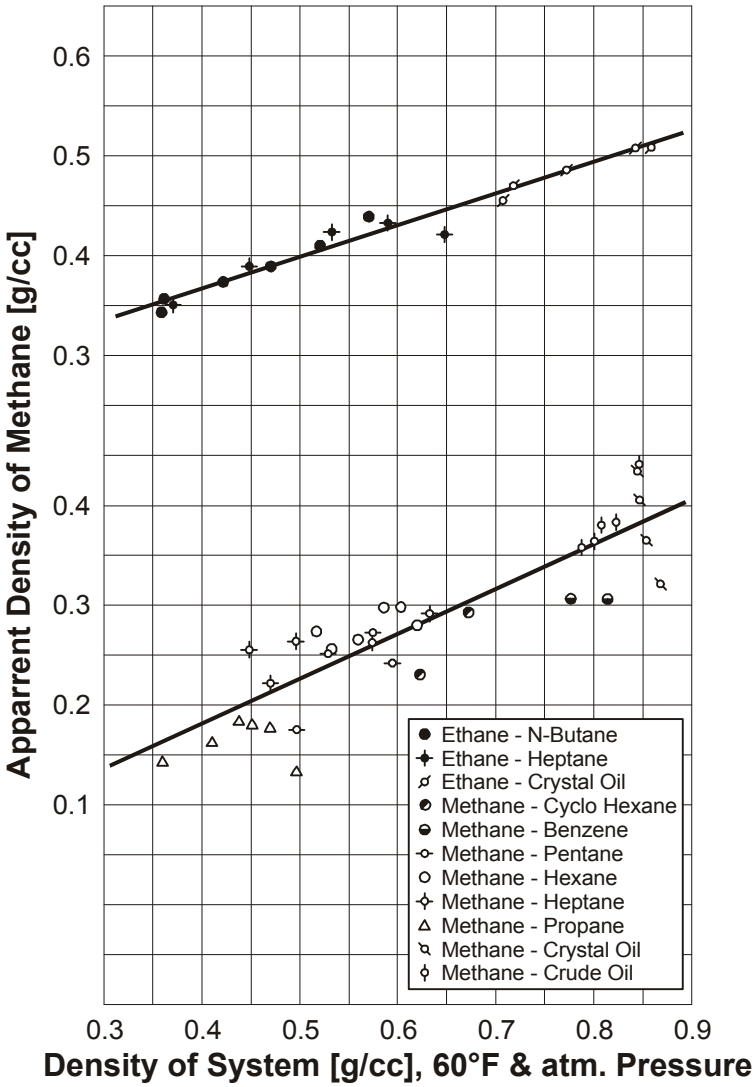

Figure 5.11: Variation of apparent density of methane and ethane with density of the system (from STANDING and KATZ, 1942)

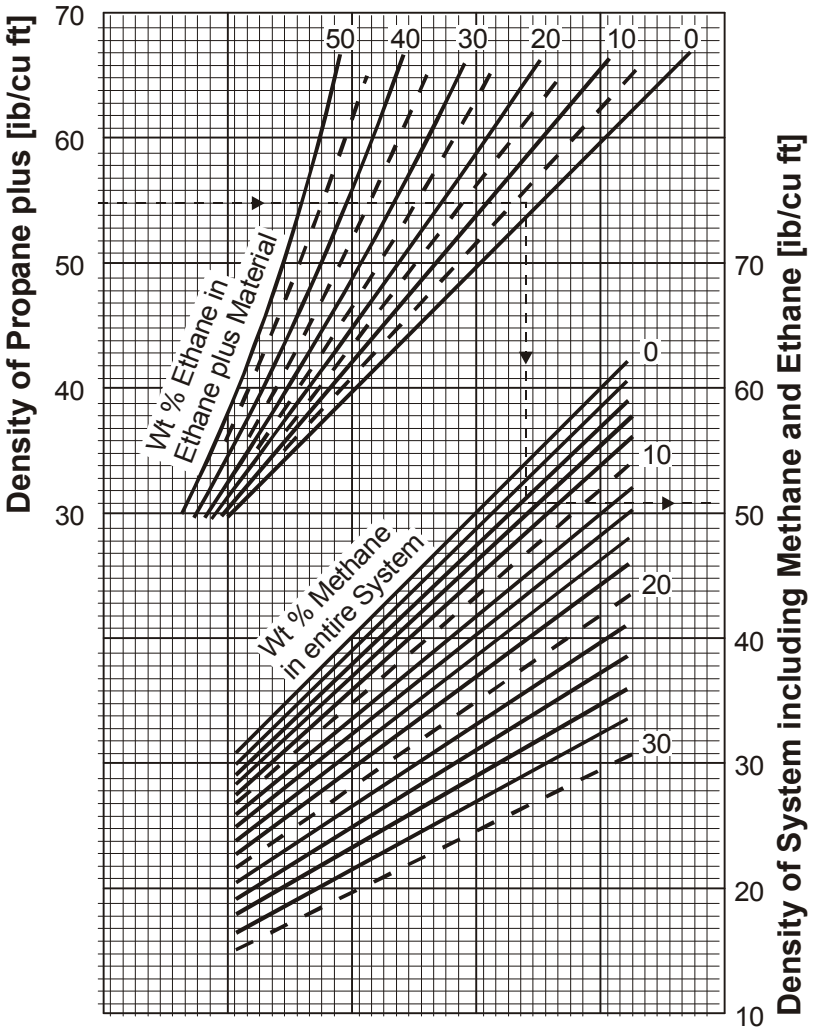

Figure 5.12: Pseudo-liquid density of systems containing methane and ethane (from STANDING, 1952)

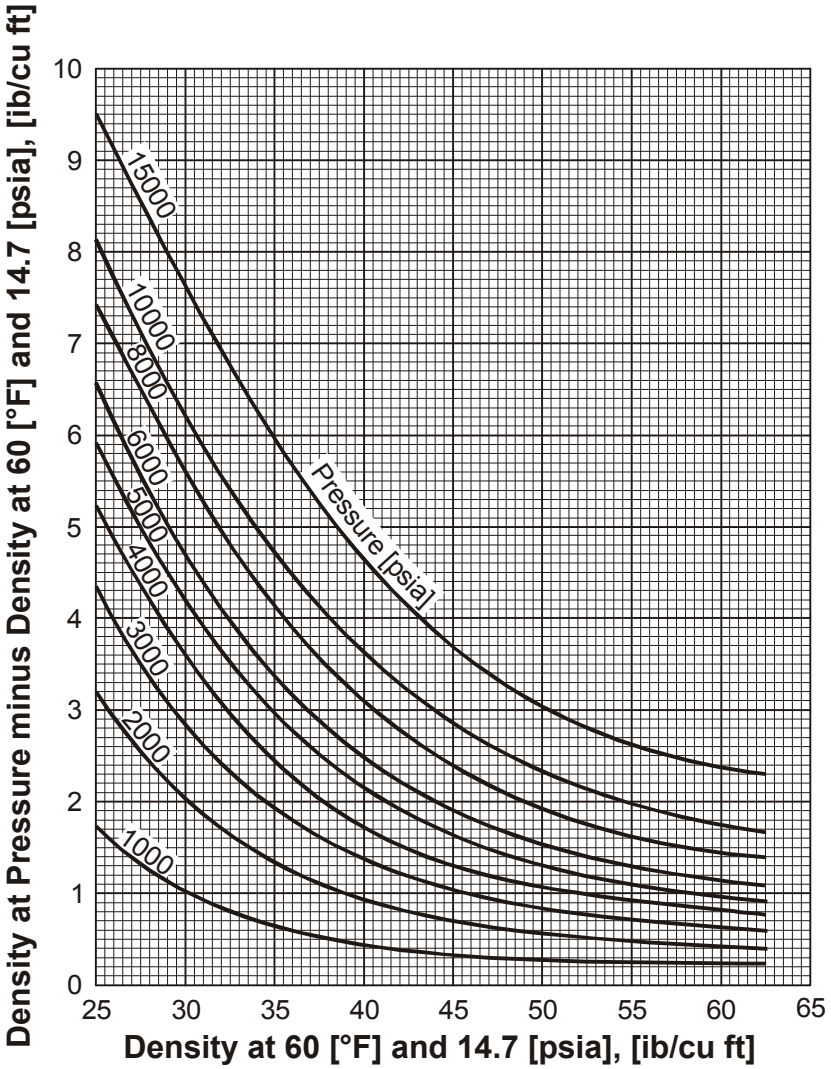

Figure 5.13: Density correction for compressibility of liquids (from STANDING, 1952)

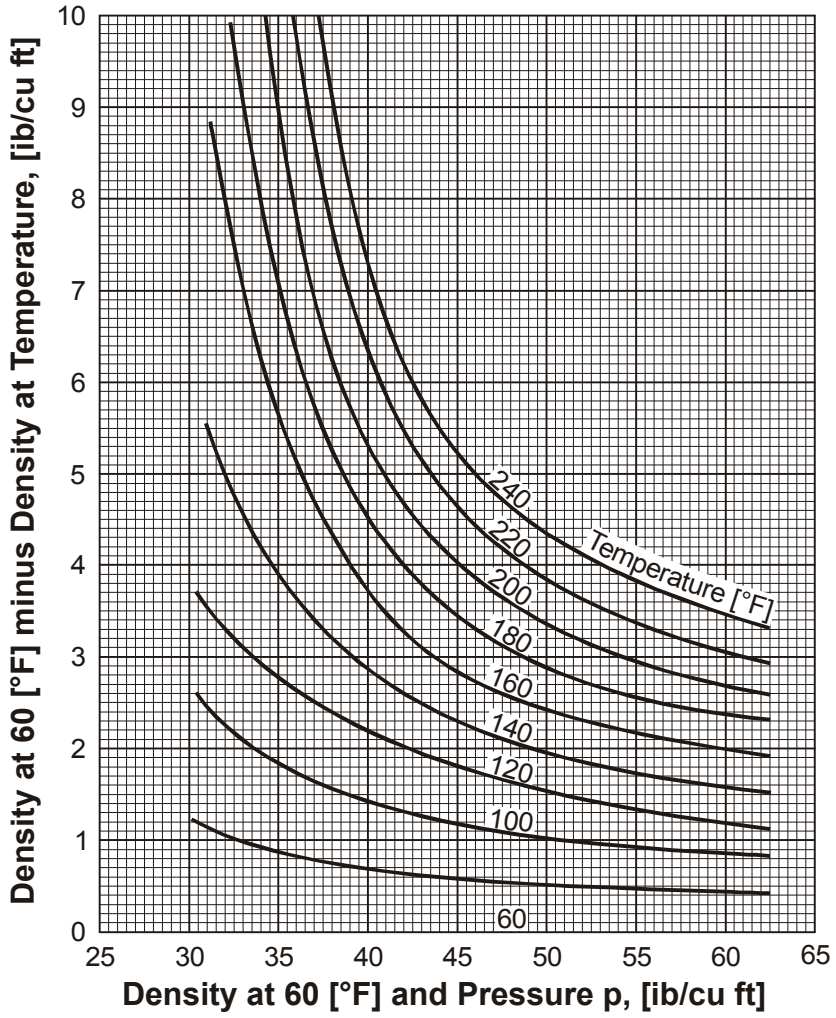

Figure 5.14: Density correction for thermal expansion of liquids
(from STANDING, 1952)

Example 5.5

Determination of the volume of 1 mole oil at bubble point through STANDING-KATZ correlations. The bubble point is defined by

$$p_{ob} = 3300 psia (22.55 MPa)$$

and

$$T_{ob} = 220^{o} F (105 °C).$$

The composition of the system is tabled below.

Composition	Mole Fraction $z_i = x_i$	Mole Weight M_i kg/kmole	$z_i M_i$	Density ρ_i kg/m^3	Volume V_i^* m^3
C_1	0.4404	16.0	7.046		
C_2	0.0432	30.1	1.300		
C_3	0.0405	44.1	1.786	507.5	0.0035
C_4	0.0284	58.1	1.650	575.0	0.0029
C_5	0.0174	72.2	1.256	626.0	0.0020
C_6	0.0290	86.2	2.500	662.5	0.0038
C_{7+}	0.4001	287.0	114.829	907.0	0.1271
Σ	1.0000		130.367		0.1393

*) at standard conditions: 0.1 MPa, 15°C

The density of the propane-plus can be calculated through

$$\frac{\sum_{i=3}^{k} z_i M_i}{\sum_{i=3}^{k} V_i} = \frac{122.021}{0.1393} = 876 kg/m^3 = 54.69\ lb/cu\text{ft}.$$

Then the weight -% ethane in the ethane-plus material

$$\frac{z_2 M_2}{\sum_{i=2}^{k} z_i M_i} \times 100 \times \frac{1.300}{123.321} \times 100 = 1.05[\%]$$

and the weight -% methane in the entire system

$$\frac{z_1 M_1}{\sum_{i=1}^{k} z_i M_i} \times 100 = \frac{7.046}{130.367} \times 100 = 5.4\%$$

are calculated.

From Figure 5.12, the pseudo-liquid density of the hydrocarbon mixture at standard conditions is read off as *51.5 lb/cu ft.*

From Figure 5.13, the pressure correction for p_{ob} (3300 psia) is read off as

0.9 lb/cu ft

so that the liquid density at 3300 psia and 60°F results in

51.5 + 0.9 = 52.4 lb/cu ft.

Then the temperature correction for 220° F is read off from Figure 6.13 as

3.7 lb/cu ft

so that the oil density at 3300 psia and 220°F results in

$$\rho_{ob} = 52.4 - 3.7 = 48.7\ lb/cu\ \text{ft}$$

and

$$\rho_{ob} = 778.5 kg/m^3,$$

respectively.

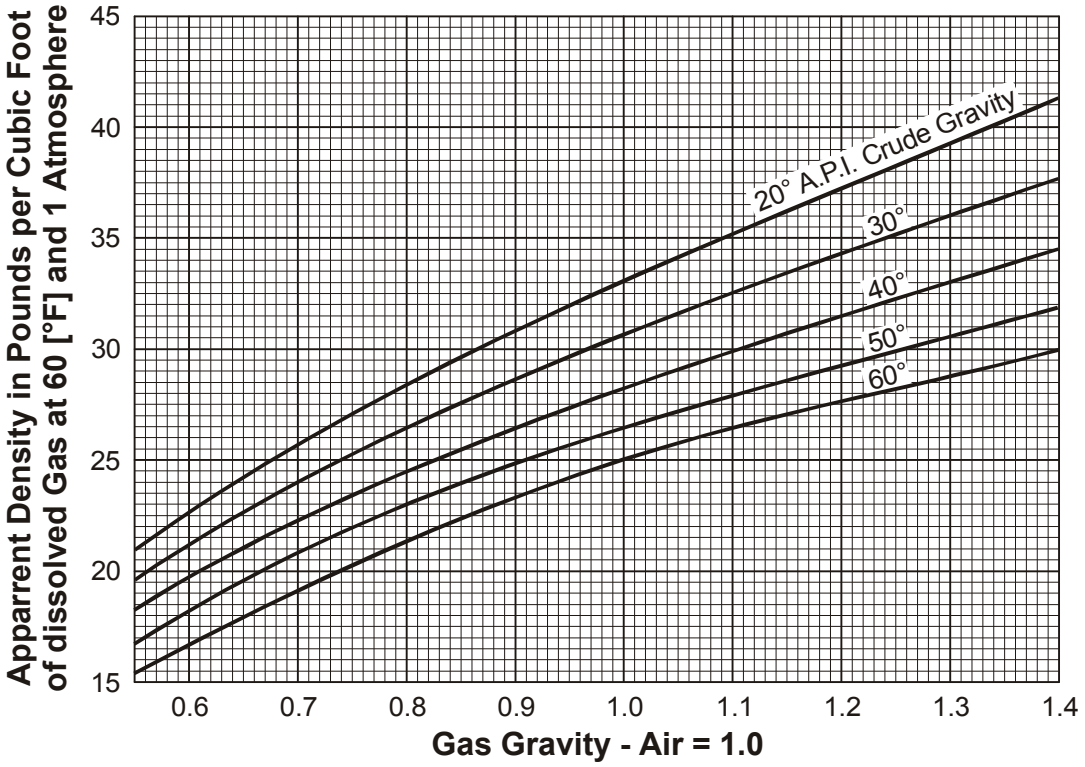

Figure 5.15: Apparent liquid density of natural gases in various API gravity oils (from KATZ, 1952)

Natural gases (dissolved gas) predominantly consist of methane. Therefore, KATZ (1942) has applied the method of the apparent liquid volume also to crude oil - natural gas systems. The easily volatilized component is marked by its gravity, γ_g, and the scarcely

volatilized fraction is the crude oil with the density ρ_o and its gravity γ_o (in °API) at standard conditions. The apparent liquid density of the respective natural gas can be determined according to Figure 5.15.

The amount of the dissolved gas is always indicated as the number of normal cubic meter per actual liquid volume at standard conditions, nm^3/m^3. This ratio is designated as R_S (solution ratio). In terms of the production, the ratio is also often designated as GOR (producing gas - oil ratio).

In other words: R_S expresses how much gas will be dissolved in one cubic meter oil (volume at standard conditions) at the operating conditions. Therefore, R_S depends on pressure and temperature, but also on the oil quality.

5.2.2 Formation Volume Factor

5.2.2.1 Definition

The oil volume inside the tank at surface conditions differs from the volume of the oil leaving the reservoir. This change in volume has three main sources:

- The most important factor is the gas liberation below bubble point pressure $p_{ob.}$
- The difference between reservoir pressure and atmospheric pressure causes slight expansion of the remaining oil phase.
- The increase in volume because of expansion is more or less compensated by the shrinkage of the oil resulting from the transfer from reservoir to surface temperature.

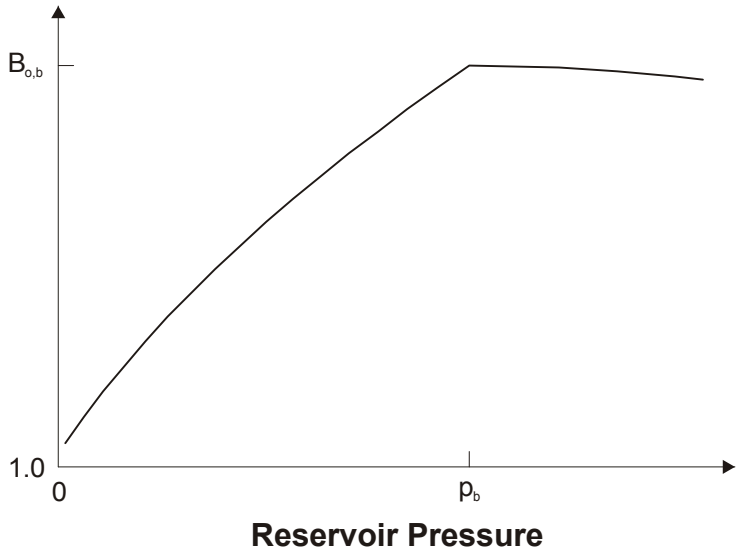

Figure 5.16: Typical graph of formation-volume factor of oil against pressure

The formation volume factor of the oil phase, which must be taken into account, is defined as

$$B_o = \frac{\text{oil volume and volume of dissolved gas at reservoir conditions}}{\text{oil volume at standard conditions}}.$$

Correspondingly, B_o can be defined as the volume of one cubic meter tank oil (oil at standard conditions) at certain operating pressure and temperature.

Figure 5.16 illustrates typical characteristics the relationship between B_o and p. As long as the pressure does not fall below the bubble point pressure p_{ob} during a pressure decrease from initial reservoir conditions, change in B_o will be ruled by the expansion of the oil. As soon as the reservoir pressure falls below p_{ob}, gas will be liberated. This gas liberation results in a shrinkage of the oil volume. Thus, B_o decreases at decreasing pressure as soon as p_{ob} has been crossed.

The reciprocal value of B_o is called "shrinkage factor".

By multiplying the tank oil volume with the actual B_o, the volume of the oil inside the reservoir is obtained. On the other side, the multiplication of the shrinkage factor with the volume inside the reservoir will result in the stock oil volume.

5.2.2.2 STANDING Nomograms

On the basis of many investigations, STANDING (1947) amplified the correlation to permit the calculation of bubble point pressures and volume factors, B_o. The respective STANDING charts are appended at the end of this textbook:

- Working with Chart 1, it is possible to take the solution ratio, gas gravity, tank oil gravity and reservoir temperature to determine the pressure at which the given amount of gas would be in solution. This pressure is the bubble point pressure of the respective hydrocarbon system, p_{ob}.
- Charts 2 permits the evaluation of B_o at bubble point conditions if *GOR* represents the solution ratio.
- The total formation volume factor, B_t, can be estimated by use of Chart 3. B_t is defined by

$$B_t = B_o + (R_{si} - R_s)B_g, \tag{5.34}$$

where

B_o: volume factor of the actual oil phase

B_g: volume factor of the actual gas phase

$R_{s,i}$: solution ratio at initial conditions

R_s: solution ratio at operating conditions.

B_o can be evaluated

- by use of the KATZ correlation (see Figure 5.15) and the STANDING diagrams (see Figure 5.13 and Figure 5.14)
- or by use of the Charts from STANDING (see appendix).

In most cases, these empirical correlations (see Example 6.6) yield values which are comparable within 3 or 4% to measured laboratory data.

Example 5.6

Evaluation of the oil volume factor at bubble point conditions from operation data tabled below both in SI-units and Field-units. The thermodynamic data of the system were given in Example 5.5. The calculation is based on one cubic meter tank oil.

	GOR $nm^3/m^3]$	GOR *cu ft/bbl*	γ_g	ρ_o kg/m^3	γ_o ^oAPI
Separator 1	74	415.5	0.640		
Separator 2	16	89.8	0.897		
Tank	4	22.5	1.540	876.2	30
SUM	94	527.8	-	-	-

In summing up the producing gas/oil ratios GOR, the initial solution ratio R_{si} results in

$$R_{si} = 94 nm^3/m^3$$

and

$$R_{si} = 527.8 \text{ cu ft}/bbl$$

respectively.

The computation of the average specific gas gravity results in

$$\gamma_g = \frac{74 \times 0.640 + 16 \times 0.897 + 4 \times 1.540}{74 + 16 + 4} = \frac{67.9}{94} = 0.722.$$

Now the amount of gas can be calculated through

$$m_g = R_{si} \varsigma_a \gamma_g ,$$

where ρ_a is the air density:

$m_g = 94 \times 1.225 \times 0.722 = 83.1$ kg

Because the specific gravities are given as

$\gamma_g = 0.722$

and

$\gamma_o = 30^\circ$ API,

the apparent liquid density of the gas can be evaluated through Figure 5.15 as

$$\rho_{g,a} = 24.3 \text{ lb/cu ft}$$

and

$$\rho_{g,a} = 389.2 \text{ kg/m}^3,$$

respectively.

Now the apparent liquid volume of the liberated gas at standard conditions *(T =15 °C* and atmospheric pressure) can be calculated through

$$V_{g,app} = \frac{m_g}{\rho_{g,a}},$$

and so

$$V_{g,app} = \frac{83.1}{389.2} = 0.214 \text{ m}^3.$$

In summarizing 1 m^3 tank oil and 0.214 m^3 apparent liquid volume of the liberated gas, as well as 876.2 kg tank oil and 83.1kg liberated gas,the pseudo-liquid density of the given hydrocarbon system at standard conditions results in

$$\rho_{o,app} = \frac{876.2 + 83.1}{1000 + 0.214} = 790.2 kg/m^3,$$

and so

$$\rho_{o,app} = 49.3 \text{ lb/cu ft}.$$

From Figure 5.13, the pressure correction of this density for *p = 3300* psia results in

$$\rho_o = 49.3 + 0.9 = 50.2 \text{ lb/cu ft}.$$

From Figure 5.14, the final temperature correction for T = 220 °F results in

$$\rho_o = 50.2 - 3.8 = 46.4\ lb/cu\,ft,$$

or, in SI-units, respectively, in

$$\rho_o = 743.7 kg/m^3.$$

On the basis of the calculated oil density under the conditions of the reservoir, the volume of one cubic meter oil under reservoir conditions results in

$$V_{ob} = \frac{959.3}{743.7} = 1.29 m^3,$$

and so

$$B_{ob} = 1.29.$$

In other words: 1.288 m^3 saturated reservoir liquid under reservoir conditions shrinks to 1 m^3 tank oil. The shrinkage results in

$$\frac{1.29 - 1.000}{1.29} \times 100 = 22.48\%.$$

5.2.3 Compressibility of Undersaturated Liquids

An undersaturated oil is a compressed liquid in the pressure range above the bubble point pressure p_b. Its isothermal compressibility is to be calculated in the same way as for the gases (see Eq. 5.10) so that

$$c_o = -\frac{1}{V}\left(\frac{\partial V}{\partial p}\right)_T = \frac{1}{B_o}\left(\frac{\partial B_o}{\partial p}\right)_T, \tag{5.35}$$

and after integration

$$B_o = B_{ob} e^{-c_o (p - p_b)}. \tag{5.36}$$

Because

$$\rho_o = \frac{C}{B_o},$$

where C is a constant, the density of an undersaturated oil phase can be calculated through

$$\rho_o = \rho_{ob} e^{c_o (p - p_b)}. \tag{5.37}$$

In general, the bubble point pressure, $p_{b,}$ is chosen as reference. Eq. 5.20 and Eq. 5.21 will develop in a Taylor series. Because c_o is very small, the terms of higher order can be disregarded so that

$$B_o \tilde{-} B_{ob}[1 - c_o(p - p_b)], \tag{5.38}$$

and

$$\rho_o = \rho_{o,b}[1 + c_o(p - p_b)]. \tag{5.39}$$

Similar formulae are also valid for water.

The compressibility of undersaturated liquids is constant within wide pressure intervals. Therefore, it can be calculated between any two states of the system, (V_1, p_1) and (V_2, p_2) by

$$c_o = -\frac{V_1 - V_2}{\overline{V}(p_1 - p_2)}, \tag{5.40}$$

where $\overline{V}$ is averaged volume between p_1 and p_2.

5.2.3.1 TRUBE Correlation

This method is based on the determination of the pseudo-critical data of the system and on the evaluation of the pseudo-reduced compressibility of the undersaturated liquid, c_r as a function the pseudo-reduced pressure, p_{pr}, and pseudo-reduced temperature, T_{pr} (see Figure 5.17). Then the oil compressibility can be calculated through

$$c_o = c_r / p_{pc}. \tag{5.41}$$

If the composition of the undersaturated system is not known, the pseudo-reduced pressure and temperature can be approximately evaluated through Figure 5.18 on the basis of

- the calculation of the pseudo-liquid density of the hydrocarbon mixture at standard conditions (see procedure of Example 5.6),
- the pressure correction of this pseudo-liquid density from Figure 5.13.

Then, the evaluated oil density is related to the density of water at the standard temperature, $\rho_w = 1000 kg/m^3$.

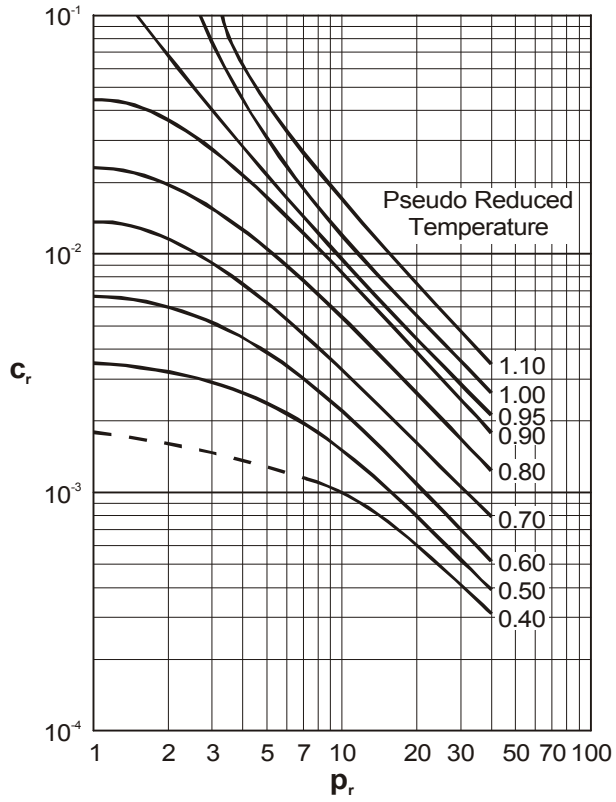

Figure 5.17: Pseudo-reduced compressibility for undersaturated reservoir fluids (from TRUBE, 1957)

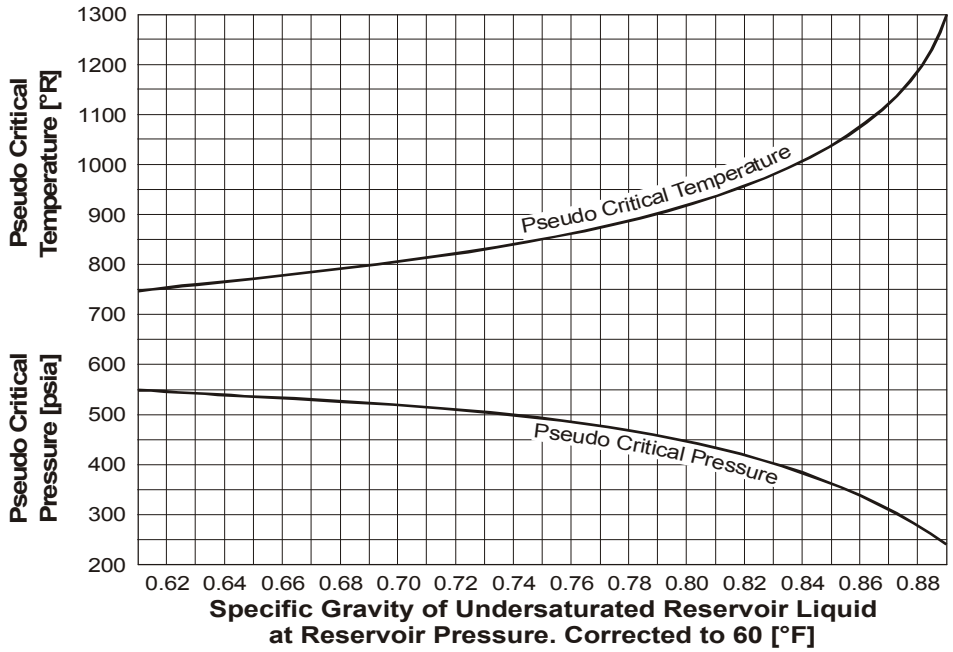

Figure 5.18: Pseudo-critical conditions of undersaturated reservoir liquids (from TRUBE, 1957)

Example 5.7

Evaluation of B_{oi} for an under saturated oil at reservoir temperature $T = 105\ ^{o}C$ and under the initial pressure $p_i = 25\ MPa$ through the reduced compressibility from TRUBE. The composition of the system was given in Example 5.5 and B_{ob} was calculated through Example 5.6. The critical data are tabled below.

The computation of the pseudo-reduced temperature and pressure results in

$$T_{pr} = \frac{T}{T_{pc}} = \frac{105 + 273.15}{374.70} = 1.01$$

and

$$.p_{pr} = \frac{p}{p_{pc}} = \frac{25}{3.655} = 6.84\,.$$

From Figure 5.17, the reduced compressibility can be read off as

$$c_r = 0.02\,.$$

The compressibility of the undersaturated oil phase can be calculated through

$$c_o = \frac{c_r}{p_{pc}} = \frac{0.02}{6.84} = 2.92\,\mathrm{E}-3 MPa^{-1}\,.$$

Because

$$B_{o,b} = 1.29\,,$$

(see Example 5.6), B_{oi} can be calculated through Eq. 5.39

$$B_{oi} = B_{ob}[1 - c_o(p_i - p_b)]$$

and results in

$B_{oi} = 1.29[1 - 0.00292(25 - 22.5)] = 1.281.$

Strictly speaking, the compressibility of an oil mixture is defined only for pressures greater then the bubblepoint pressure. If an oil is at its bubblepoint, the compressibility can be determined and defined only for a positive change in pressure. A reduction of pressure from the bubblepoint results in gas coming out of the solution and, subsequently, a change in mass of the original system for which compressibility is to be determined. Implicit in the definition of compressibility is that the system mass remains constant.

5.2.3.2 VAZQUES-BEGGS Correlation

VAZQUEZ and BEGGS suggested the following correlation for the evaluation of the instantaneous undersaturated oil compressibility, as a function of the dissolved gas, R_s, temperature, T, pressure, p, oil and gas gravity, γ_o and γ_g:

$$c_o = \frac{A}{p}, \tag{5.42}$$

where

$$A = 10^{-5}(5R_{sb} + 17{,}2T - 1{,}180\gamma_{gc} + 12{,}61\gamma_{API} - 1{,}433), \tag{5.43}$$

with the oil compressibility, c_o, in psi^{-1}, the Gas-Solution-Ratio at bubble point, R_{sb}, in scf/STB, the temperature, T, in °F, and the pressure, p, in psia.

γ_{API} is the oil gravity and γ_{gc} is the corrected separator gas specific gravity:

The gas gravity is a strong correlation parameter and unfortunately usually is one of the variables of most questionable accuracy, because it depends on conditions at which the gas/oil separation is made. For this reason VAZQUEZ and BEGGS decided to use a value of gas gravity obtained from particular conditions of separator pressure. The value of 100 psig was chosen as a reference pressure because it was the pressure resulting in a minimum oil shrinkage for the separator tests available.

Therefore, the gas gravity first must be corrected to the value that would have resulted from a separation at 100 psig. Regression analysis resulted in the following equation for correcting gas gravity for separator conditions:

$$\gamma_{gc} = \gamma_{g,sep} \cdot \left[1 + 5{,}912 \times 10^{-5}\gamma_o T \log\left(\frac{p}{114{,}7}\right)\right], \tag{5.44}$$

where

γ_{gc} is the corrected gas gravity,
$\gamma_{g,sep}$ is the gas gravity obtained at actual separator conditions,
p is the actual separator pressure in psia
T is the actual separator temperature in °F, and
γ_o is the oil gravity in °API.

With this correlation for the oil compressibility, undersaturated oil formation volume factor can be calculated analytically from

$$B_o = B_{ob}\left(\frac{p_b}{p}\right)^A. \tag{5.45}$$

If measured pressure/volume data are available, these data can be used to determine A by

plotting V_o/V_{ob} vs. p/p_b on a log-log paper. Constant A can then be used to compute compressibilities from the simple relation $c_o=A/p$. Constant A determined in this way is a useful correlating parameter, one that helps to identify erroneous undersaturated p-V_o data.

5.2.3.3 STANDING Correlation

STANDING gives a graphical correlation for undersaturated c_o, see Figure 5.19, that can be represented by

$$c_o = 10^{-6} \exp\left[\frac{\rho_{ob} + 0{,}004347(p - p_b) - 79{,}1}{(7{,}141 \times 10^{-4})(p - p_b) - 12{,}938}\right], \tag{5.46}$$

with c_o in psi^{-1}, ρ_{ob} in lbm/ft³, and p in psia.

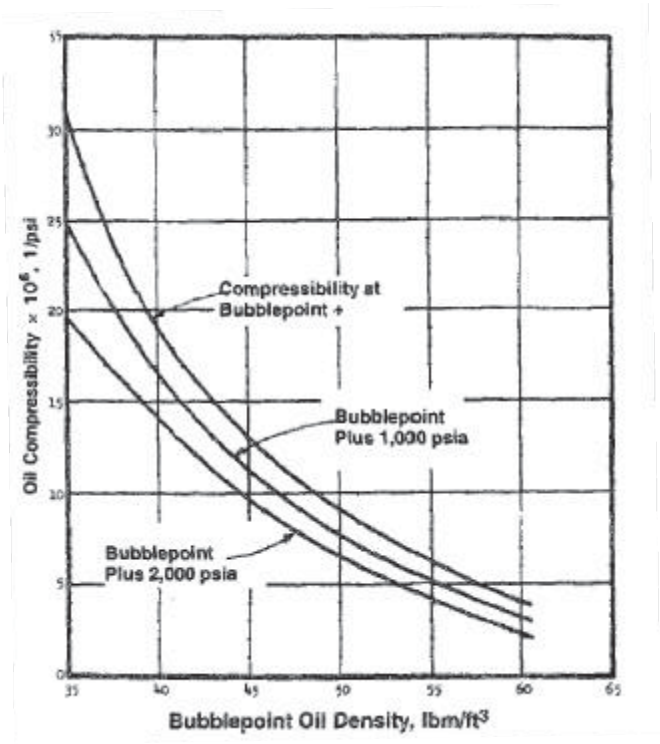

Figure 5.19: Undersaturated oil compressibility (from STANDING)

5.2.3.4 Volume Translation

One weakness of the conventional Equations of State is the bad prediction of liquid properties, such as the liquid density. Further, the prediction of the critical Z-value was

erroneous: For hydrocarbons, $Z_c < 0.29$ was measured, however, the VAN DER WAALS Equations results in 0.375. The values from the REDLICH-KWONG Equation and the PENG-ROBINSON EOS are better, 0.335 and 0.307, but still not satisfactory.

Usually, the molar volume is calculated from the Z-Factor:

$$V_M^{EOS} = \frac{RTZ}{p} \tag{5.47}$$

PENELOUX et al. proposed the following correction term for the molar volume:

$$V_M = V_M^{EOS} - c\,, \tag{5.48}$$

where V_M^{EOS} is the volume calculated with the cubic EOS, V_M is the corrected volume and c is a component specific parameter, which is often referred to as a third EOS parameter, besides a and b.

This shift in volume is like adding a third parameter to the EOS, but the correction does not change the vapor-liquid equilibrium conditions.

PENELOUX et al. also showed that there is no influence in equilibrium conditions and volumes by defining the correction term c as:

$$c = \sum_{i=1}^{N_c} c_i x_i\,. \tag{5.49}$$

They determined c_i to match saturated liquid density at $T_r = 0.7$ for the first ten n-Alkanes.

JAHVERI and YOUNGREN introduced a relationship between b_i and c_i:

$c_i = s_i b_i$ where s_i is the Dimensionless Shift Parameter.

5.2.4 Viscosity

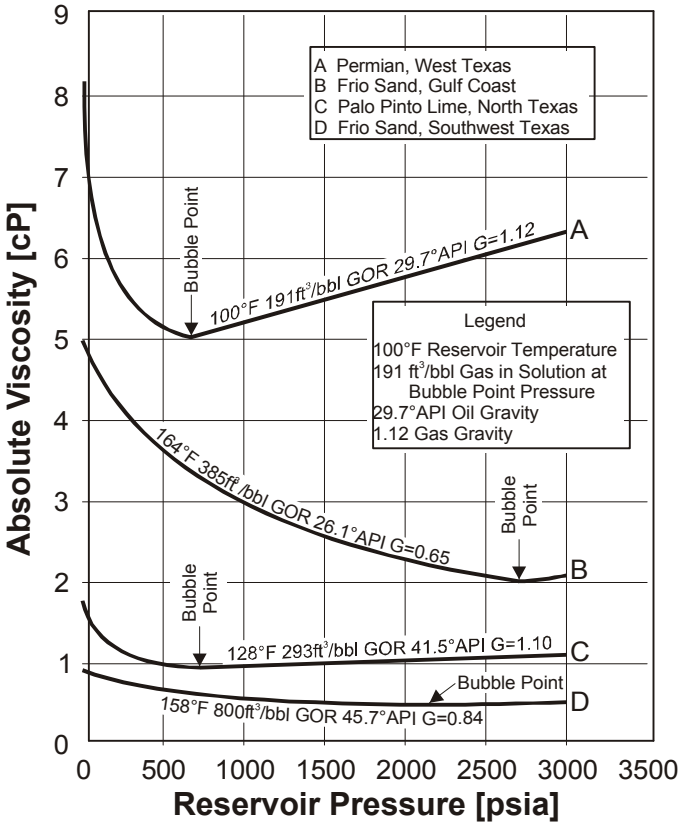

Figure 5.20: Viscosity of subsurface samples of crude oil (from HOCOTT and BUCKLEY, 1941, after BEAL, 1946)

In general, liquids decrease in viscosity with increasing temperature and increase in viscosity with increasing pressure. HOCOTT and BUCKLEY (1941) presented measurements of the viscosity of crude oils containing dissolved gases. Figure 5.20 demonstrates that with increasing pressure, the viscosity decreases up to the bubble point because of the increasing fraction of light components. The dependence on pressure is more significant for high viscous oils than for low viscous oils. Anyway, above the bubble point pressure, the viscosity increases with increasing pressure.

The viscosity of the crude oil can be determined with sufficient accurancy on the basis of the known viscosity of the tank oil μ_1 at the reservoir temperature T and atmospherical pressure, the solution ratio R_{si} and the undersaturated pressure in the reservoir, $\Delta p = p_i - p_b$. Example 5.8 elucidates the respective correlation procedure.

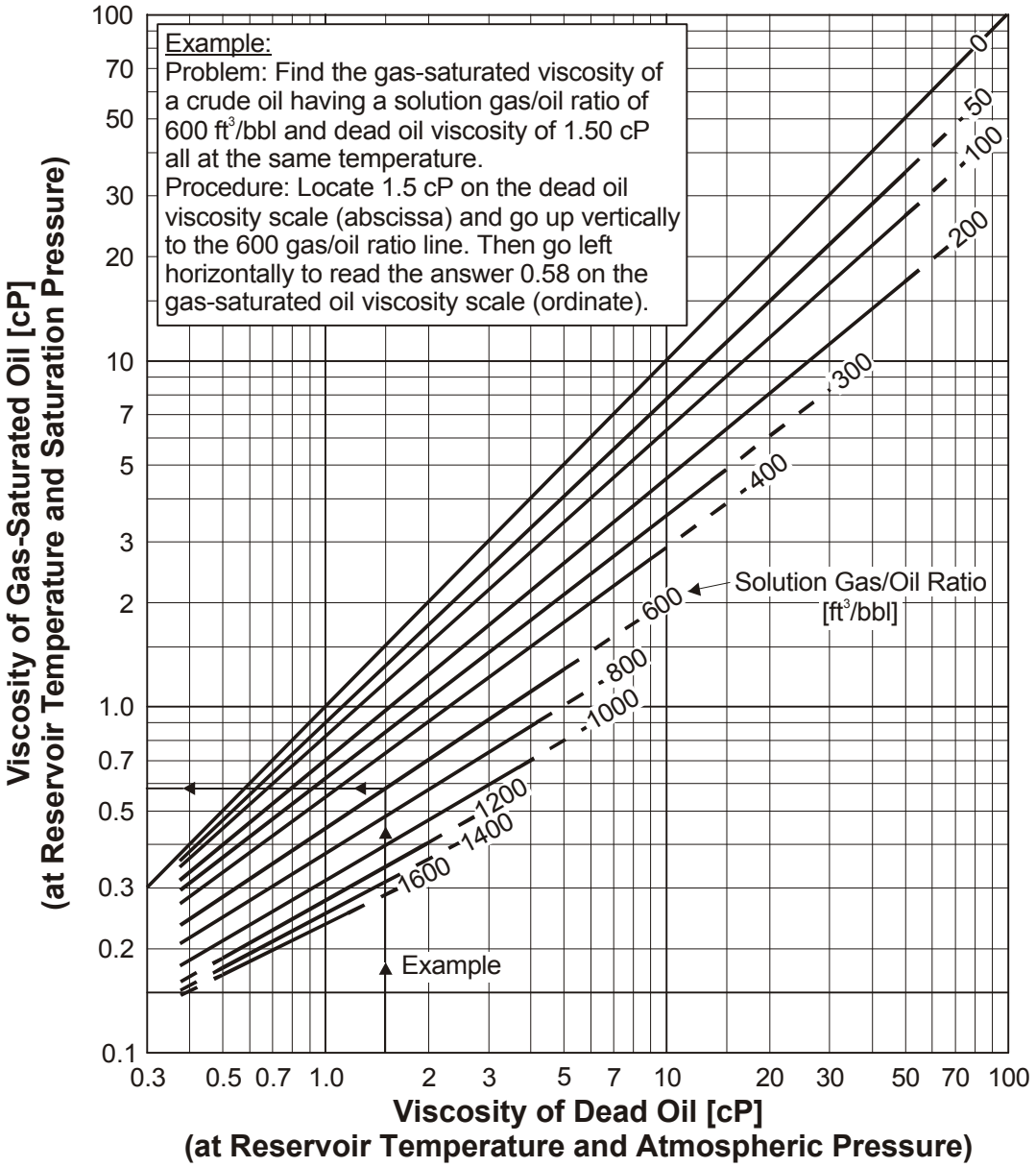

Figure 5.21: Viscosity of gas-saturated reservoir crude oils at reservoir conditions (from CHEW and CONNALLY, 1959)

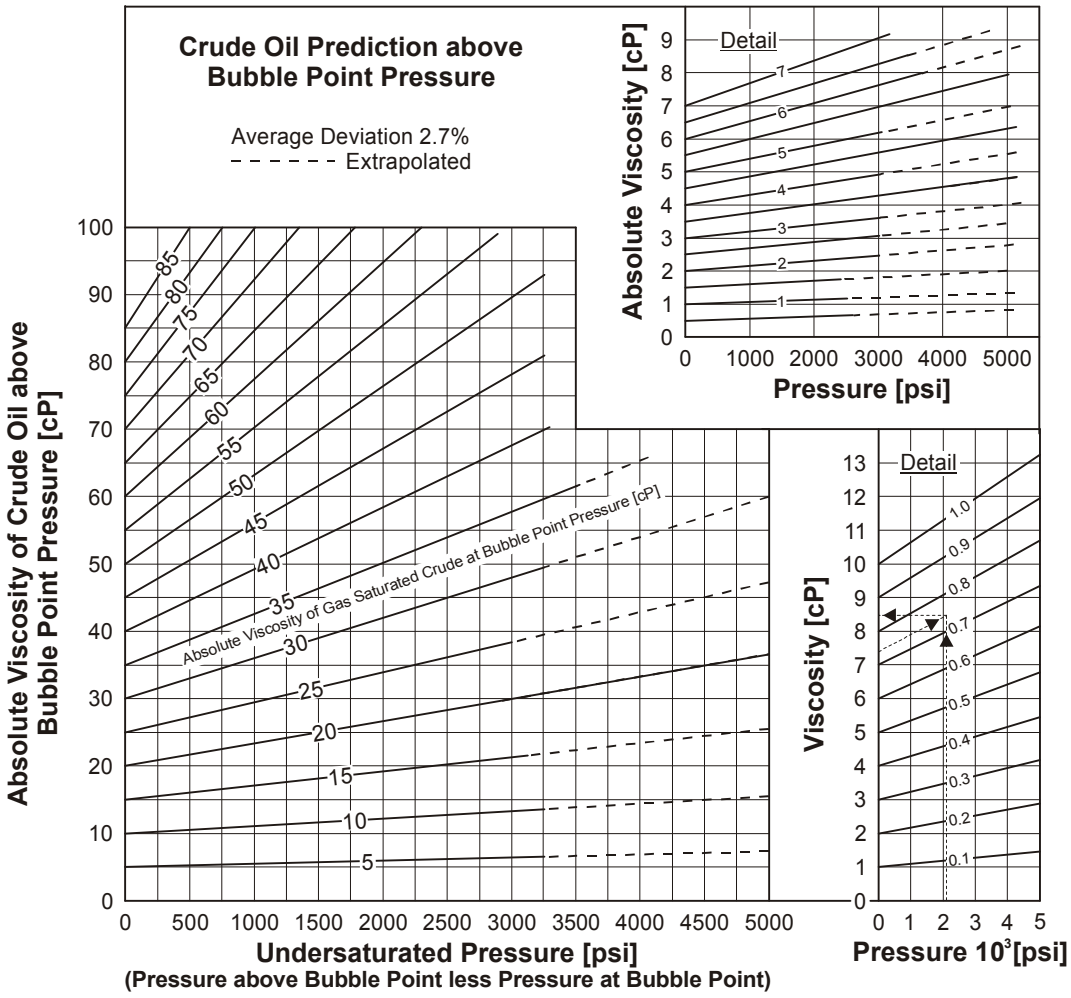

Figure 5.22: Prediction of crude oil viscosity above bubble point pressure (from BEAL, 1946)

Example 6.8

Evaluation of the oil viscosity at reservoir conditions which are given below as well as the interesting production data.

μ_{ob} = 0.45cP.

		SI-Units	Field Units
Reservoir Temperature	T	105 °C	220 °F
Bubble Point Pressure	pb	22.55 MPa	3300 psia
Reservoir Pressure	p	25.00 MPa	3600 psia
Initial Solution Ratio	Rsi	94 nm^3/m^3]	527.8 cu ft/bbl
Standard Oil Viscosity	μ_1	0.9 mPas	0.9 cP

From Figure 5.21, the oil viscosity at bubble point conditions can be read off as

$$\mu_{ob} = 0.45\text{cP}.$$

From Figure 5.22, the viscosity of the under saturated crude oil at p = 3300 psia can be evaluated:

$$\mu_{oi} = 0.48\text{cP}$$

or

$$\mu_{oi} = 0.48[mPas].$$

LOHRENZ, BRAY and CLARK have provided a general correlation to calculate the phase viscosity, applicable for gas as well as liquid. The method is described in Chap. 6.

5.3 Brines

It has been recognized relatively late that water is - without any exception - one of the reservoir fluids. GARRISON (1935) and SCHILTHUIS (1938) have been the first who presented detailed information on the distribution of oil and water in porous rock and on the origin and occurrence of "connate water" (formation water, capillary water, interstitial water). Furthermore, they established a relationship between the water saturation and the rock permeability.

Nowadays, knowledge of the chemical and physiochemical data of the respective reservoir water is of great importance for the petroleum engineer. Water analyses

- give valuable information about the area of prospecting,
- help to answer questions about the origin of the produced water,
- make sure that injected water is chemically compatible with the reservoir water or with added water (plugging by precipitations must be avoided),
- are indispensable for feasibility studies in case of chemical EOR processes.

Last but not least, data such as density, compressibility, formation volume factor and viscosity are required for calculating the displacement process and for establishing a material balance.

Additionally, this section presents an unusual phenomenon, the so-called "gas hydrate formation", during which water and natural gas form a solid phase at temperatures above the freezing point of water.

5.3.1 Composition of Brines

Reservoir water always contains dissolved inorganic salts, above all sodium chloride, *NaCl*. Therefore, these waters are sometimes called "brines" although they cannot be compared with sea water because both the total salt concentration and the content of distinctions are different.

The cations usually dissolved in reservoir brine are

$Na^+, K^+, Ca^{2+}, Mg^{2+}$

In certain cases,

$Ba^{2+}, Li^+, Fe^{2+},$

and sometimes Sn^{2+} can be found.

The generally present anions are

Cl^-, SO_4^{2-}, HCO_3^-

and, in some cases, also

$CO_3^{2-}, NO_3^-, Br^-, J^-, S^{2-}$.

The elements are present in reservoir water within the following concentration ranges:

Na, Cl	*in%*
Ca, SO_4	*in% or ppm*
K, Sr	*in 100 ppm*
Al, B, Ba, Fe, Li	*in 1 - 100 ppm*
Cr, Cu, Mn, Ni, Sn, Ti, Zr	*in ppb (in most cases)*
Be, Co, Ga, Ge, Pb, V, W, Zn	*in ppb (in some cases)*

where

%:	g substance per 100 g brine
ppm:	mg substance per 1 kg brine
ppb:	mg substance per 10^3 kg brine

Usually micro-organisms of different species are also present in oil field brines. The origin of these organisms is not yet totally clear. They contribute to corrosion in the bore hole and to permeability reduction during water flooding.

There is a wide variability of concentrations and chemical characteristics resulting from many factors. Such factors may be

- the non-marine origin of a few sediments,
- dilution with ground water,
- enrichment because of vaporization by migrating gas,
- adsorption and cation exchange with clay minerals,
- dissolution of mineral salts in the migrating formation water,
- the chemical reaction with components of adjacent sediments.

Therefore, it is important that water from a certain horizont is characteristically distinct from all the other brines, even those from the immediate neighbourhood. Thus, water analyses are mainly used for identifying the produced water with regard to the geological formation it originates from. In doing so, a simple and easily readable representation of the great data set from a water sample is desired. The graphical method proposed by STIFF (1951) may be the simplest graphical method, has maximum utility and, hence, is the most popular.

This graphical method is shown in Figure 5.23. Horizontal lines extend right and left from a centrally located vertical line. The positive ions are plotted on the left of the vertical line, while the anions are plotted on the right. Characteristic positions are designated for the ions which are most frequently found in reservoir brines.

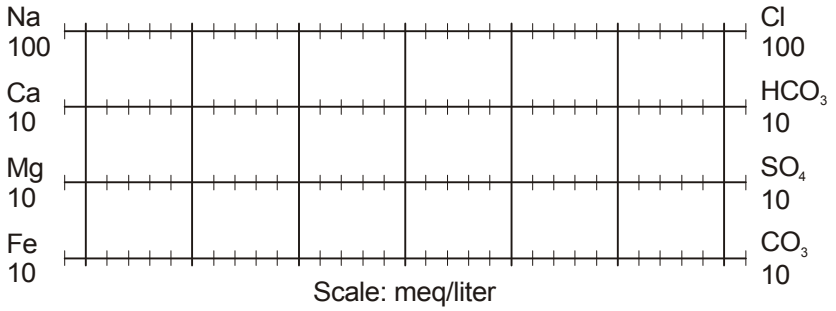

Figure 5.23: Essential feature of the water pattern analysis system (from STIFF, 1951)

The analysis data for all ions in question are indicated in *ppm* (milligram per liter). To make these values comparable with each other, the contents have to be converted to **meq** (milliequivalents) by dividing the respective value with the milliequivalent weight (ionic weight in mg per valence). If there is a difference between Σ meq of the positive and Σ *meq* of the negative ions, the difference is presented as sodium.

Although various scales can be employed, most reservoir waters may be plotted with sodium and chloride on a scale of *100 meq* and a scale of *10 meq* for the others. When the data of the water analysis are plotted on the graph and the adjacent points are connected by straight lines, a closed "pattern" is formed as a "fingerprint" of the respective brine.

One of many practical applications in correlating producing formations is illustrated by Figure 5.24. The characteristic pattern of the formations is evident.

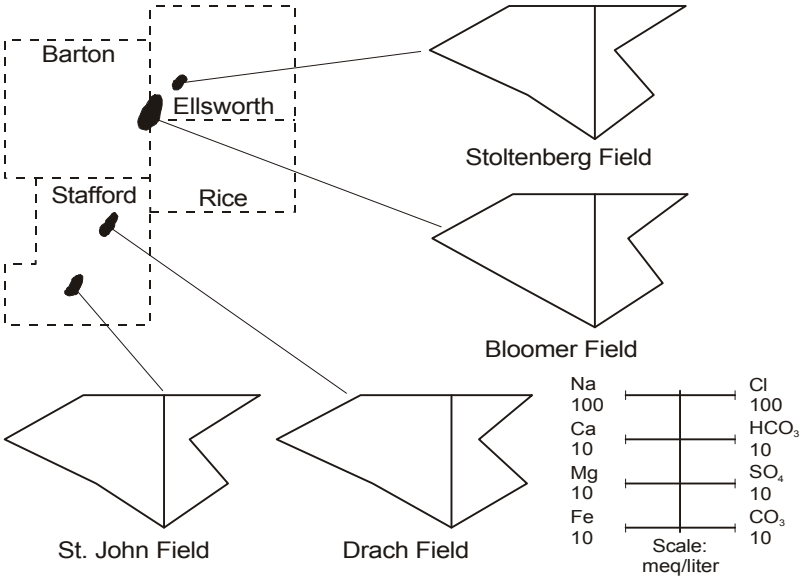

Figure 5.24: Course of Arbuckle formation through Kansas shown by water patterns (from STIFF, 1951)

5.3.2 Solubility of Gas in Water

Gas will also be dissolved in the water phase and this has influence on the water compressibility. To give a general impression, the brine will dissolve less then 30 scf/STB (5.3432 sm^3/sm^3) gas at a temperature of 300°F (148.8 °C) and a pressure less than 5000 psia (344.73 bar), and increase the water compressibility by 25%.

The solubility of natural gases in water is rather complicated to estimate from empirical correlations. Therefore, the solubility will often be neglected in a simulation model or it will be restricted to a single component which can either be methane or CO_2. The method in use is similar for both compounds:

At first the gas solubility will be calculated for pure water using the CULBERSON and MCKETTA equation for methane, and a different empirical equation for CO_2. Both equations are functions of the temperature and the pressure. The influence of the salinity will be correlated by using the SETCHENOW constant k_s, also called "salting out coefficient" which is a function of the temperature. SOREIDE and WHITSON defined the function for methane and CLEVER and HOLLAND for CO_2.

The following empirical equation gives a reasonable fit for the CULBERSON and MCKETTA solubility of methane in pure water, at conditions $100 < T < 350$°F and $0 < p < 10{,}000$ psia:

$$x_{wc1} = 10^{-3}\left[\sum_{i=0}^{3}\left(\sum_{j=0}^{3} A_{ij}T^{j}\right)p^{i}\right], \tag{5.50}$$

where A_{00}=0.299, A_{01}= -1.273.10^{-3}, A_{02}=0., A_{03}=0., A_{10}= 2.283.10^{-3}, A_{11}= -1.870.10^{-5}, A_{12}= 7.494.10^{-8}, A_{13}= -7.881.10^{-11}, A_{20}= -2.850.10^{-7}, A_{21}= 2.720.10^{-9}, A_{22}= -1.123.10^{-11}, A_{23}= 1.361.10^{-14}, A_{30}= 1.181.10^{-11}, A_{31}= -1.082.10^{-13}, A_{32}= 4.275.10^{-16}, A_{33}= -4.846.10^{-19}, with T in °F and p in psia.

The gas solubility is expressed as a solution gas/water ratio, R_{ws}:

$$R_{sw}^{0} = \frac{7,370x_{wg}^{0}}{1-x_{wg}^{0}} \approx 7,370x_{wg}^{0}\ [scf/STB]. \tag{5.51}$$

Analogously for CO_2, at first, the gas fraction in fresh water $x_{w,\,CO_2}^{o}$ is calculated from the following empirical equation:

$$x_{w,\,CO_2}^{o} = A + B\cdot p - C\cdot e^{-D\cdot p} + T^{-n}. \tag{5.52}$$

The pressure p is in bar and the temperature T is in °C.

The constants that best fit the experimental data for CO_2 are given in Table 5.2.

Table 5.2: Constants for CO_2 Solubility in Fresh Water

A	0.0184
B	0.00001256
C	0.02
D	0.03
n	1.6

Using this gas fraction $x_{w,\,CO_2}^{o}$, we calculate the solubility of CO_2 in fresh water expressed as solution gas-water ratio R_{sw}^{o} [sm^3/sm^3] by

$$R_{sw}^{o} = 1242\cdot\left(\frac{x_{w,\,CO_2}^{o}}{1-x_{w,\,CO_2}^{o}}\right). \tag{5.53}$$

For both CO_2 and Methane this fresh water solubility R_{sw}^{o} has to be corrected for the brine salinity which can be done using the following equation:

$$\frac{R_{sw}}{R_{sw}^{0}} = \frac{x_{wg}}{x_{wg}^{0}} = 10^{-k_s c_s} \approx 10^{-(17{,}1 \times 10^{-6}) k_s C_s}. \tag{5.54}$$

In the equations, R_{sw}^{o} and R_{sw} are the solution gas-water ratios in fresh water and brine, respectively, c_s is the salinity of the brine in the gridblock in ppm, k_s the salting out coefficient.

The definition of the SETCHENOW constant is

$$k_s = \lim_{c_s \to 0} \left[c_s^{-1} \log \frac{(\phi_i^{\infty})_w}{(\phi_i^{\infty})_w^{0}} \right], \tag{5.55}$$

where k_s is the "salting out coefficient" in 1/molarity (molarity = number of moles of solute per liter of solvent, molality = number of moles of solute per kg of solvent,), c_s is the salt concentration of the brine in the gridblock in ppm, $(\phi_i^{\infty})_w$ and $(\phi_i^{\infty})_w^{0}$ are the fugacity coefficients of component i at infinite dilution in the salt solution and in pure water, respectively.

For $k_s > 0$, the gas solubility is less in brines then in pure water, a fact that has led to the term "salting out coefficient".

Correlations are available for methane and CO_2 in NaCl solution:

For methane (SOREIDE and WHITSON):

$$k_s = 0,1813 - (7{,}692 \times 10^{-4}) T + (2{,}6614 \times 10^{-6}) T^2 - (2{,}612 \times 10^{-9}) T^3, \tag{5.56}$$

with T in °F and k_s in M^{-1}.

For CO_2 (CLEVER and HOLLAND):

$$k_s = 0,257555 + -(0{,}157492 \times 10^{-3}) T - (0{,}253024 \times 10^{-5}) T^2 + (0{,}438362 \times 10^{-8}) T^3 \tag{5.57}$$

with T in °K and k_s in M^{-1}.

5.3.3 Density

The correlation for the water density, described below is valid for SI-units. Here TRANGENSTEIN´s modification of KELL´s correlations is used to calculate the water density:

$$\rho_w = \frac{A_0 + A_1 T_c + A_2 T_c^2 + A_3 T_c^3 + A_4 T_c^4 + A_5 T_c^5}{1 + A_6 T_c} \exp[c_w (p - A_7)], \tag{5.58}$$

where

$A_0 = 999{,}83952$ $A_4 = 105{,}56302 \times 10^{-9}$

$A_1 = 16{,}955176$ $A_5 = -280{,}54353 \times 10^{-12}$

$A_2 = -7{,}987 \times 10^{-3}$ $A_6 = 16{,}87985 \times 10^{-3}$

$A_3 = -46{,}170461 \times 10^{-6}$ $A_7 = -10{,}2$

and c_w is the water compressibility.

5.3.4 Compressibility

From Figure 5.25a the coefficient of the isothermal water compressibility, c_w, can be evaluated without considering the gas in solution. At a given pressure and temperature, the effect of gas in solution is to increase c_w (see Figure 5.25b).

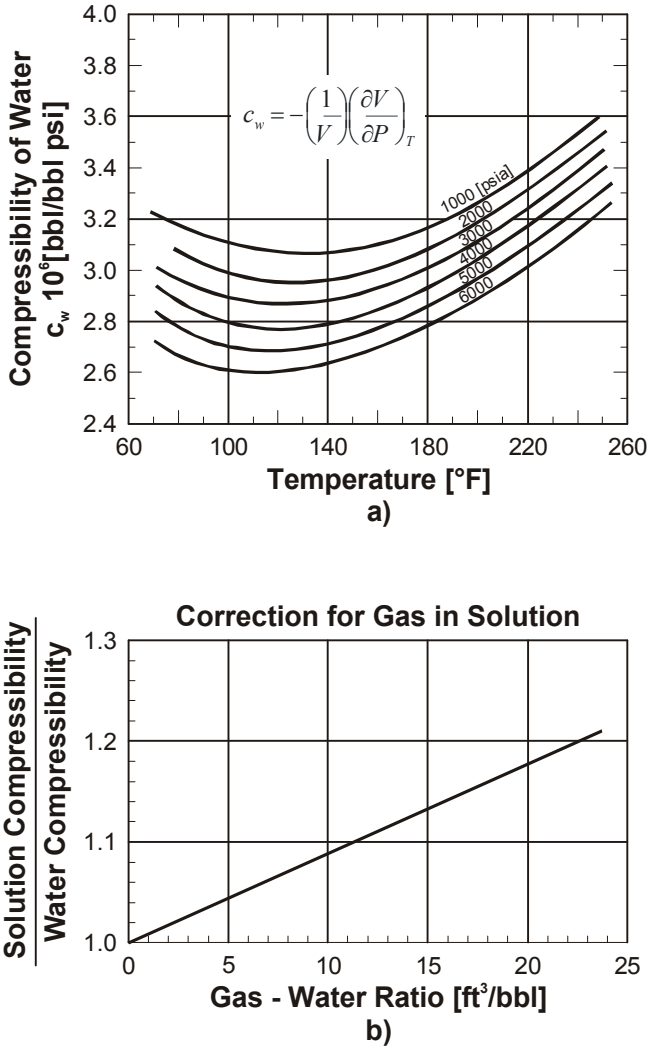

Figure 5.25: The isothermal coefficient of compressibility of pure water, including effects of gas in solution (from DODSON and STANDING, 1944)

Example 5.10

Evaluation of the compressibility of reservoir water at the reservoir data of Example 5.9.

From Figure 5.25a at 3000 psia and 200 ^{o}F, c_w can be read off as

$$c_w = 3.1 \text{ E - 6 psi}^{-1}.$$

From Figure 5.26a, the gas solubility in pure water results in

$$R_{sw} = 15.3 \text{ cu ft bbl}^{-1}.$$

Correction of gas solubility from Figure 5.26b:

$$R_w = 15.3 \times 0.88 = 13.46 \text{ cu ft / bbl .}$$

After evaluating the effect of the dissolved gas from Figure 5.26b, the compressibility of the reservoir brine results in

$$c_w = 1.12 \times 3.1\ E-6 = 3.47 \text{ E - 6 psi}^{-1},$$

or

$$c_w = 5.03 \text{ E - 10 Pa}^{-1},$$

respectively.

With the compressibility data reported by ROWE and CHOU covering the conditions $70 < T < 350$°F, $150 < p < 4{,}500$ psia, and $0 < w_s < 0.3$ (weight fraction of NaCl), a recent correlation for the compressibility of a brine (without solution gas), c'_w, is

$$c'_w(p, T) = (A_0 + A_1 p)^{-1}, \tag{5.59}$$

where

$$A_0 = 10^6[0{,}314 + 0{,}58 w_s + (1{,}9 \times 10^{-4})T - (1{,}45 \times 10^{-6})T^2] \tag{5.60}$$

and

$$A_1 = 8 + 50 w_s - 0{,}125 w_s T, \tag{5.61}$$

with c'_w in psi^{-1}, p in psia, T in °F, and w_s in weight fraction of NaCl.

DODSON and STANDING give a correction for the effect of dissolved gas on the water/brine compressibility.

$$c_w(p, T, R_{sw}) = c'_w(p, T)(1 + 0{,}00877 R_{sw}), \tag{5.62}$$

with R_{sw} in scf/STB.

The equations mentioned above are valid for field units.

5.3.5 Formation Volume Factor

The definition of the formation volume factor of water B_w corresponds to the definition of B_o. Similarly to the hydrocarbon liquids, the change in volume may have three reasons:

- liberation of dissolved gas due to pressure decrease,
- expansion of the brine because of pressure decrease,

- contraction of the brine due to temperature reduction.

In contrast to the solubility of natural gases in oil, their solubility in water is low (see Figure 5.26a). Additionally, the solubility decrease with increasing salinity of the brine (see Figure 5.26 b). Consequently, the contribution of the gas liberation to the volume change is low.

Since the expansion due to the decrease in pressure and the contraction because of temperature decrease are also insignificant, B_w is always numerically small, rarely above 1.06.

Figure 5.27 shows a typical relationship between B_w and p. In the present case, the initial reservoir pressure is higher than the bubble point pressure. If the reservoir pressure is reduced from initial pressure to the bubble point pressure, B_w increases because of the water expansion. A further pressure reduction leads to gas liberation. This loss of liquid volume only balances partly the continuing expansion so that B_w further increases with further pressure drop. Along with the reduction of the pressure to atmospheric pressure, B_w will reach its maximum value. The difference between this value and 1.0 represents the thermal contraction resulting from the cooling of the brine from the reservoir temperature to the standard temperature of 15 ^oC. However, B_w will be smaller than 1.0, if the increase in volume by dissolved gas is too low to compensate the volume reduction resulting from high pressure.

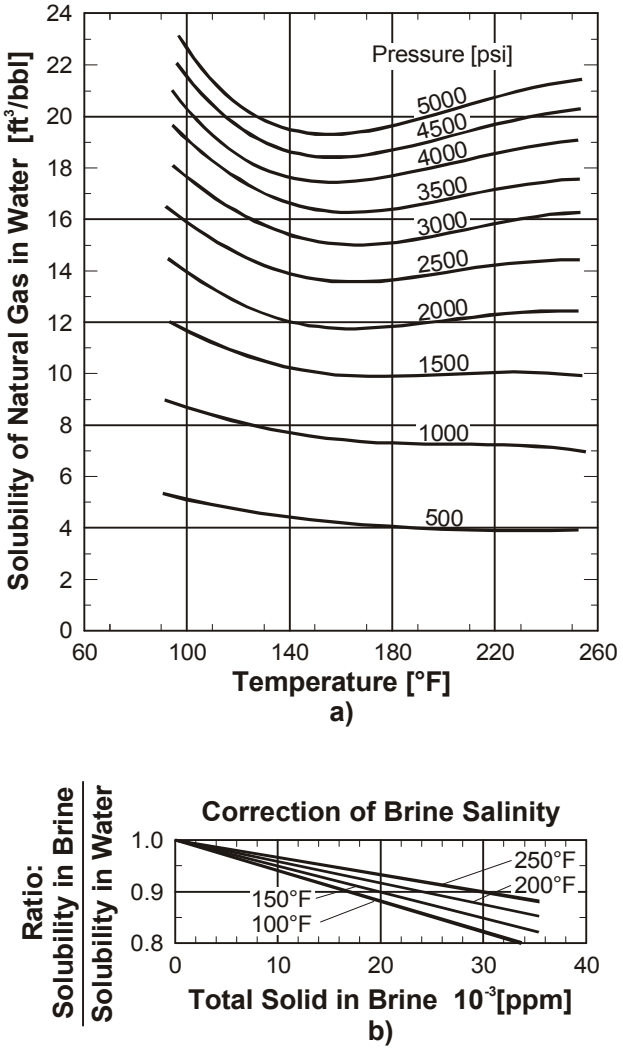

Figure 5.26: Solubility of natural gas in water (from DODSON and STANDING, 1944)

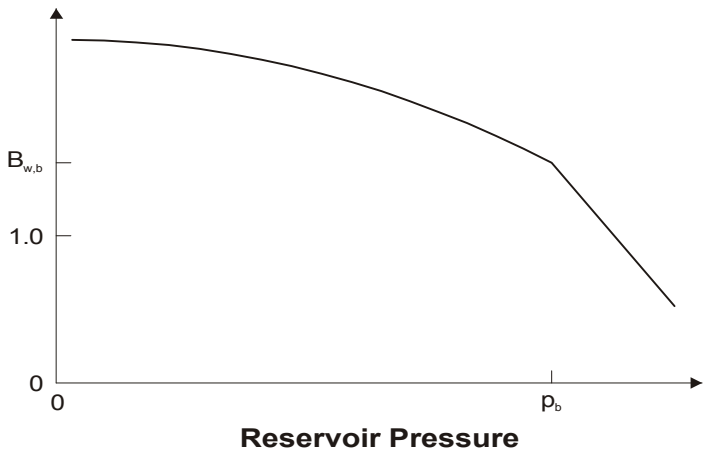

Figure 5.27: Typical graph of formation volume factor of water against pressure

The assumption is customary that the bubble point pressure of a gas-saturated brine is equal to the bubble point pressure of the crude oil inside the corresponding reservoir.

Figure 5.28 presents data of B_w for pure water saturated with natural gas (solid lines). Naturally, gas saturated pure water has a higher volume factor than pure water at a given pressure and temperature (dashed lines). B_w for a reservoir water can be computed with aid of Figure 5.28 and Figure 5.26 as follows:

- The volume factors for pure water and pure water saturated with natural gas are read from Figure 5.28 for the given reservoir data.
- The gas solution ratio, R_{sw}, for pure water is read from Figure 5.26a. and corrected for salinity using Figure 5.26b.
- Assuming the effect of gas solubility on B_w to be linear, the volume factor is computed by interpolation.

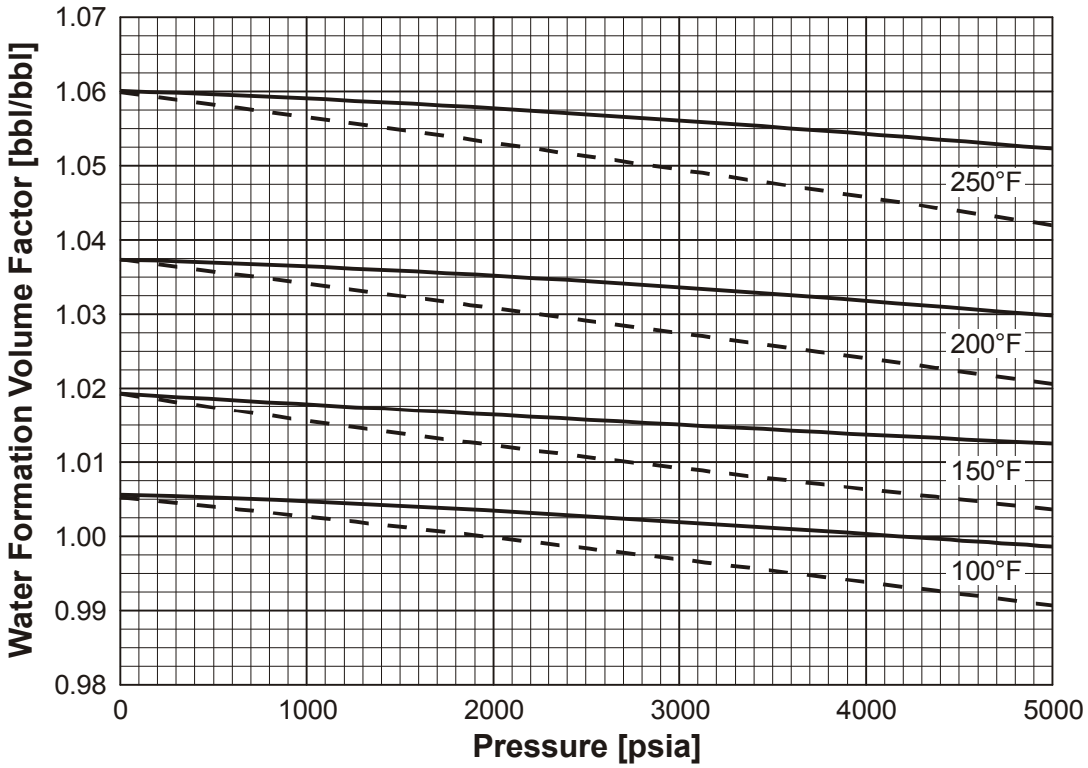

Figure 5.28: B_w for pure water (dashed lines) and pure water saturated with natural gas (solid lines) as a function of pressure and temperature (from DODSON and STANDING, 1944)

Example 5.9

Formation volume factor of reservoir water. The reservoir conditions as well as the salinity of the brine are given below both in SI- and Field units.

		SI Units	Field Units
Reservoir Temperature	T	93.3 °C	200 °F
Reservoir Pressure	p	20.56 MPa	3000 psia
Salinity		30,000 ppm	30,000 ppm

The evaluation of B_w for pure water from Figure 5.28 results in

$$B_w = 1.0275.$$

B_w for pure water saturated with natural brine can be read off from Figure 5.28 as

$$B_w = 1.034.$$

The gas solution ratio in pure water from Figure 5.26a results in

$$R_{sw} = 15.3 \text{ cu ft/bbl.}$$

After correction of the gas solubility from Figure 5.26b, R_{sw} results in

$$R_{sw} = 15.3 \times 0.88 = 13.46 \text{ cu ft/bbl.}$$

Then the formation volume factor of the reservoir water results in

$$B_w = 1.0275 + (1.034 - 1.0275)\ \frac{13.46}{15.3} = 1.033\,.$$

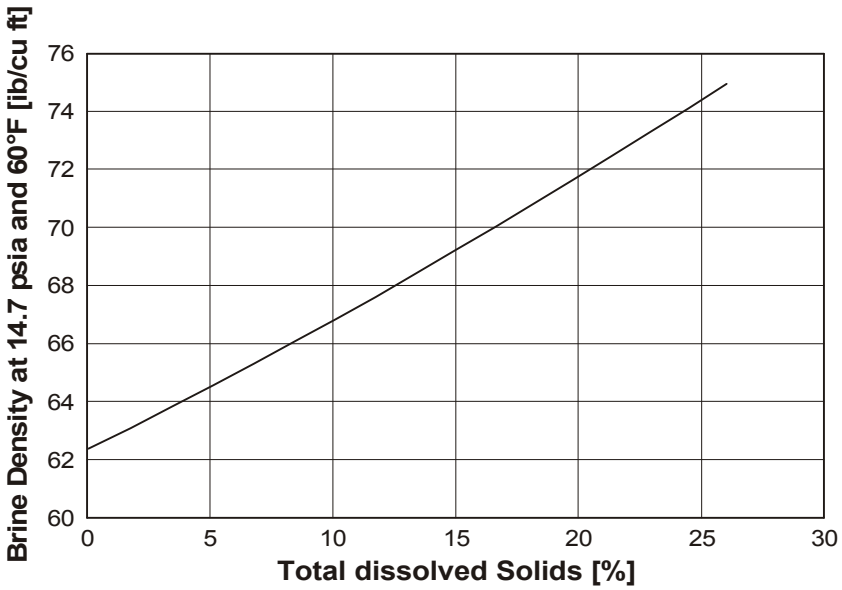

Figure 5.29: Density of brine as a function of total dissolved solids (from McCain, 1973)

In Figure 5.29, the density of reservoir water at standard conditions is plotted as a function of the total salt concentration. By dividing the respective density with B_w, the

corresponding density under reservoir conditions can be received.

The effect of pressure on the formation volume factor can be calculated by use of the definition of water compressibility,

$$c_w' = -\frac{1}{B_w}\left(\frac{\partial B_w}{\partial p}\right)_{c_s,\,T}, \tag{5.63}$$

where c'_w is the brine isothermal compressibility without solution gas.

Eq. 5.63, when integrated gives

$$\ln\frac{B'_w(p,T)}{B^0_w(p_{sc},T)} = -\int_0^p c'_w(p,T)\,dp\,. \tag{5.64}$$

Solving Eq. 5.64 for the Formation Volume Factor of a brine without solution gas, B'_w, gives

$$B'_w(p,T) = B^\circ_w(p_{sc},T)\left(1+\frac{A_1}{A_0}p\right)^{(1/A_1)}, \tag{5.65}$$

where A_0 and A_1 are given by Eq. 5.60 and Eq. 5.61, applying the correlation by ROWE and CHOU.

5.3.6 Viscosity

Regarding the viscosity of oil field brines, only few data are available. Figure 5.30 shows the water viscosity as a function of the temperature. The viscosity should rise with pressure and increase significantly with increasing salt concentration. These dependencies can be observed in Figure 5.30. It is recommended to use this graph for estimating the viscosity of reservoir waters without considering both the pressure and the salinity of the brine.

The fact that low molecular paraffins are dissolved in water under reservoir conditions should furthermore lead to a considerable reduction of the brine viscosity. Unfortunately, no corresponding data have been published until now.

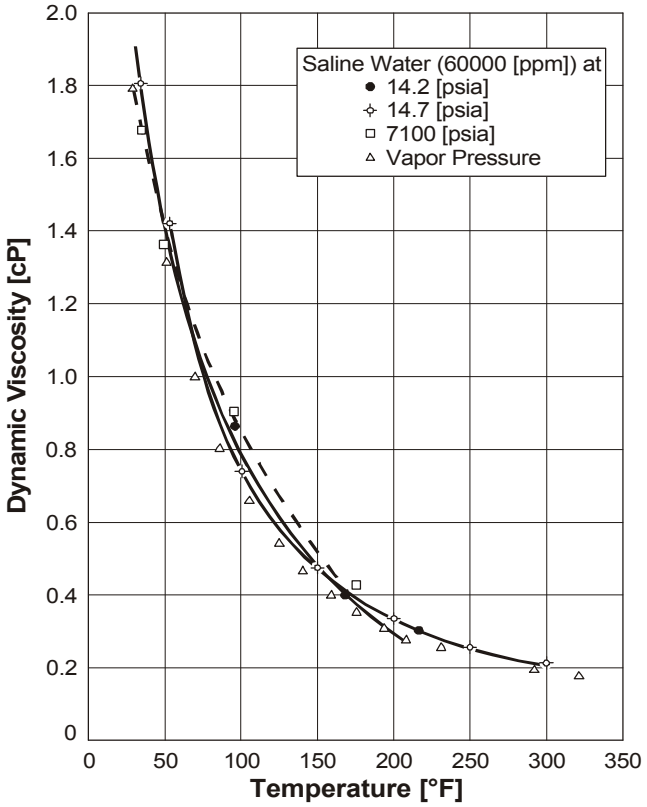

Figure 5.30: The viscosity of water at oil field temperature and pressure (from VAN WINGEN, 1950)

KESTIN et al. presented a correlation for the determination of water and brine viscosity as functions of temperature and salinity, which results in an accuracy of ±0,5 % in the range $70<T<300$°F, $0<p<5000$ psia, and $0<C_{sw}<300{,}000$ ppm.

Standard values of the ratios of viscosity at a temperature T to its value at 20°C have been derived because the uncertainty of this ratio is an order of magnitude smaller than that of the absolute values. The ratios are used to generate absolute values with the aid of the standard μ = 1.002 cP at 20 °C. The viscosity ratios are correlated with two empirical equations.

The water viscosity according to KESTIN et al. is calculated by

$$\mu_w = (1 + A_0 p)\mu'_w, \tag{5.66}$$

$$\log\left(\frac{\mu'_w}{\mu^\circ_w}\right) = A_1 + A_2 \log\left(\frac{\mu^\circ_w}{\mu^\circ_{w20}}\right), \text{ where} \tag{5.67}$$

$$A_0 = 10^{-3}[0{,}8 + 0{,}01(T - 90)\exp(-0{,}25 c_{sw})], \tag{5.68}$$

$$A_1 = \sum_{i=1}^{3} a_{1i} c_{sw}^{i}, \tag{5.69}$$

$$A_2 = \sum_{i=1}^{3} a_{2i} c_{sw}^{i}, \tag{5.70}$$

$$\log\left(\frac{\mu^\circ_w}{\mu^\circ_{w20}}\right) = \sum_{i=3}^{4} a_{3i} \frac{(20-T)^i}{96+T}, \tag{5.71}$$

and $\mu^\circ_{w20} = 1{,}002$ cp,

where $a_{11}=3.324*10^{-2}$, $a_{12}=3.624*10^{-3}$, $a_{13}=-1.879*10^{-4}$, $a_{21}=-3.96*10^{-2}$, $a_{22}=1.02*10^{-2}$, $a_{23}=-7.02*10^{-4}$, $a_{31}=1.2378$, $a_{32}=-1.303*10^{-3}$, $a_{33}=3.060*10^{-6}$ and $a_{34}=2.550*10^{-8}$, with μ given in cP, T in °C, and p in MPa.

The effect of dissolved gas on the water viscosity has not yet been reported. Intuitively, one might suspect that it decreases with increasing solubility, although COLLINS et al. suggest that the dissolved gas might increase brine viscosity.

5.3.7 Natural Gas Hydrates

Natural gas and liquid water can form solid material which remind of wet snow. This process takes place at temperatures slightly higher than the freezing point of pure water. These solid substances are called “gas hydrates”.

The phenomenon is of special interest for petroleum industry. For example, the pressure decreases in the production line, such as across a choke or in a separator. This can cause a reduction in the temperature of the gas (adiabatic process) and, therefore, the condensation of water from the gas. The conditions necessary for hydrate formation could be established.

Gas hydrates behave rather like dissolutions of gases in ice than like chemical compounds. The lattice of the hydrate crystal is mainly formed by water molecules while the hydrocarbon molecules occupy vacancies within the lattice. Therefore, the hydrate formation is rather of physical than of chemical nature. The water lattice seems to be similar to ice, because the formation enthalpy is comparable.

Although gas hydrates can be compared rather to solid solutions than to chemical compounds, a certain number of water molecules is associated to each gas molecule. This may be caused by the crystal structure. The ratio of hydrocarbon to water depends mainly on the size of gas molecules.

The presence of liquid water is the most important prerequisite for hydrate formation. However, even if liquid water is present, a meta-stable equilibrium between water and hydrocarbon gas may occur (under conditions at which generally hydrate formation takes place). Seed crystals can immediately induce the hydrate formation.

Figure 5.31 shows a part of the phase diagram of a mixture of water and a light hydrocarbon. The point Q_2 is a "quadruple point" at which four phases are in equilibrium. The quadruple point Q_1 is at approximately 0 ^oC (ice, gas hydrate, water and natural gas are in equilibrium). The connection Q_1 - Q_2 represents the equilibrium natural gas-water-hydrate. This line is of special interest.

Figure 5.32 presents the hydrate formation conditions for natural gases of different gravities. The curves can be used to estimate the conditions of hydrate formation. Anyway, the results should be applied with caution because of the large discrepancies of the few published experimental data and the correlation present, especially in case of high gas gravity and temperature.

Additionally, it has to be taken into account that electrolytes present in the water will lead to decreasing temperatures at which hydrate formation will occur. Thus, water-soluble substances are often added to the system to inhibit or suppress the hydrate formation. The effect of the concentration of various inhibitors on the hydrate-formation temperatures of a natural gas is plotted in Figure 5.33.

Hydrate portion of the phase diagram for a typical mixture of water and a light hydrocarbon (from McCain, 1973)

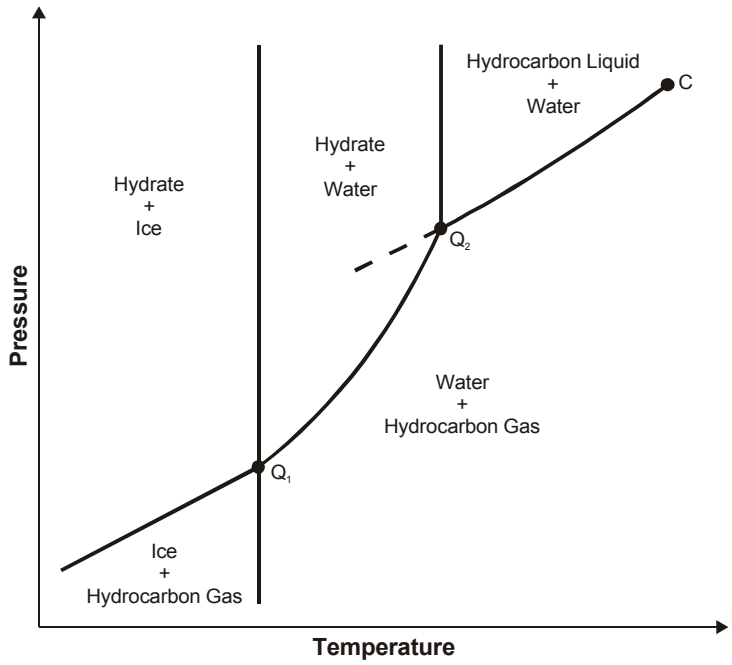

Figure 5.31: Hydrate portion of the phase diagram for a typical mixture of water and a light hydrocarbon (from McCain, 1973)

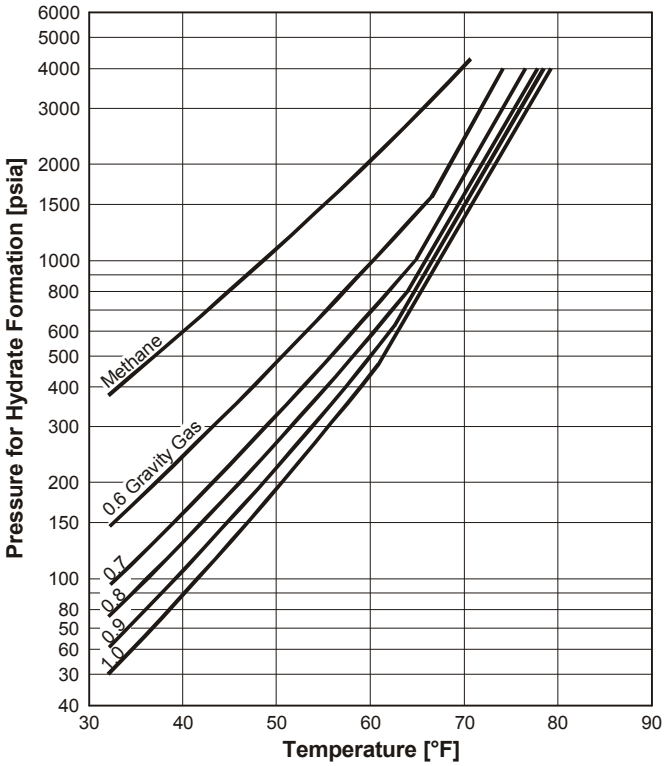

Figure 5.32: Pressure-temperature curves for predicting hydrate formation (from KATZ, 1945)

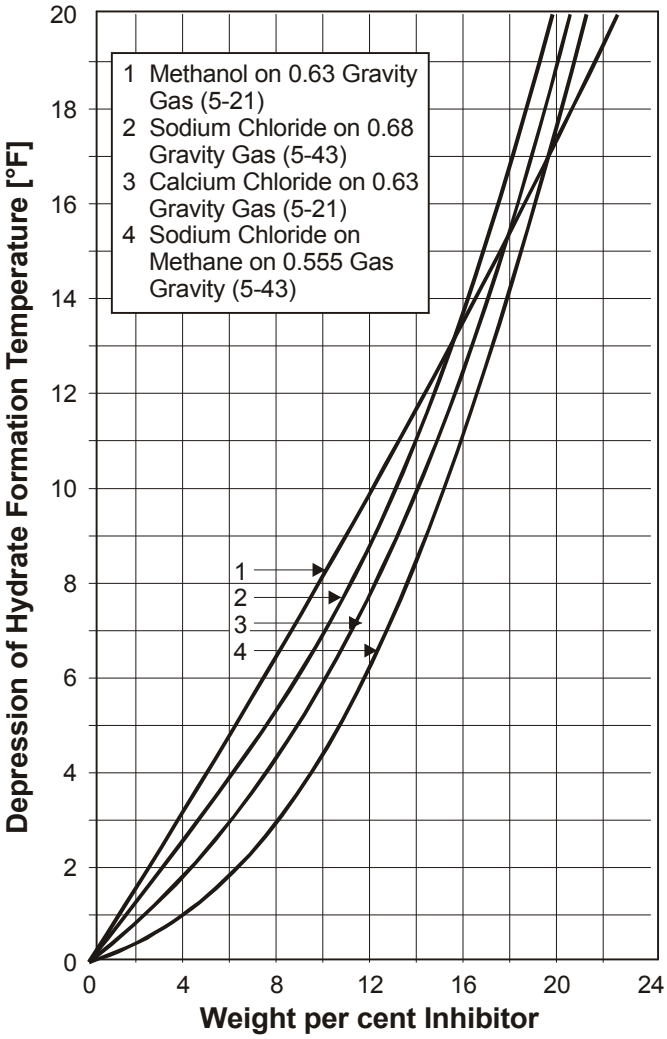

Figure 5.33: Depression of hydrate formation temperature by inhibitors (from KATZ et al., 1959)

Temperature calculations have been carried out for typical natural gases, and the results have been combined with the hydrate formation conditions given in Figure 5.32. This has been done to evaluate diagrams by which the maximum adiabatic pressure reduction without gas hydrate formation can be estimated. One of these diagrams is given by Figure 5.34.

Example 5.11

Evaluate the maximum of adiabatic expansion of a natural gas without any danger of hydrate formation. Up to which pressure can this gas be expanded adiabatically without hydrate formation and what will the temperature be?.

	SI-Units	Field-Units
Gas Gravity	γ_g 0.80	0.80
Initial Pressure	p_i 20.68 [MPa]	3000 psia
Initial Temperature	T_i 71[°C]	160 °F

Solution steps:

- The ordinate of Figure 5.34 was entered at p_i = *3000 psia*.

- It follows a horizontal movement to the 160 °F isotherm.

- The next step consists of the vertical movement to the abscissa. 800 psia is the lowest final pressure which will preclude hydrate formation.

The intersection of the 800 psia line with the dashed line results in *65 °F (18.3 °C)* after expansion to *800 psia (5.52 MPa)*.

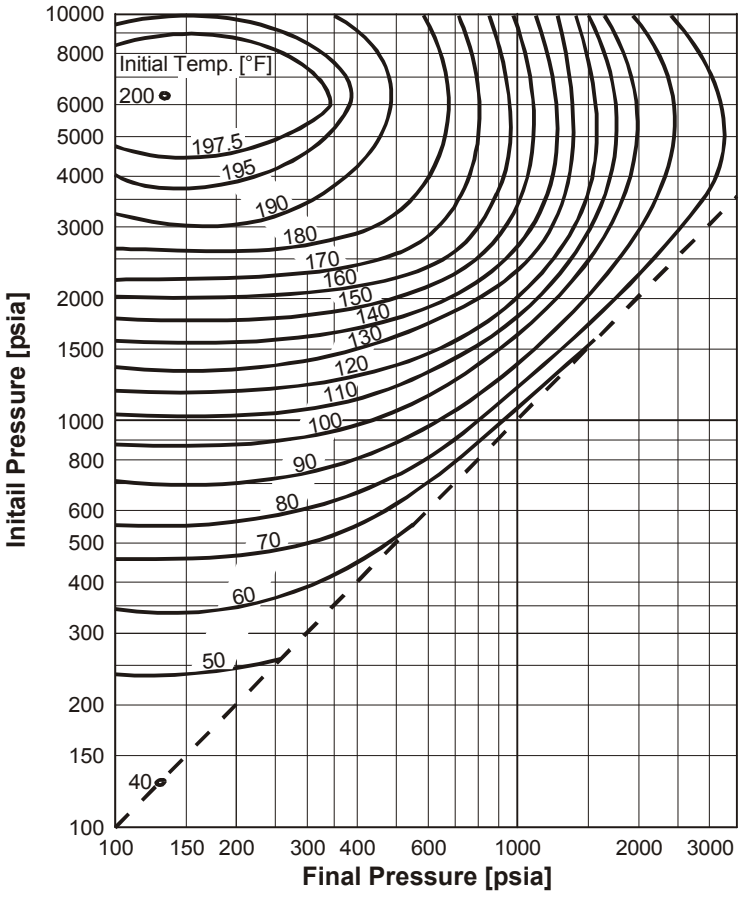

Figure 5.34: Permissible expansion of 0.8 gravity gas without hydrate formation (from KATZ, 1945).

Chapter 6

Miscellaneous

6.1 Interfacial Tensions

6.1.1 Parachor

The parachor is a temperature-independent parameter and may be determined from the structure of the molecule. The parachor must be entered in (cm³/mol)*(dyn/cm)^0.25.

If no values are specified and the internal library cannot provide the parachor P for the component i, it will be estimated from the following formula:

$$P_i = 25{,}2 + 2{,}86 \cdot M_i \tag{6.1}$$

The surface tension σ between the liquid and the vapor phase of a multi-component mixture is calculated from the MACLEOD-SUDGEN correlation:

$$\sigma^{1/s} = \sum_{i=1}^{N_c} P_i \cdot (\rho_{m,l} x_{l,i} - \rho_{m,v} y_{v,i}), \tag{6.2}$$

where the default value of s is 4.

6.1.2 Capillary Pressure and Relative Permeabilities

The surface tension σ is given in dyn/cm. For single phase states the surface tension is zero, and as the phases become miscible the surface tension will decrease sharply towards zero. Thus, this equation can be used together with the reference surface tension to model the transition between the immiscible and the miscible state. The transition applies to the

gas-oil capillary pressure and the gas and oil relative permeability function.

The transition function F is obtained from

$$F = (\sigma / \sigma_{ref})^N. \tag{6.3}$$

where σ_{ref} is the reference surface tension (usually the average initial surface tension). This interpolation factor can then be used to obtain a weighted average of miscible and immiscible hydrocarbon relative permeabilities.

$$k_{r,\,corr} = F \cdot k_{r,\,imm} + (1 - F) \cdot k_{r,\,mis} \tag{6.4}$$

The two contributions are scaled so that they have the same critical saturation, given by $FS_c^{imm} + (1 - F)S_c^{mis}$. (6.5)

Normally, the miscible critical saturation is zero and the immiscible critical saturation is obtained from a user-defined rock curve.

Capillary Pressures also must go towards zero as the surface tensions decrease. Here, a linear relationship can be assumed. The corrected gas-oil capillary pressure is calculated by

$$P_{cgo} = P_{cgo} \cdot (\sigma / \sigma_{ref})^N, \tag{6.6}$$

N may be specified by the user, or is set to 0.25 by default.

6.2 Viscosity Correlations for Liquid and Vapor

The following correlations can be applied to calculate liquid and vapor viscosities.

LOHRENZ-BRAY-CLARK

It has become standard in compositional reservoir simulation. Since the determination of relative permeability is prone to relatively large errors, the requirement for accuracy in oil viscosity calculations is not very severe. Errors of ±25% are acceptable and the LOHRENZ method was evaluated with 260 different reservoir oils, resulting in an average deviation of 16%.

The correlation of JOSSI, STIEL and THODOS developed for pure components is used.

$$[(\mu - \mu^*)\zeta + 10^{-4}]^{1/4} = A + B\rho_r + C\rho_r^2 + D\rho_r^3 + E\rho_r^4, \tag{6.7}$$

where the values for the coefficients are as given below:

A = 0.1023,
B = 0.023364,
C = 0.058533,
D = -0.040758,
E = 0.0093324,
and

$$\rho_r = \frac{\rho}{\rho_c'} \tag{6.8}$$

is the reduced density. ρ_c' is the pseudocritical density which is calculated by

$$\rho_c' = 1/\sum_{\substack{i=1 \\ i \neq C_{7+}}}^{N_c} (x_i V_{ci} + x_{C_{7+}} V_{cC_{7+}}), \tag{6.9}$$

where

$$V_{C7+} = 21{,}573 + 0{,}015122 M_{C7+} - 27{,}656\gamma_{C7+} + 0{,}070615 M_{C7+}\gamma_{C7+} \tag{6.10}$$

ζ is the mixture viscosity parameter and is defined by:

$$\zeta = \frac{\left[\sum_{j=1}^{N_c} x_i T_{ci}\right]^{\frac{1}{6}}}{\left[\sum_{j=1}^{N_c} x_i M_i\right]^{\frac{1}{2}} \left[\sum_{j=1}^{N_c} x_i p_{ci}\right]^{\frac{2}{3}}}. \tag{6.11}$$

μ^* is the viscosity of a gas mixture at low pressure:

$$\mu^* = \frac{\sum_{i=1}^{N_c} x_i \mu_i^* \sqrt{M_i}}{\sum_{i=1}^{N_c} x_i \sqrt{M_i}}. \tag{6.12}$$

The low-pressure pure component gas viscosities are calculated for all components of the mixture using the STIEL and THODOS correlation as follows

$$\begin{aligned} \mu_i{}^*\zeta_i &= 34{,}0 \times 10^{-5} \cdot T_{ri}^{0{,}94} && ,T_{ri} < 1{,}5 \\ \mu_i{}^*\zeta_i &= 17{,}78 \times 10^{-5}(4{,}58T_{ri} - 1{,}67)^{\frac{5}{8}} && ,T_{ri} \geq 1{,}5 \end{aligned} \quad , \tag{6.13}$$

where T_{ri} is the reduced temperature of component i and

$$\zeta_i = \frac{T_{ci}^{\frac{1}{6}}}{M_i^{\frac{1}{2}} p_{ci}^{\frac{2}{3}}} . \tag{6.14}$$

Kelvin and atm are used in the last equation. In all other equations T is in °R, p in atm, μ is in cp and ρ in lb/ft^3.

REICHENBERG:

If the reduced density is less than 0.02, the REICHENBERG correlation is recommended to be used to obtain a better gas viscosity. This correlation is as follows:

$$\mu = \mu^* \left(1 + \frac{A p_r^{1{,}5}}{B p_r + (1 + C p_r^D)^{-1}} \right) , \tag{6.15}$$

where the constants A, B, C, and D are functions of the reduced temperature T_r as shown below.

$$\begin{aligned} A &= \frac{\alpha_1}{T_r} e^{\alpha_2 T_r^{-\alpha_3}} \quad , \quad B = A(\beta_1 T_r - \beta_2) \\ C &= \frac{\gamma_1}{T_r} e^{\gamma_2 T_r^{-\gamma_3}} \quad , \quad D = \frac{\delta_1}{T_r} e^{\delta_2 T_r^{-\delta_3}} \end{aligned} \tag{6.16}$$

$$\begin{array}{llll} \alpha_1 = 1{,}9824 \times 10^{-3} & \beta_1 = 1{,}6552 & \gamma_1 = 0{,}1319 & \delta_1 = 2{,}9496 \\ \alpha_2 = 5{,}2683 & \beta_2 = 1{,}2760 & \gamma_2 = 3{,}7035 & \delta_2 = 2{,}9190 \\ \alpha_3 = 0{,}5767 & & \gamma_3 = 79{,}8678 & \delta_3 = 16{,}6169 \end{array} \tag{6.17}$$

Note:

The calculation of the parameters A, B, C and p_r^D can cause problems, because the term

is in the range of machine accuracy, and their value has to be estimated in advance.

PEDERSEN et al.

Here, viscosities are calculated from a modified form of the corresponding states method. A group of substances obey the corresponding states principle if the functional dependence of the reduced viscosity μ_r on, say, reduced density and temperature, ρ_r and T_r, is the same for all components within the group, namely:

$$\mu_r(\rho, T) = f(\mu_r, T_r) \quad , \tag{6.18}$$

in which case comprehensive viscosity data is only needed for one component of the group, which is denoted as the reference substance (subscript (*o*), all other components have the subscript (*x*).

The critical viscosity can be estimated from the inverse of Eq. 6.18:

$$\mu_r(\rho, T) = \mu(\rho, T) T_c^{-\frac{1}{2}} \cdot V_c^{-\frac{1}{2}} \cdot M_w^{\frac{2}{3}} \quad . \tag{6.19}$$

Thus, the viscosity of a component c with a density ρ at a temperature T is given by:

$$\mu_r(\rho, T) = \frac{T_{c,x}^{\frac{1}{2}}}{T_{c,o}} \cdot \frac{V_{c,x}^{-\frac{2}{3}}}{V_{c,o}} \cdot \frac{M_{w,x}^{\frac{1}{2}}}{M_{w,o}} \cdot \mu_o(\rho_o, T_o) \, , \tag{6.20}$$

where $\mu_o = \rho \frac{\rho_{co}}{\rho_{cx}}$, $T_o = T \frac{T_{co}}{T_{cx}}$ and μ_o is the viscosity of the reference substance at T_o and ρ_o.

Of course, not all components with molecular weights between 16 (Methane) and 1100 (C_{80}) can be expected to belong to the same corresponding group. So, a third parameter had to be introduced, accounting for the shape of the molecules, such as the accentric factor. A corresponding state principle was introduced depending on the reduced temperature and pressure, where

$$\mu_r = \frac{\mu}{T_c^{-1/6} \cdot p_c^{2/3} \cdot M_w^{1/2}} \tag{6.21}$$

The difference to the simple corresponding states principle is expressed in terms of a rotational coupling coefficient, denoted α to give:

$$\mu_{mix}(\rho, T) = \frac{T^{-1/6}_{c,\,mix}}{T_{c,\,o}} \cdot \frac{p^{\frac{2}{3}}_{c,\,mix}}{p_{c,\,o}} \cdot \frac{M^{\frac{1}{2}}_{w,\,mix}}{M_{w,\,o}} \cdot \frac{\alpha_{mix}}{\alpha_o} \cdot \mu_o(\rho_o, T_o), \tag{6.22}$$

where

$$p_o = p\frac{p_{co}}{p_{c,\,mix}} \cdot \frac{\alpha_o}{\alpha_{mix}} \text{ and } T_o = T\frac{T_{co}}{T_{c,\,mix}} \cdot \frac{\alpha_o}{\alpha_{mix}} \quad . \tag{6.23}$$

The critical temperature and volume for unlike pairs of molecules are given by:

$$T_{c,\,ij} = (T_{c,\,i} \cdot T_{c,\,j})^{1/2} \text{ and } V_{c,\,ij} = \frac{1}{8} \cdot (V^{1/3}_{c,\,i} + V^{1/3}_{c,\,j})^3, \tag{6.24}$$

where the critical volume of a component can be expressed in terms of the critical temperature and pressure using the real gas law and the critical *Z*-Factor.

Assuming a constant Z_c for all components, Eq. 6.24 becomes:

$$V_{c,\,ij} = \frac{1}{8} \cdot constant\left(\left(\frac{T_{c,\,i}}{p_{c,\,i}}\right)^{1/3} + \left(\frac{T_{c,\,j}}{p_{c,\,j}}\right)^{1/3}\right)^3 \quad . \tag{6.25}$$

The mixture critical temperature is then:

$$T_{c,\,mix} = \frac{\sum_{i=1}^{N}\sum_{j=1}^{N} z_i z_j \left[\left(\frac{T_{c,\,i}}{p_{c,\,i}}\right)^{1/3} \cdot \left(\frac{T_{c,\,j}}{p_{c,\,j}}\right)^{1/3}\right]^3 (T_{c,\,i} \cdot T_{c,\,j})^{1/2}}{\sum_{i=1}^{N}\sum_{j=1}^{N} z_i z_j \left[\left(\frac{T_{c,\,i}}{p_{c,\,i}}\right)^{1/3} \cdot \left(\frac{T_{c,\,j}}{p_{c,\,j}}\right)^{1/3}\right]^3} \tag{6.26}$$

and the mixture critical pressure is:

$$p_{c,\,mix} = \frac{8 \cdot \sum_{i=1}^{N}\sum_{j=1}^{N} z_i z_j \left[\left(\frac{T_{c,\,i}}{p_{c,\,i}}\right)^{1/3} \cdot \left(\frac{T_{c,\,j}}{p_{c,\,j}}\right)^{1/3}\right]^3 (T_{c,\,i} \cdot T_{c,\,j})^{1/2}}{\left(\sum_{i=1}^{N}\sum_{j=1}^{N} z_i z_j \left[\left(\frac{T_{c,\,i}}{p_{c,\,i}}\right)^{1/3} \cdot \left(\frac{T_{c,\,j}}{p_{c,\,j}}\right)^{1/3}\right]^3\right)^2} . \tag{6.27}$$

The mixture mole weights are defined as:

$$M_{w,\,mix} = 1{,}304 \cdot 10^{-4} \cdot (\overline{M}^{2{,}303}_{w} - \overline{M}^{2{,}303}_{n}) + \overline{M}_n, \tag{6.28}$$

where $\overline{M}_w$ and $\overline{M}_n$ are the weight average and number average mole weights.

The α-parameter for the mixture is:

$$\iota_{mix} = 1{,}0 + 7{,}378 \cdot 10^{-3} \cdot \rho_r^{1{,}847} \cdot M_{w,\,mix}^{0{,}5173} \quad , \tag{6.29}$$

where the α of Methane, the reference substance, is given by:

$$\alpha_o = 1{,}0 + 0{,}031 \cdot \rho_r^{1{,}847} \quad . \tag{6.30}$$

Chapter 7

pVT-Measurements

Accurate crude oil data are necessary to control the production of a hydrocarbon reservoir efficiently. They are of importance for further calculations of the processes which take place inside a reservoir.

7.1 Sampling

7.1.1 Objectives

The objectives of sampling are to receive samples from a suitable place in the production wells or surface facilities. The samples should represent the system in the reservoir under its initial conditions. Only then, the determination of its type, volumetric and phase behavior, and its composition is assured to supply data for

- geological and reservoir engineering evaluation and forecasting,
- laboratory studies concerning enhanced oil recovery (EOR) methods modifying *PVT* properties (and the viscosity) of the system.

7.1.2 General Criteria

Based on the general remarks about the types and behavior of hydrocarbon systems, conclusions can be drawn about general sampling criteria. It is obvious that - except in case of dry and wet gases - characteristic samples can be received only in the early life of the reservoir. Therefore, it can be generally stated that the best time of sampling is at the beginning of production.

To meet all requirements, the careful selection of wells for sampling is very important. Representative samples cannot be received from wells which are perforated at the water/oil or gas/oil contact and are producing water and/or non-equilibrium gas. The wells should be allocated at characteristic sections of the reservoir. Number of samples will depend on the dip of the structure as well as on the pay thickness. To determine the fluid properties along with the depth of the pay zone (where monophase system exists), a minimum of one sample per 30 m can be recommended.

There are restrictions which must always be considered:

- Considering the gravitational effect, it is clear that the sampling in closed wells could easily lead to misleading data.
- No characteristic fluid can be received within the flowing wells, where a multiphase system exists or is developing.
- Reliable sampling conditions in the flowing wells and at the wellhead only exist, if the total composition of the system entering the well and leaving it at the wellhead remains constant.

Favorable conditions at steady state flow are indicated by stabilization of the pressure and temperature at the wellhead and in the separator. Moreover, the production gas/liquid ratio, *GOR,* should remain constant during a long period of time.

7.1.3 Sampling Methods

There are three methods of sampling. Samples can be taken from the flowing wells (**subsurface sampling**) or from the equilibrium phases of the separators (**separator samples**). The third possibility is to get representative samples from the wellhead (**wellhead sampling**). In every case, steady state conditions must be maintained. The method used depends on the type of system to be sampled.

There are certain approximations for selecting sampling methods which consider some of the properties of the produced fluids. Values summarized in Table 7.1 represent average characteristics which can be used as some rule of thumb. It is clear, however, that the behavior of any system also depends on reservoir conditions which are missing on the tabulated data. Therefore, preliminary screening must be used cautiously.

On the basis of the general remarks on the phase behavior of different systems in their

Table 7.1: Screening sampling methods

Type	Density of the produced liquid $[kg/m^3]$	Gas/liquid ratio $[m^3/m^3]$
Dry gas	-	
Wet gas	$\leq$ 740	11000 - 20000
Gas/condensate system	740 - 780	1000 - 13000
High shrinkage oils	780 - 800	200 - 1500
Low shrinkage oils	$\geq$ 800	$\leq$ 200

initial state and on the changes in their behavior in the depression zone and in the wells, the following guidelines can be applied in screening sampling methods.

Sampling of equilibrium phases from separators can be used for all systems, but steady state conditions must exist. Note, that no separator sampling is needed for dry gases and for saturated and undersaturated oils, if no free water enters the production well and if there is a considerable length along which a1-phase oil.

For sampling, only those separators can be used where construction ensures highly efficient separation of the entering phases. In a wide region of flow rates, no liquid droplets should depart the system with the gas.

Separators must contain pressure gauges and thermometers as well as devices for the accurate measurement of the gas volumes (liberated and/or delivered), liquid hydrocarbons, and of water. Each phase can be sampled through sampling valves built in the separator at that part where pure gas, oil, and water exist.

To determine the phase boundary during the time of sampling, separators often contain high pressure windows for visual control. When highly paraffinic systems are produced exhibiting a cloud point in the vicinity of the separator temperature, separators should be heated. The continuous monitoring of the concentration of some key components in the gas phase is recommended. This procedure should be considered to control the development and maintenance of steady-state flow.

Samples of the equilibrium phases should be take using specially designed bottles with valves at their extreme ends. These bottles are in vertical position during sampling. The upper valve is connected with the sampling valve of the separator by a flexible tubing which is resistant to pressure and corrosion by phases sampled.

Sometimes, the bottles and the connecting tube are filled up with an indifferent liquid (mercury or water from the separator or from other sources) to maintain pressure and to

exclude air. It is then displaced by the sampled phase (gas or liquid). Whenever the temperature in the separator is lower than the ambient temperature, the use of mercury (or brine) is recommended in sampling the liquid phase. In doing so, about 90% of mercury (or brine) has to be displaced by the separator liquid. After closing the valves into he container and in the separator and after dismounting the container, additional 10% of mercury (or brine) should be removed by opening the lower valve. The created gas cap will prevent uncontrollable pressure increase during shipping. The valves in the contains must be protected by steel caps during shipping. Data for identification must be delivered with the sample.

Bottom hole sampling

Bottom hole sampling can be used when only the phase to be sampled is present at the perforated zone. If water is also produced with the hydrocarbons but remains at the bottom under steady-state conditions, samples can be taken above the water level. However, the flow of a 1-phase hydrocarbon fluid must be assured. The method can be controlled by sampling at different depths and by analyzing the water content of samples. No sampling within the wells is needed for dry gases or - in general - for systems which exist in a 1-phase state up to the wellhead.

Bottom hole samplers are specially designed devices containing one valve or two valves at their extreme ends. They are run into the well through a sealed tube mounted to the christmas tree by a mechanically driven cable. After reaching the desired depth (usually with open valves to allow the flushing of the sampler by the flowing fluids), the valves are closed. The valves are operated mechanically or electrically from the surface or within the sampler at the predetermined depth or time.

At the surface, the sample should immediately be transferred to containers through a flexible steel tube which - together with the shipping bottle - is filled up with an inert liquid (e.g. mercury). The sample is displaced by injection of the inert liquid into the sampler using a volumetric pump or - in a simple manner - by gravitational effects. The protection of the samples in the shipping bottles and their correct marking for identification are important as it has already been mentioned.

Sampling at the wellhead

Sampling at the wellhead is a suitable process in case of the production of dry gas or undersaturated oil at wellhead conditions.

The container is connected with a valve at the wellhead and flushed with the fluid produced. The previous remarks referring to the protection and identification of the shipping bottles are also valid for wellhead samples.

7.1.4 Special Problems

There are sometimes problems arising from low permeability oil reservoirs (wells being produced with high depression). As a result, the ratio of the phases entering the wells does not characterize the initially-in-place fluids (bubble point oil system), especially if water is also present. In this case, it is only possible to take samples from the equilibrium phases of the separator and to recombine them under separator conditions corresponding to their volume ratio. Afterwards, pressure and temperature are increased up to the reservoir conditions.

The basic concept of this method is that - if the liquid is in equilibrium with other phase(s) - the composition of the oil phase is not influenced by the contacted volume of the other phase(s) being in equilibrium with the oil. However, no processes in the reservoir/well system should take place which may result in a difference between the overall composition of the reservoir fluid and the produced fluid.

A similar approach can also be used for gas-condensate systems.

Whenever water production cannot be avoided and the volume of the produced water is high, dissolved gases may be liberated from the water having a composition which could largely differ from that of the equilibrium hydrocarbon system. In this case, a similar procedure as above should be used to restore the composition of the hydrocarbon phase.

However, the samples must be preserved in their original state. As for liquids, it is important

- to prevent any loss - especially in their lighter fractions -,
- to avoid the contact with air because oxidation processes could drastically modify the composition of hydrocarbon liquids, primarily those of oils.

Specially designed sampling is needed to determine the microbiological contamination of the produced fluid(s). This procedure is often necessary in case of reservoirs containing only water from which water will be produced for industrial or public supply. Sterile samplers and shipping bottles but also anaerobic conditions (in the course of sample transfer) must be guaranteed.

7.2 Experimental Determination of the Volumetric and Phase Behavior

To determine the volumetric and phase behavior of naturally occurring systems under reservoir/well/surface conditions, equipments and methods have been developed for the petroleum industry. A general scheme of the set of equipments used for *PVT* studies shown in Figure 7.1.

7.2.1 Equipment

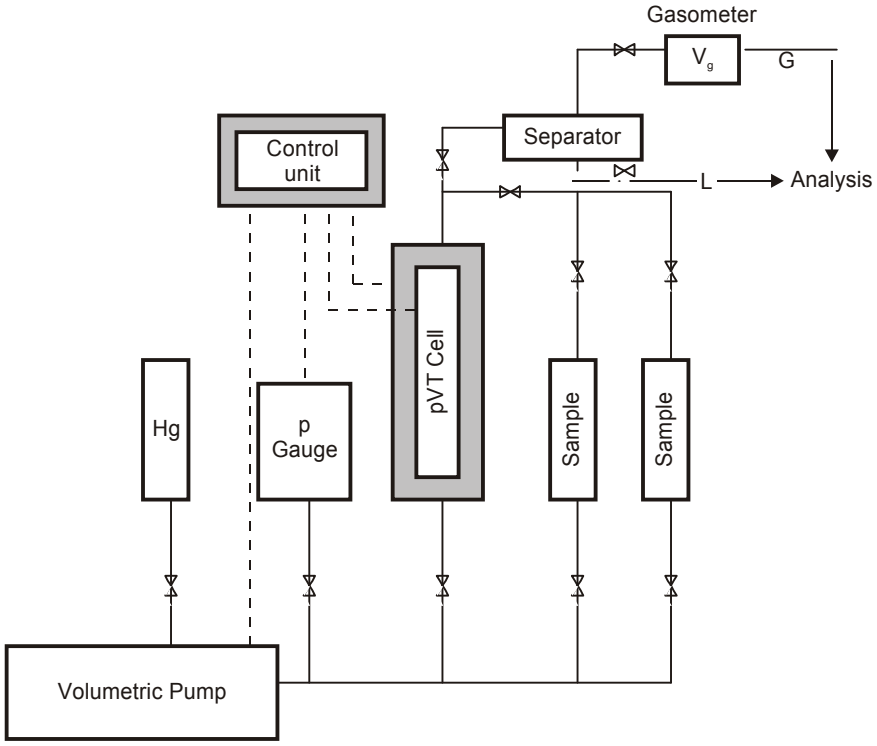

Figure 7.1: Scheme of *PVT* equipments

Samples to be studied are transferred to the **P V T cell.** Some known volume of an inert liquid is injected into the sampling bottle(s), while the same liquid is withdrawn from the cell initially filled with it.

The selection criteria for the inert liquid are:

- It must exhibit low volatility under (i) ambient conditions and also (ii) under temperatures and pressures which represent the working conditions.
- It should not react with the fluids contacted.

- Its physical and chemical properties must be well known.

Although mercury is widely used, sometimes low melting point alloys are used. No restriction is needed, however, if the liquid transported by the volumetric pump(s) is separated from the samples. In this case, the samples will be transferred and measured by a piston built into the containers and the ***PVT*** cell.

Double-acting or two single-acting volumetric pump(s) are needed for this process. Sometimes only one pump may be used for this purpose, if the inert liquid leaves the cell through a suitable operated valve at the bottom of the cell. This valve controls the rate and volume of the out-flowing inert liquid.

The sample being transferred into the cell must be in a 1-phase state. Therefore, liberated gas or condensate in the shipping bottle has to be dissolved or evaporated in advance. Referring to separator samples, the proportions of gas and liquid to be injected into the *PVT* cell must be equal to those measured into the field separator at the time of sampling.

7.2.2 PVT-Cells

Evaluation of the *PVT* behavior is carried out on the system transferred into the *PVT* cell. The cell has to be a heat- and pressure-resistant vessel which is equipped with valves made of non-corrosive materials. The cell is mounted into a thermostatic bath which ensures from detrimental temperature inconstancy in the cell. The electrically heated (or cooled) medium circulating around the cell could be air or liquid. To obtain the desired rapid establishment of the equilibrium conditions at any given pressure and/or temperature, the cell is agitated or stirred inside.

However, the accuracy of measurements depends on the resolution of the measuring instruments. Nevertheless, the relative error can be decreased by a reasonable increase of the sample volume studied. Therefore, “micro *PVT* cells” are not used in practice. Moreover, considering the change in volume of the system within the pressure range applied in the *PVT* studies, larger cell volumes are used to study (i) gases, (ii) gas-condensate systems, (iii) critical oils, and (iv) water. On the other hand, relatively smaller ones are used to investigate characteristic oil systems.

Although many different *PVT* cells are specified, two basic types can be distinguished:

- **blind** *PVT* **cells** (without any possibility of visual observation of the system to be measured),

- **windowed** *PVT* **cells**, where the volumetric and phase behavior can directly be observed through one or more pressure- and temperature- resistant windows built into the cell body. The inside of the cell is lighted from outside by transmitted or reflected (from the inner wall of the cell) light.

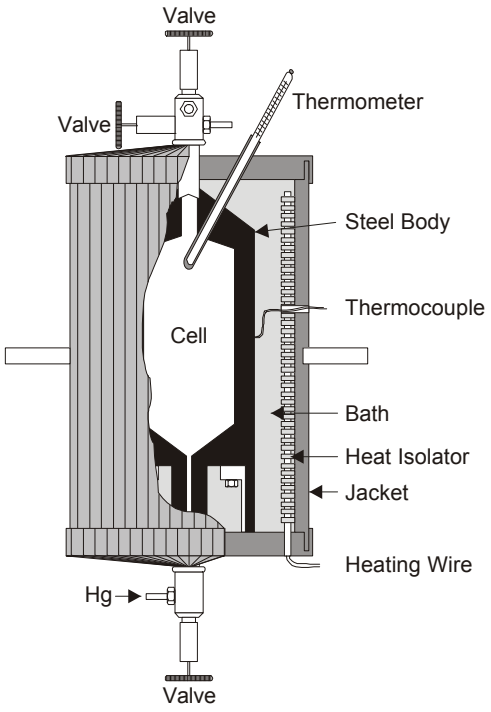

Figure 7.2: Blind *PVT* cell

Blind *PVT* cells are usually used to study systems in which no phase transition takes place or phase transition can easily be determined using the isothermal p - V relationship (dry gases, oil systems, water). A characteristic blind cell is shown in Figure 7.2. Its volume is about $0.001[m^3]$ which is large enough to be used for gas and oil studies as well.

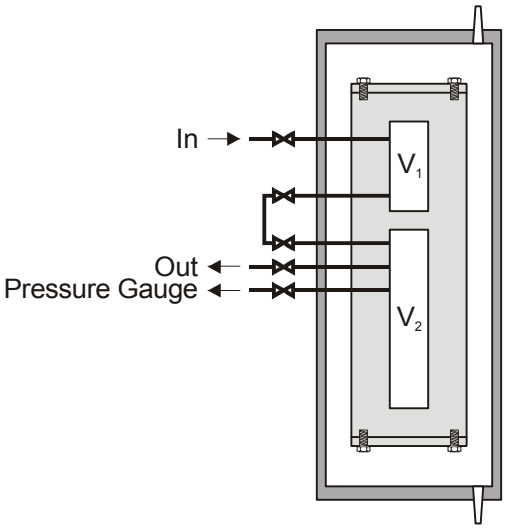

Figure 7.3: *PVT* cell (after BURNETT)

A special *PVT* cell for gases was developed by BURNETT (see Figure 7.3). It contains two or more chambers with different volumes which are separated by valves. The chamber possessing the smaller volume contains the gas under given pressure. By opening

successively the valves of the evacuate other chambers with known volume, the change in pressure can be measured. No volumetric pumps are needed in this case.

Windowed *P V T* cells

Windowed *PVT* cells are usually used to evaluate systems where the knowledge of the volumes of coexisting phases is necessary (e.g. wet gases under well or separator conditions, gas condensate systems). It is also required whenever phase transition cannot exactly be determined by isothermal p - V relationships (volatile oils or partially miscible liquid/liquid systems with or without free gas phase).

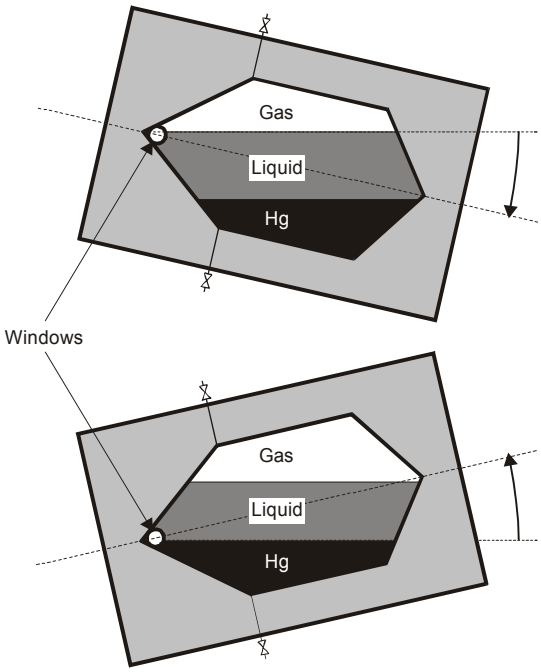

Figure 7.4: *PVT* cell (after DEAN-POETTMAN)

A typical one-windowed cell is shown in Figure 7.4. The volumes of the liquid phase can be determined by the angle of rotating the cell until liquid phases appear in the window.

A *PVT* cell with variable volume is presented in Figure 7.5. The condensed phase can be moved to the window by simultaneous lifting (or sinking) the two built-in plungers. The volume corresponding to that motion can be read on the calibrated stem of the plungers.

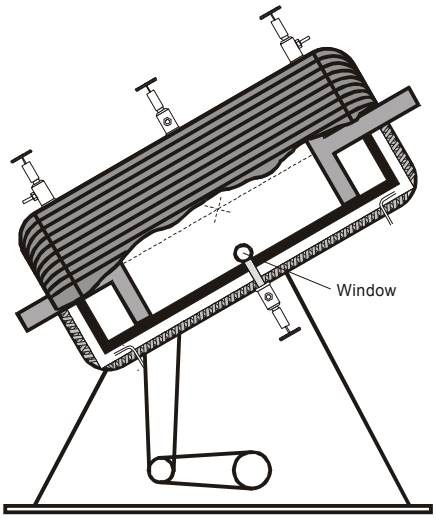

Figure 7.5: Variable volume cell (after VELOKIVSKIY et al.)

As far as SLOAN's windowed cell (see Figure 7.6) is concerned, there are three sections. In the upper part, a plunger is moved by the fluid injected or withdrawn by a volumetric pump. In the lower part, the condensed liquid is collected and can be lifted up to the windows which are built into the middle part. This can be done by injecting inert fluid. Meanwhile, pressure can be kept at the desired constant value by the simultaneous lifting of the plunger.

Another type contains one capillary glass tube within the cell through which the inner volume can be lighted and observed using an optical system. It serves also for the measurement of the volume of phases. The scheme of this cell is shown in Figure 7.7. Three windows are built into the body of the most generally used cell as shown in Figure 7.8.

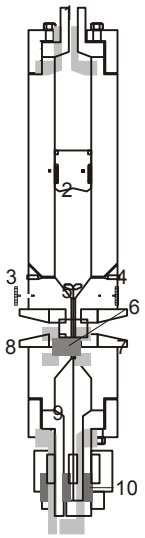

1 Orifice for Introduction of Mercury through the Upper Cap, for Operation of the Piston
2 Piston with joist Packing
3 Hole and Valve for Introduction of Gasoline
4 Hole and Valve for Introduction and Sampling of Gas
5 Spiral for stirring Gas. The Liquid is stirred by a Spiral Coil Wound around the axis
6 Sapphire Viewing Window
7 Viewing Window
8 Lighting Window
9 Liquid Volume Measurement Chamber
10 Magnetic Agitator

Figure 7.6: *PVT* cell (after SLOAN)

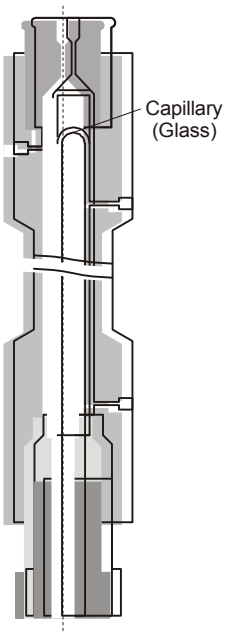

Figure 7.7: *PVT* cell (after WELLS-ROOF)

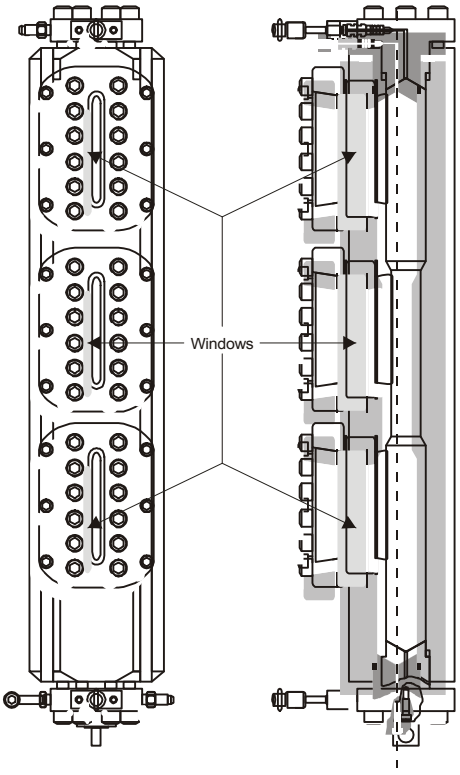

Figure 7.8: RUSKA cell

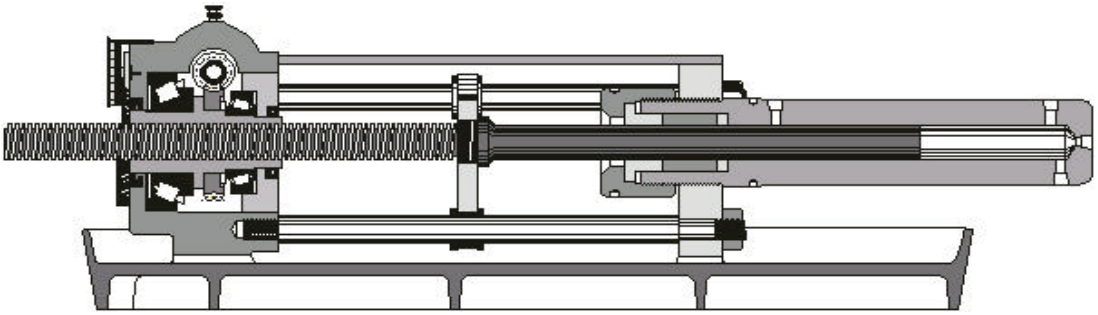

Figure 7.9: RUSKA volumetric mercury pump

7.2.3 Volumetric Pumps

Volumetric pumps - the so called **positive displacement pumps** - are used to measure the volume of the inert liquid injected to and withdrawn from the cell respectively. The pressure can be increased or decreased. The transported volume is proportional to the change in volume of the system studied.

In the generally used types, the inert liquid is displaced by a plunger from a pressure resistant and thermostatically controlled cylinder. The movement of the connecting screw-spindle can be read on a calibrated rod and on a dial to increase the accuracy.

In practice, hand- and mechanically operated pumps are used, the latter sometimes with variable speed. A special type of volumetric pumps is the **double-acting** one: Two plungers are working simultaneously, but in opposite directions.

A scheme of a hand-operated volumetric pump is shown in Figure 7.9. Its general construction does not differ from the pump which is mechanically driven.

7.2.4 Auxiliary Equipment

The *PVT* cell, the volumetric pump(s), and other parts of the *PVT* system are interconnected by pressure-resistant stainless steel tubes. In order to separate single parts of the equipment, valves are mounted in the network of tubes.

Pressure in the system is measured by gauges containing BOURDON-tubes. However, also dead weight gauges can be used for this purpose and for the calibration of the BOURDON-tube-gauges as well. There are also gauges in which an electric signal is proportional to the pressure measured. These gauges are also built into the tube network. They are filled with the inert liquid used in the volumetric pumps.

In order to store the inert liquid (mercury), a container is used which is also interconnected

through valves with the different parts of the *PVT* system.

The temperature of the volumetric pump(s), in the *PVT* cells, and in the thermostat around the cell is usually measured by thermocouples (may be controlled by thermometers). Whenever pressure, temperature, and the volume in the pumps are measured electrically, the process can be automated and computerized.

If the gas phase liberated in the *PVT* cell will be displaced, its volume must be measured. For this purpose gasometers are used. However, gas could condense under ambient conditions or at pre-selected pressures. Therefore, a laboratory separator must be inserted between the *PVT* cell and the gasometer.

7.3 Methods

Basically, there are three methods generally used in *PVT* studies. They are distinguishable by considering the change and the direction of change in the composition of the system.

7.3.1 Flash Process

In the course of flash processes, pressure is gradually increased or decreased at constant temperature under equilibrium conditions. At each pressure step, the volumes of the system and that of the existing phases are measured and the development of phases is observed. Measurements are usually repeated at other temperatures, too, covering some range between reservoir and surface temperatures (in the separator or in the stock tanks).

Measurements start at or above the reservoir pressure. The lowest pressure applied is determined by the system studied. For systems in which no phase transition takes place, the lowest pressure selected could be the atmospheric one. In this case the flash process simulates the whole course of production.

Whenever phase transition occurs, measurements should be carried out in a pressure region which correctly characterizes the phase transition and the 2-phase (or multiphase) behavior of the system. In this case the flash process - carried out at reservoir temperature - simulates the behavior of the system far inside the reservoir where its composition is not influenced by the production. A scheme of the flash process has been presented in Figure 4.3.

7.3.2 Differential Process

The differential process describes the change in the volumetric and phase behavior of the system at reservoir temperature and under equilibrium conditions, where any decrease in the reservoir pressure results from the stepwise production of one of the equilibrium phases (usually liberated or free gas).

In contrast to the flash process during which the composition is maintained and the volume is varied, the differential process is carried out at constant volume and by variation of the system composition.

In the course of the differential study - also explained in Figure 4.3 -, the volumes of the system and those of the existing phases are measured. The development or disappearance of phases is observed. To follow the change in composition of the system and to characterize the displaced phase (gas), the composition of the latter is also determined. By use of a laboratory separator in which pressure and temperature correspond to those during the field separation process, further information on the volume (and composition) of phases separated can be given.

The differential process is repeatedly carried out, usually down to the lowest possible reservoir (separator) pressure. As a result of the gradually changing composition, the values of characteristic parameters will differ from those determined by the flash process. except the starting point representing the intact system under initial reservoir conditions.

7.3.3 Reverse Differential Process

The reverse differential process is used to study the effect of any gas injection process on the volumetric and phase behavior of systems. This can be done under initial conditions (gas cycling) or by starting from a given depleted state (gas injection with pressure increase). Both are constant volume processes. In the course of gas injection (using a pre-selected gas), the phase volumes are measured and phase transition(s) are observed at reservoir temperature. There are two subgroups of the reverse differential process.

If the effect of **pressure maintenance by gas injection** is being studied after each step of the differential measurement, p is re-established by injecting a measured volume of the pre-selected gas. This method is used, when

- in the initial state of a gas condensate system, the liquid phase exists beyond the restriction of retrograde condensation,
- partial or total evaporation of the immobile liquid condensate is needed.

In depleted (gas condensate or oil) reservoirs, the effect of **increasing the pressure by pre-selected gas** can also be studied. In the course of a stepwise process, an isothermal pressure increase is realized under constant volume conditions. The highest pressure to be

reached corresponds to the fracturing pressure of the formation, or - if this information is not available - it is about 10% higher than the initial reservoir pressure. If some 1-phase system develops below this pressure, it is obviously no need to continue the process in a higher pressure region. The effect of gas injection is often the combination of the methods discussed above.

Chapter 8

References

1. Amyx, J.W., Bass, D.M.Jr. and R.L. Whiting: Petroleum Reservoir Engineering - Physical Properties, McGraw-Hill Book Company, N.Y. - Toronto - London (1960) 610p
2. Beal, C.: The Viscosity of Air, Water, Natural Gas, Crude Oil and its Associated Gases at Oil Field Temperatures and Pressures, Trans. AIME, 165 (1946) 94-115
3. Brill, J.P. and Beggs, H.D.: "Two-Phase Flow in Pipes, "paper presented at the University of Tulsa INTERCOMP Course, 1974.
4. Brown, G.G.: A Series of Enthalpy-Entropy Charts for Natural Gases, Trans.AIME, **160**(1945)65-76
5. Brown, G.G., Katz, D.L., Oberfell, G.G. and Allen, R.C.: Natural Gasoline and the Volatile Hydrocarbons, NGAA, Tulsa, OK (1948)
6. Burcik, E.J.: Properties of Petroleum Reservoir Fluids, International Human Resources Development Corporation, Boston, MA, (1979) 190p
7. Carr, N.L. Kobayashi, R.and Burrows, D.B.: Viscosity of Hydrocarbon Gases under Pressure, Trans. AIME, **201** (1954) 264-272
8. Chew, J.N. and Connally, C.A.: A Viscosity Correlation for Gas-Saturated Crude Oils, Trans.AIME **216** (1959) 23-25
9. Collins, A.G.: "Properties of Produced Waters," Petroleum Engineering Handbook, H.B. Bradley et al. (eds.), SPE, Richardson, Texas (1987), Chap. 24, 1-23.
10. Dodge and Newton (1937): Ind.Eng.Chem., **29**
11. Dodson, C.R. and M.B.Standing (1944): Pressure-Volume-Temperature and Solubility Relations for Natural Gas-Water Mixtures, Drilling and Production Practice, American Petroleum Institute (X)
12. Dourson, R.H. Sage B.H. and Lacey, W.N.: Phase Behavior in the Methane-Propane-Pentane System, Trans AIME, **151** (1943) 206-215
13. Dranchuk, P.M. and Abou-Kassem, J.H.: "Calculation of Z-Factors for Natural Gases Using Equations of State, "Journal of Canadian Petroleum Technology, Volume 14, 1975.
14. Edmister, W.C. and Lee B.I.: Applied Hydrocarbon Thermodynamics, Vol.1,2nd ed., Gulf Publishing Co. Houston, TX (1984) 233p
15. Gyulay, Z.: Reservoirmechanik, Teil I: Thermodynamik der Lagerstättenflüssigkeiten, Fernstudium Bergakademie Freiberg (1967) 156p
16. Haas, J.L.Jr.: "Physical Properties of the Coexisting Phases and Thermochemical Properties of the H2O component in Boiling NaCl-Solutions, "Geological Survey

Bulletin (1976) 1421-A and -B.
17. Hall, K.R. and Yarborough, L.: "A New EOS for Z-factor Calculations, "Oil & Gas Journal, 1973.
18. Hocott, C.R. and Buckley, S.W.: Measurements of the Viscosities of Oil under Reservoir Conditions, Trans.AIME, 142 (1941) 131-136
19. Katz, D.L.: Prediction of the Shrinkage of Crude Oils, API Drill.Prod.Practice (1942) 137
20. Katz, D.L., Cornell, D., Kobayashi R., Poettmann, F.H., Vary, J.A., Elenbaas, J.R. and Weinaug, C.F.: Handbook of Natural Gas Engineering, McCraw-Hill Book Company, N.Y.-Toronto-London (1959), 802p
21. Kay, W.B.: Liquid-Vapor Phase Equilibrium Relations in the Ethane-n- Heptane System, Ind.Eng.Chem., 30/4 (1938) 459-465
22. Kestin et al.: "Tables of the Dynamic and Kinematic Viscosity of Aqueous NaCl Solutions in the Temperature Range 20-150°C and the Pressure Range 0.1-35 MPa," J. Phys. Chem. Ref. Data (1981) 10, No. 1, 71.
23. Kortüm, G.: Einführung in die chemische Thermodynamik, Verlag Chemie GmbH., Weinheim (1972) 474p.
24. Lee, B.I. and Kesler, M.G.: "A Generalized Thermodynamic Correlation Based on Three-Parameter Corresponding States, "AIChE Journal, Volume 21, 1975.
25. Lewis, G.N. and Randall, M.: Thermodynamics and the Free Energy of Chemical Substances, McCraw-Hill Book Company, Inc., New York (1923)
26. Lohrenz, J., Bray, B.G. and Clark, R.C.: Calculating Viscosities of Reservoir Fluids From their Compositions, J.Pet.Tech. (Oct. 1964) 1171-76.
27. Matthews, T.A, Roland, C.H. and Katz, D.L.: High Pressure Gas Measurement, Petr.Refiner **21/6** (1942) 58
28. McCain, W.D.Jr. (1973): The Properties of Petroleum Fluids, Petroleum Publishing Company, Tulsa, OK (1973) 326p
29. Equilibrium Ratio Data Book, Natural Gasoline Association of America, Tulsa, OK (1957)
30. Nghiem, L.X., Aziz, K. and LI, Y.K.: A Robust Iterative Method for Flash Calculations Using the Soave-Redlich-Kwong or the Peng Robinson Equation of State, Soc.Pet.Eng.J. (June 1983)521-530.
31. Peng, D.Y. and Robinson, D.B.: A New Two-Constant Equation of State, Ind.Eng.Chem.Fundam. **15/1** (1946) 59-64
32. Redlich, O. and Kwong, J.N.S: On the Thermodynamics of Solutions. V - An Equation of State. Fugacities of Gaseous Solutions, Chem.Reviews, 44 (1949) 233-244
33. Sage, B.H. and Lacey, W.N.: Volumetric and Phase Behavior of Hydrocarbons, Gulf Publishing Company, Houston, TX (1949)
34. Sage, B.H., Lacey, W.N. and Schaafsma, J.G.: Phase Equilibria in Hydrocarbon Systems, Ind.Eng.Chem., 26 (1934) 214-217
35. Soave,G.: Equilibrium Constants from a Modified Redlich-Kwong Equation of State, Chem.Eng.Sci., 27 (1972) 1197-203
36. Standing, M.B.: Volumetric and Phase Behavior of Oil Field Hydrocarbon System, Reinhold Publ. Corporation, New York (1952) 130p
37. Standing, M.B.: Volumetric and Phase Behavior of Oil Field Hydrocarbon Systems, SPE of AIME, Dallas, TX (1977)130p
38. Standing, M.B. and Katz, D.L.: Density of Crude Oils saturated with Natural Gas,

Trans.AIME, 146 (1942) 159-165
39. Stiff, H.A.Jr.: The Interpretation of Chemical Water Analysis by Means of Patterns, Trans.AIME 192 (1951)376-379
40. Trube, A.S.: Compressibility of Undersaturated Hydrocarbons Reservoir Fluids, Trans. AIME, **210** (1957) 341-44
41. Van der Waals, J.D.: Over de Continuiteit von den Gas en Vloeistoftoestand, Dissertation, Leiden(1873)
42. Van Wingen, N.: Viscosity of Air, Water, Natural Gas, and Crude Oil at Vary-ing Pressures and Temperatures, Secondary Rescovery of Oil in the United States, American Petroleum Institute (1950).
43. Wichert, E. and Aziz, K.: "Compressibility Factor of Sour Natural Gases," Canadian Journal of Chemistry Engineering, Volume 49, 1971.
44. Wichert, E. and Aziz, K.: "Calculate Z´s for Sour Gases, "Hydrocarbon Processing, Volume 51, 1972.

Chapter 9

Nomenclature

Symbols

a	- EOS parameter
b	- EOS parameter
B	- Formation volume factor
c	- compressibility
C	- Number of Components
F	- Degree of Freedom
f	- Fugacity
K	- K-Factor
m	- mass [kg]
M	- Molecular weight [kg/kmol]
n	- Number of moles in the system
P	- Number of Phases
p	- Pressure
R	- Gas Solution Ratio
T	- Temperature
V	- Volume
W	- Average Mole weight
x	- Mole fraction in the liquid phase
y	- Mole fraction in the vapor phase

z - Mole fraction in the total system

Z - Compressibility factor

Greek

γ specific gravity

κ - isothermal compressibility

κ - binary interaction coefficient

α - cubic expansion coefficient

β - pressure coefficient

ϕ - fugacity coefficient

μ - viscosity

ρ density, [kg/m^3]

ω acentric factor

Super-/Subscripts

b - at the bubble point

C - number of components

c - component

g - gas

i - component

i - initial

liq - liquid phase

N_c - total number of components

N_p - total number of phases

o - Standard Condition

o - oil

P - number of phases

p - phase

pc - pseudo-critical

pr - pseudo-reduced

r - reduced

t - total system

vap - vapor phase

w - water

Conversion Factors

bar = psia*0.06894757

m = ft*0.3048

kg = lb*0.453592

$1000m^3$ = MMSCF*26.795

kg/m^3 = lb/ft^3*16.01846

°F = °R-459.67

$$°C = \frac{(°F-32)}{1,8}$$

$$°API = \frac{141,5}{\text{Spec. Gravity}-131.5}$$